Mediterranean evergreen vegetation dynamics

Detection and modelling of forest and shrub-land development in the Peyne catchment

Utrecht Studies in Earth Sciences

ISSN 2211-4335

Utrecht Studies in Earth Sciences 002

Mediterranean evergreen vegetation dynamics

Detection and modelling of forest and shrub-land development in the Peyne catchment

Wiebe Nijland

Utrecht 2011

ISBN 978-90-6266-280-7

Cartography and figures:

Communication & Marketing (8017), Faculty of Geosciences, Utrecht University

Printed in the Netherlands by Labor Grafimedia bv, Utrecht.

Contents

Preface

Onderzoek doen is als eerste natuurlijk gewoon heel leuk. Zeker als je dat in het mooie zuiden van Frankrijk kunt doen aan een onderwerp als vegetatieontwikkeling. Bijna altijd is het mooi weer (zowel bij zon als bij regen), dagenlang ben je bezig in de mooiste bossen en landschappen, en dan maken ze daar ook nog eens prima wijn voor weinig en elke dag vers stokbrood. Als tweede moeten er natuurlijk ook resultaten komen en moet het hele onderzoek ook nog een beetje leuk opgeschreven. Van het totaal ligt er nu het resultaat en ik ben blij dat het is gelukt. Natuurlijk heb ik het hele proces niet in mijn eentje hoeven doorlopen en daarom wil ik bij deze graag iedereen bedanken die heeft bijgedragen aan mijn dagelijks leven en de totstandkoming van dit proefschrift.

Als eerste de direct betrokkenen:
Elisabeth, als eerste bedankt voor het zetje –of flinke duw– die je me hebt gegeven om aan dit hele project te beginnen. Ik had het bijna aan mij voorbij laten gaan en dat zou toch jammer zijn geweest. Als tweede was je er eigenlijk gewoon altijd om mee te denken, en met aansporingen of wijze raad die ik evenzovaak niet heb opgevolgd. Ik kan gerust zeggen dat ik maar geboft heb met jou als dagelijks begeleider, ik kon ondanks dat jij altijd gelijk hebt toch heel goed met je opschieten en dat is best speciaal.
Steven, ook jij was erg nauw betrokken met mijn werk en met jou als promotor heb ik nooit wat te klagen gehad. Integendeel. Echt leuk werd het als we eens met een goed glas wijn in de Franse avondzon konden zitten en er echt tijd was voor het spuien van allerlei ideetjes of een flinke discussie. Je hebt altijd de vrijheid gegeven om mijn eigen valkuilen te graven, maar stond er toch ook om te voorkomen dat ik er in viel.
Freek, je stond vanuit Enschede op iets meer afstand van mijn project, maar desondanks heb je toch steeds interesse getoond en kwam je vaak met nieuwe kijk of op de zaken of vragen die tot dan toe bij mij nog niet op waren gekomen. Mark, tijdens mijn eerste bezoek aan het ITC kwam je met het idee om eens wat geofysische methoden te bekijken voor het onderzoek aan vochtbeschikbaarheid in de bodem. Dit heeft tot een heel leuk hoofdstuk geleid en tot een hoop gesleep met al die apparatuur in het struikgewas. Esther, bedankt voor het meedenken en jouw ervaring op boomringen gebied. Zonder de inbreng van jou en Martha en het gebruik van jouw labfaciliteiten was mijn boomringenavontuur misschien wel hopeloos gestrand.
Voor de boomringen was ook de inzet van het FG-Lab onmisbaar, net zoals voor al mijn andere veldwerken waarvoor altijd weer alle spullen voor geregeld konden worden ondanks mijn soms gebrekkige planning. Chris, Marcel, Bas, Henk, bedankt! Ook voor de extra schep of hamer die ik nog mee kreeg en die steeds weer van pas bleek te komen.
Bij het veldwerk in het mooie Peyne gebied waren ook vele MSc. studenten betrokken waaronder de club van 2007 in Mas Delon (Mark, Peter, Liesbeth, Menno, Daan) en in 2008 Rik en Erik. Bedankt voor jullie gezelschap en voor sommigen van jullie ook voor de nuttige data die verzameld is en die ik weer voor dit proefschrift heb kunnen gebruiken. Peter nog dank voor de extra week veldwerk in juni, jouw inzet toen was onmisbaar.

Dan de mensen in Utrecht,
De bewoners van kamer 112: Reinder, ons verschil in levenshouding was interessant, maar een amusante discussie of een bak koffie kon er altijd van af. En mijn tweede kamergenoot, Top. Alle AIO's en aanverwanten uit het promovendioverleg: de oude garde (Hans, Susan, Menno, Hanneke, Loes), de club uit de kelder (Gilles, Mark, Ingwer, Noemi, Sanneke, Nelleke, Willem) de eerste verdieping (Arien, Lara, Edwin, Frederiek, Liesbeth, Oliver) en van boven (Paulus, Frans, Germari, Wouter en de hele club van zand en zee), ik vond het erg interessant om in een groep te zitten met zo'n breed onderzoeks gebied. Ook alle andere stafleden, o.a. Edzer, Derek, Rens, Geert, etc. moeten natuurlijk even genoemd.
In het speciaal wil ik alle mensen bedanken voor de vele verfrissende wandelingen in de botanische tuin. Nu ik klaar ben zullen jullie zelf een pasje moeten meenemen. Dank ook aan onze rots in de branding voor een werkend koffieapparaat en het secretariaat Juul, en verder aan alle bewoners en bezoekers van de koffiehoek voor de gezelligheid.

Buiten de universiteit zijn er natuurlijk ook nog een hoop vrienden enzo die ook meer dan eens zijn vermoeid met verhalen en flessen wijn meegebracht uit La Peyne.
Rogier, je had eigenlijk gemakkelijk bij de direct betrokkenen kunnen staan zo veel heb je geholpen met veldwerk, bomen zagen, wijn proeven discussies over onderzoek etc. En dan hebben we ook nog foto's gemaakt, wijn gedronken, camera's omgebouwd, wijn gedronken, de bx geklust, wijn gedronken etc. Wilco, ik was je vaste excuus voor een road trip naar Zuid-Frankrijk, en dat leverde steeds weer een heel gezellig weekeinde op en een hoop roering in het anders zo stille Neffiès.
Dank aan iedereen waarmee ik mij heb vermaakt tijdens weekeinden wadden, zeeland, of verdere reizen, en thuis op Warande 115, de 2e Hogeweg, en in de Lessepsstraat. Zonder deze momenten van afleiding of bezinning was het lang niet zo leuk geweest. Ake, bedankt voor alles en veel succes met jouw werk in Siberië.

Ik wil ook nog een paar niet menselijke zaken bedanken. Mijn trouwe (voor zover van toepassing) BX, en het citroen-forum.nl voor snelle diagnose en oplossingen. De brug bij Millau voor het aanzienlijk bekorten van de tocht naar mijn veldwerkgebied, en natuurlijk het Peyne gebied zelf met alle geneugten die Frankrijk te bieden heeft.

Als laatste noem ik mijn familie omdat ze er toch wel voor me zijn of ik ze nou bedank of niet. Al mijn ouders: mijn opvoeding heeft een stevige basis gelegd om dit onderzoek te kunnen doen. Ik heb van jullie ongelofelijk veel geleerd en doe dat nog steeds. Broer Reindert, ik vond het heel leuk om in jouw proefschrift een aanmoediging te lezen voor dit werk.

1. Introduction

Mediterranean regions are regarded as outstandingly rich with respect to history, geography and biodiversity. The landscape has a unique combination of climate, landforms, vegetation and long term human history. Mediterranean ecosystems are under pressure due to demographic development. The region is an attractive place for living and as such it attracts a wide variety of economic activities and services e.g. high tech industry like software companies, universities, and research institutes. These economic activities draw people to the area resulting in increased use of space for living, recreation and transport. Furthermore, these activities increase the already high pressure on the available environmental resources (Grenon and Batisse, 1989; UNEP, 2009). The presence of 'natural' vegetation types in the landscape is strongly influenced by centuries of human occupation of the landscape and the successive establishment and abandonment of agricultural fields, mainly vineyards. Natural vegetation is limited to areas unfit for agricultural use because of relief, soils, or accessibility. The natural areas are presently used for practices such as cattle grazing and wood harvest by coppicing, while at the same time they represent value towards tourism and the reduction of soil erosion and flooding hazards.

Vegetation development in Mediterranean landscapes is often a slow process. The typical Mediterranean climate -with long dry periods in summer, mild winters and concentrated rainfall events in spring and autumn- is an important constraint on growth, enhanced by the often marginal and degraded soil conditions. Broadleaved evergreen species are characteristic to Mediterranean areas and are the dominant vegetation type in large parts of the Mediterranean areas in the world. The sclerophyll, leather-like, leaves allow the evergreens to survive the dry summers and benefit from the mild and humid periods of the year. These specific adaptations allow the evergreen trees and shrubs to grow in a landscape where summer drought and poor soil conditions strongly limit plant productivity. The low growth potential and slow succession make this landscape vulnerable to disturbances and modern climate change. Regional climate-change scenarios predict that the extreme character of the Mediterranean climate will increase: higher temperatures, longer periods of drought and more violent rainfall events (Gao and Giorgi, 2008; Giorgi and Lionello, 2008). These changing environmental conditions will possibly have a deteriorating impact on the Mediterranean ecosystems and landscapes.

This thesis aims at improving the abilities of monitoring and modelling the growth and development of Mediterranean evergreen shrub and forest vegetation. The anticipated climate changes for the next century may have large effects on the vegetation development in the area and it is thus important to create reliable predictions of future vegetation development and to have accurate methods to monitor the natural areas. Analysis of the current spatial patterns and temporal variability in key vegetation characteristics such as biomass, leaf area, water use, and growth provides information on the ecosystem that can be used to create more accurate projections for future development of the landscape and vegetation.

1.1 Research questions

The research presented in this thesis is carried out on the evergreen natural vegetation in the Peyne study area in southern France. The combination of field measurements, earth observation, and dynamical modelling provides the tools to better understand vegetation patterns in space and time. The measurement of important variables for tree growth is far from trivial and raises questions that are of general interest to science by itself. In this thesis some of these questions are addressed within the general scope of monitoring and modelling vegetation functioning. The progress made in each of the specific subjects contributes to science in general and may be useful outside of the Mediterranean basin or even outside vegetation science. The issues regarding vegetation functioning centre on evergreen Mediterranean species, specifically *Quercus ilex* and *Arbutus unedo.*

The overall objective of this thesis is:
To increase the understanding of, and abilities to monitor the growth and development of evergreen Mediterranean vegetation and to improve the projections of vegetation change as an effect of modern climate change.

Within this objective lies the quest to better understanding of vegetation functioning and to determine and size the most important actors on tree growth in the Mediterranean landscape. Detection of vegetation growth and analysing its patterns within the landscape and over the years and seasons provides important information about the actual functioning of the vegetation system. This information is used to improve the simulation models that are used to create projections based on future climate scenarios. The different parts of this process are addressed in these main research questions:

1: What is the optimal spatial unit to retrieve quantitative measurements on Mediterranean evergreen vegetation from earth observation imagery?
Given the fact that Mediterranean vegetation grows in open, complex spatial patterns, the resolution of remotely sensed imagery and the scale of vegetation analysis is non-trivial and has to be carefully considered when using and selecting imagery to obtain measurements on biophysical vegetation parameters like leaf area and aboveground biomass.

2: What do the spatial and temporal patterns of remotely sensed thermal and spectral information tell about the sensitivity of the vegetation to the variability in the climate and landscape?
Monitoring of the landscape by means of remotely sensed images provides information on the status and development of vegetation. Analysis of the spatial and temporal patterns of vegetation vigour of may provide information about its sensitivity towards variability in the climate or the landscape.

3: What method is best suited to detect soil-water availability to trees in the rocky and stony substrates?
Available soil water is a major limiting factor for Mediterranean vegetation growth. Our knowledge on where and at what depth from the rocky soil and substrate water is extracted by vegetation is very limited. Traditional methods of determining soil water content and water

extraction by trees fail in rocky soils. New methods are therefore needed to obtain measurements on soil-water use at spatial scales relevant to tree growth.

4: How has climate variability influenced tree growth over the past 40 years, and which are the most influential variables and seasons?
The effect of year-to-year and season-to-season variability of precipitation and temperature on vegetation growth is reflected in tree rings. By relating climate records over the last four decennia to tree-ring properties we can determine how these climate variations influenced tree growth. Knowledge about the relation between temperature, precipitation and tree growth is important for constructing process models simulating vegetation development under changing climate conditions.

5: Can vegetation development in Mediterranean areas be accurately modelled for the next decades and what are probable projections of vegetation growth based on the anticipated climate change?
Given the most probable climate change scenarios for the Mediterranean region i.e. warmer and drier summers and warmer and wetter winters, can our process simulation models make reliable projections for the next five decennia of the Mediterranean vegetation development in the Peyne area.

1.2 Outline

The study presented in this thesis investigates growth and development of Mediterranean evergreen shrubs and forest vegetation with respect to climate and stand characteristics, and aims at contributing to mapping and modelling of the these vegetation types. The thesis consists of six chapters next to the introduction and the synthesis. Chapter 2 provides an extended background on Mediterranean landscape an ecosystem as well as on the expected changes in the Mediterranean climate. It also identifies gaps in our knowledge with respect to monitoring and modelling Mediterranean vegetation. Chapter 2 also contains a more thorough introduction of the study area where in each of the chapters only very short information is given on a need-to-know basis.

Chapter 3 aims at finding an optimal detection unit for remote sensing studies on Mediterranean vegetation. Apart from a fundamental contribution towards improving the abilities to obtain quantitative information from remote sensing images, it provides a basis for the work in chapter 4 as well as a method for creating continues maps of leaf area and biomass based on limited field data and remotely sensed images. Chapter 4 covers both spatial and temporal issues of vegetation functioning by presenting an analysis of seasonal changes in vegetation vigour on the most import geological landscape units in the study area.

Chapter 5 evaluates the possibilities of using electrical resistivity tomography as a novel technique to detect soil moisture abstraction in inaccessible substrates. Soil water availability and rooting depth are important for vegetation growth in Mediterranean landscapes because trees have to rely on soil moisture as their only water source during the dry summer season.

Chapter 6 has a temporal focus and analyses tree ring-records for climate signals in order to derive the most important climatic variables for tree growth. The patterns observed in the tree rings also provide an important basis for evaluating the performance of growth simulation models. In chapter 7 a vegetation-productivity model accumulates the knowledge from all previous chapters into a simulation exercise. The model performance is evaluated based simulations of forest growth in the past 60 years and comparison with tree-ring and field data. In the end the model is used to project future vegetation development based on climate scenarios for the end of this century.

2. Study area and geographical setting

2.1 The Mediterranean Landscape

The Mediterranean type landscapes are defined by their climate and are located between 30° and 45° latitude nearby oceans or seas. The Mediterranean climate is characterized by warm, dry summers and temperate, wet winters and is an intermediate between humid, temperate climates and warm, arid climates and therefore classified as sub-humid to semi-arid. According to the Köppen classification (Csa/Csb), precipitation in the dry summer months should be less than 30mm and maximum one third of the wettest month and average monthly winter temperatures are above 0°C. The largest region with a Mediterranean climate is the European and North-Afrikan Mediterranean Basin, but Mediterranean landscapes are also found in California, Chile, South Africa and Australia. The combined total area of Mediterranean landscapes in the world is about 2.76Mkm² (Joffre and Rambal, 2001).

The Mediterranean regions are widely recognized as being biodiversity hotspots (Gomez-Campo, 1985; Vogiatzakis et al., 2006; Medial and Quézel, 1999) with a species density surpassed only in tropical forests. While Mediterranean ecosystems occupy about 2.6% of the earth's land surface, circa 20% of the world's vascular plants can be found here with over 40% of the species being endemic. Although the genera and species in Mediterranean ecosystems are diverse, a striking similarity is visible in the plant functional types and growth habits (Di Castri et al., 1983; Raven et al., 1973 ; Mooney and Dunn, 1970). All Mediterranean ecosystems are dominated by broadleaved evergreen sclerophyllous species, which cover a broad range of vegetation communities from open types with herbs and shrubs, dense woodlands and forests. Most Mediterranean communities are only marginally productive with an annual Net Primary Production (NPP) ranging from 40 to 460g dry matter (DM) $m^{-2}y^{-1}$, the range of aboveground biomass is wide from below 0.5 to over 25kgDM m^{-2} (Rambal, 2001). In this chapter I discuss details about the Mediterranean region and its vegetation in general, and more specific about our study area 'Peyne' in southern France.

2.2 Field site: the Peyne catchment

The focus study area of this thesis is the 'Peyne' catchment in southern France (fig 2.1). The area is located at the foot of the 'Massif Central' and about 30km from the Mediterranean Sea. The Peyne is a 33km long stream and tributary to the Hérault river which ends in the Mediterranean see at Cap d'Agde. Center coordinates of the study area are 43°3'N; 3°2'E. The Peyne area has a Mediterranean sub-humid climate which is at the temperate end of the spectrum of Mediterranean type climates. The Peyne area is a long term study site of the remote sensing and land-degradation group of Utrecht University. Therefore data availability in the area is excellent both from field campaigns and earth observation by satellite and experimental airborne hyperspectral sensors. The site was selected as one of the research locations of the European Degradation Monitoring project (Hill, 1997) because it is representative for many

degradation problems typical to the Mediterranean climate. The location has stable cloudless weather in summer, which increases its potential for remote sensing studies. The high spatial variability in geological substrates, land-use and vegetation types allow the study of a wide range of circumstances within a relatively compact area.

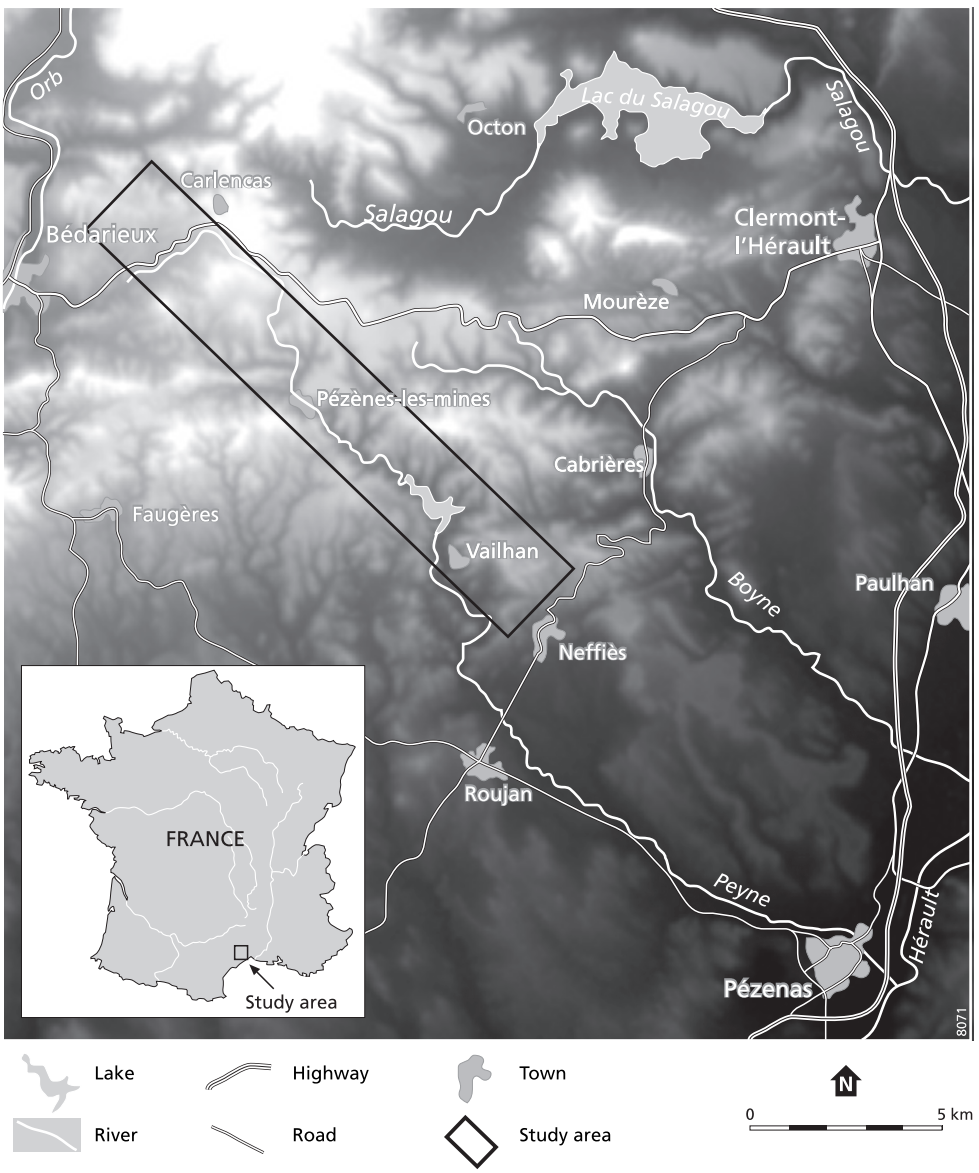

Figure 2.1: Generalized topographical map of the Peyne study area.

Climate

The Peyne area has a Mediterranean sub-humid climate (Köppen classification Csb) with warm dry summers and temperate humid winters. The mean annual temperature is around 14°C with monthly average summer temperatures between 20 to 27°C and monthly average winter temperatures between 2 and 10°C. Annual precipitation sums are extremely variable between 400 and 1200mm with a long-term average just below 800mm. Maximum precipitation falls in early spring and autumn. In summer there are long periods without any rain in which evaporation exceeds precipitation, resulting in water stress conditions for the vegetation and the Peyne River to run dry. The high precipitation in spring and autumn often falls in intense rain storms that can easily exceed 50mm within 24 hours. In autumn, vegetation productivity is at its minimum and the dry soils allow little water infiltration and are very prone to erosion. From south to north in the Peyne catchment there is a gradient of precipitation as a function of altitude (Bonfils, 1993). As a result, the high-elevation parts of the catchment receive higher volumes of precipitation than the lower parts. Precipitation from air rising against the higher Massif Central is the main cause of this pattern.

Vegetation types

The natural vegetation types in the study area range from sparse grasslands with some odorous herbs and *Cistus* species, to dense low forests that are dominated by evergreen species, mainly *Quercus ilex* and *Arbutus unedo*. The climax vegetation for the region is considered to be a mixed deciduous – evergreen oak forest with dense understory vegetation (Miller and Hajek, 1981). However, this vegetation type does usually not develop because centuries of human exploitation and land use have degraded many of the soils in the area. Furthermore, the better grounds in the area are currently all in use for agriculture, mainly vines. Many of the forests present in the area were cultivated as coppices in the past (Mather et al., 1999) which is still visible from the many stems sprouting from a common root system. This type of forests has a dense canopy and no understory vegetation. The types of vegetation occurring in the study area and their characteristics as Leaf Area Index (LAI), biomass and productivity show few changes in the past 60 years (Sluiter, 2005). This has a strong background in historical land use (e.g. forest\coppice vs. agriculture), but it also shows the limited potential for vegetation recovery that is linked to the geological substrates, water availability, soil degradation and slow seedling recruitment (Mouillot et al., 2005; Roda et al., 1999).

Landscape history

The Mediterranean area played a crucial role in the history of mankind, human habitation of the area had an important part in the landscape development. Agriculture and animal husbandry began before 10000BP in the eastern Mediterranean and around 8000BP in Greece and the western Mediterranean (Joffre and Rambal, 2001). The long-term disturbance and management of Mediterranean ecosystems resulted in widespread changes in the landscape like decreased forest cover and soil degradation, but also led to a more diversified landscape with a high biodiversity. Highest population densities and the most intense agriculture took place between 1830 and 1900. The development of the Peyne area between 1910 and 1960 was characterized mainly by land abandonment (Mather et al., 1999; Debussche et al., 1996). Most of the former agricultural lands on steep slopes and marginal soils were abandoned and are now covered with semi-natural vegetation. Recently abandoned fields still have little vegetation cover, and

transition towards a denser shrub or forest cover is very slow or may even never happen as a result of soil quality and past degradation. Some parts of the area have been forested for a long time and are managed as coppices for the production of charcoal or firewood. Even the densely forested areas were once used for agriculture as can still be seen in the abundant man-made terrace walls that are present on practically all slopes. These areas show that given enough time, it is possible for the forest to recover on abandoned agricultural fields.

The location of naturally vegetated areas in the landscape is almost entirely determined by negative agricultural selection (Sluiter and De Jong, 2007). This means that natural vegetation only grows in areas less favourable for agriculture. The unfavourable conditions for agriculture often stem from a combination of factors such as steepness, poor soils and water-holding capacity, large rocks or boulders, and high erosion risk. The vegetation type and variables such as LAI and biomass of the naturally vegetated areas is related to the time since abandonment, substrate quality, water availability, and disturbances such as wildfires, grazing or coppicing. From these factors, time since abandonment is very important because recruitment of trees and shrubs on abandoned agricultural fields is a very slow process, while once established, the evergreen forests are resilient against disturbance and quickly recover through resprouting (Mouillot et al., 2005).

Geology and Soils

The study site is situated at the southern border of the Massif Central and has a high variability in geological substrates (Alabouvette, 1982). In the formation of the Massif Central, tectonic activity deformed the geological formations in the area and pushed them to the sides. Formations that were originally on top of each other now surface side by side. The older formations are sedimentary sandstones, mudstones and limestones and are moderately metamorphic. On top of these substrates young volcanic tuffs and basalt outflows of Quaternary age are present. The basalts were originally formed in the valleys of the landscape, but because of their resistance to weathering and erosion they are now positioned as high plateaus which are intersected by lower v-shaped valleys. In some of the valley bottoms recent alluvial substrates are found, but they cover only small portions of the area.

Soil formation is slow in the Mediterranean climates, because heat and humidity occur during different seasons, and most soil forming processes require both. The steep slopes are also vulnerable to erosion when exposed to the violent rainfalls that are common during autumn. During past times, human habitation of the area caused widespread land degradation because the natural vegetation was removed in favor of agriculture. The soils currently present are shallow and classify as lithosols, regosols or luvisols (Driessen et al., 2001; Bonfils, 1993). Differences between the soil types in the area are mainly caused by the geological substrates and in most areas the water-holding capacity is very limited. The metamorphic substrates in the study area are highly fractured and all soils therefore have free drainage.

The warm and the humid season are out of phase in Mediterranean areas, limiting soil development and slowing down the mineralization process. Organic material in the soils breaks down slowly and nutrient release is therefore limited.

2.3 Vegetation adaptation: Evergreen & Sclerophyll

The typical Mediterranean climate and landscapes cause specific circumstances unfavourable for plant growth. Photosynthesis is limited by temperature during the winter, and by water availability during summer. Vegetation ha to be successfully adapted to both cold and drought. The widespread dominance of evergreen sclerophyllous trees and shrubs in Mediterranean areas shows that this plant functional type has an advantage above others (Aerts, 1995). It is also striking that in all Mediterranean areas around the globe, species from different genera have all developed to this same growth form.

Evergreen plants are found to have two important advantages: the ability to be productivity any time of the year when conditions are favorable, and higher nutrient-use efficiency (Aerts, 1995; Mooney and Dunn, 1970). Evergreen species retain their leaf area throughout the whole year and can therefore be productive very early in spring as soon as temperatures are high enough, and also very late in autumn when deciduous species already lost their leaves. This allows the evergreens to maintain enough annual productivity even when photosynthesis is stopped for an extended period during summer drought. The advantage of evergreens on nutrient efficiency is very important and has two reasons. The longer leaf lifespan reduces the leaf building costs because a leaf can be used longer. Longer leaf lifespan also limits litter production which is especially beneficial in areas where nutrients are slowly released from litter (Aerts, 1995).

The sclerorophyllous leaves of many Mediterranean species allow for a strong stomatal control on transpiration as a coping strategy for summer drought. During water shortage, the stomatal conductance is greatly reduced, specifically during periods of the day with high atmospheric demand (Baldocchi and Xu, 2007). During the dry season this limits water losses and permanent damage to the plants caused by drought. In addition to this strategy, Mediterranean species are also observed to withstand very high negative water potentials and still recover when the dry period ends (Hoff and Rambal, 2003).

The coping strategies do not only function at the leaf level, but also at the tree or stand level. Many tree species are known to have long tap roots to access water that is stored in deep soil layers, or as is the case in our study area trees having roots penetrating deeply into bedrock fractures that may retain some water. Although the deep rooting is well known, little quantitative information is available on the deep water abstraction by plants in rocky soils or fractured bedrock. At the stand or canopy level the leaf area is lower and tree cover is scarce in regions with lower water availability.

2.4 Climate and Ecosystem changes

Predicted Climate Change

The global climate is always changing by natural causes and currently also as an effect of the human-induced increased levels of atmospheric greenhouse gasses and their ongoing human emissions. Over the past century the global average temperature rose by approximately 1°C and the projected global temperature for the next century is between 2 and 3°C on top of

that (IPCC, 2007). In Mediterranean areas, climate changes as a consequence of this global warming may result in reduces water availability, decreased vegetation productivity and increased frequency of wildfires (UNEP, 2009).

Regional climate simulations for the Mediterranean basin based on the IPCC climate predictions for the next century indicate that the extreme character specific to the Mediterranean climate will further increase (Gao and Giorgi, 2008; Hertig and Jacobeit, 2008). Temperatures show an increase for the whole Mediterranean area for all months of the year in the period 2071–2100 compared to 1990–2019. For the Peyne area temperature rise will range between 2 and 5°C, with the largest change expected during the summers. Average yearly precipitation is not expected to change much, but the distribution of precipitation over the year will change towards wetter winters and longer dry periods during the summer. The combination of decreased summer precipitation and overall higher temperatures will increase water shortage over the whole Mediterranean area and may cause a substantial increase and northward extension of arid regimes (fig 2.2).

Ecosystem response

Vegetation types typical to the Mediterranean areas are highly adapted to Mediterranean climates, and many species such as Q. ilex occupy a wide range of climate and site conditions. The coping strategies of the broadleaf evergreen trees and shrubs enable these species to grow in the Mediterranean climate. Although higher temperatures and higher atmospheric CO2 concentrations may promote growth (Sabaté et al., 2002), increased aridity will lead to a decrease in productivity and leaf area (Limousin et al., 2009; Van der Tol et al., 2008; Reichstein et al., 2002). Besides a direct reduction in leaf area and productivity, climate change may also affect the resilience of the vegetation towards wood harvesting, grazing or wildfires. Decreased productivity will slow down vegetation recovery after removal or wildfires (Mouillot et al., 2005), while at the same time, wildfires are promoted by increased temperatures and aridity (Lavorel et al., 1998). Evaluation of a severe drought from flux measurements shows a strong effect of drought on ecosystem respiration, water use efficiency and gross assimilation indicating a high sensitivity of Mediterranean vegetation to climate change (Rechstein et al., 2003). The availability of deep soil water is found to be an important factor in the response of vegetation to climate change. In areas with deep groundwater, yearly rainfall sums and winter recharge have an important role in water availability, while in areas with shallow soils and no permanent groundwater table, vegetation depends entirely on precipitation during or just before the growing season.

Predicting the ecosystem response to future climate change is difficult, but also very important for policy makers and future generations (Scarrascia-Mugnozza et al., 2000). Dynamical models of ecosystem productivity may provide predictions of future vegetation growth given a climate-change scenario, and are therefore an important tool for impact assessment. Before a model can be used, however, it has to be thoroughly tested against the current vegetation state and the sensitivity of the growth to variability in the past and current climate.

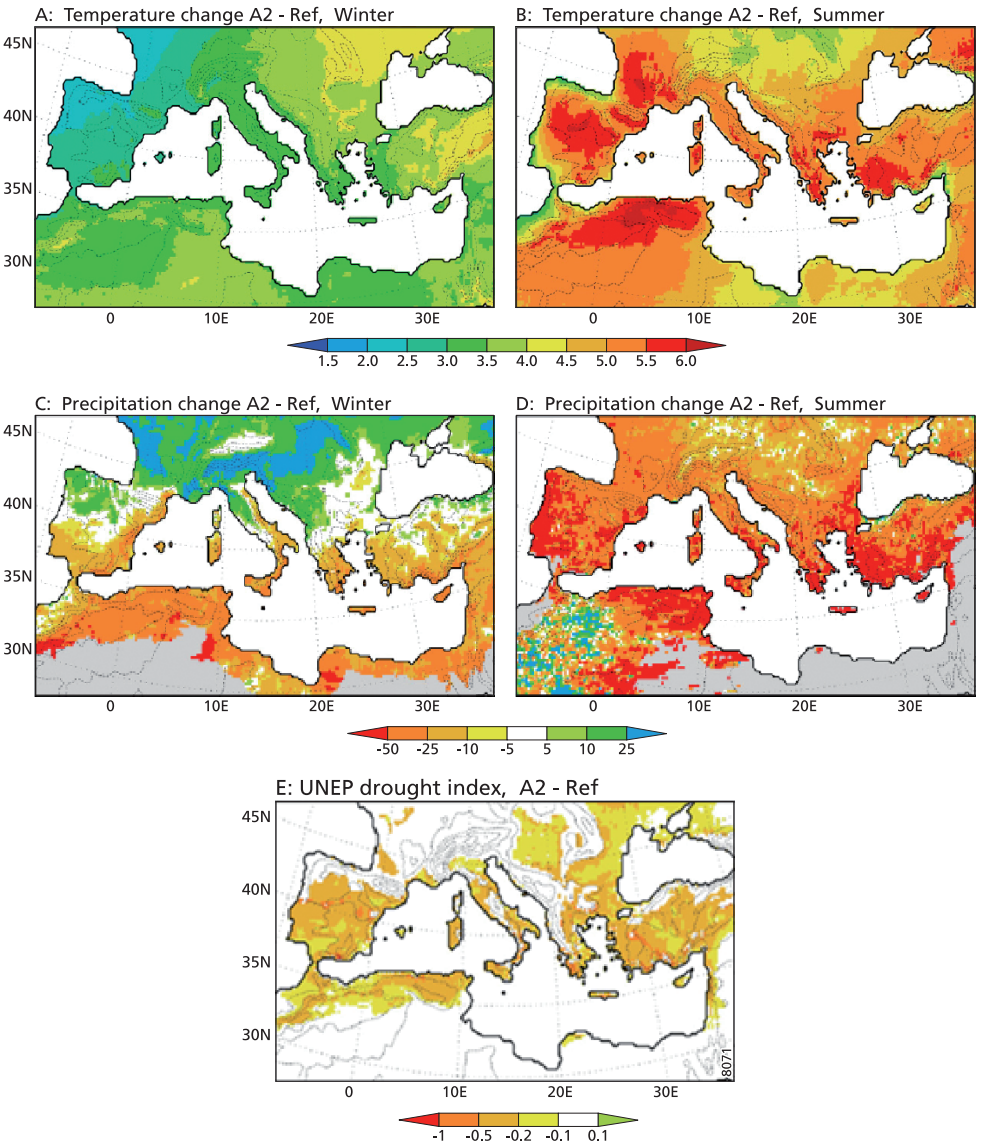

Figure 2.2: Predictions for Temperature, Precipitation and UNEP aridity index (P/PET) in 2070 in the Mediterranean basin. Based on the IPCC A2 climate change scenarios from Gao and Giorgi (2008).

2.5 Spatial and temporal scales

The starting point for the research in this thesis is the vegetation at a stand level. The characteristics of the individual trees or even leaves in the canopy are integrated over a unit ground area in the selected descriptors of the vegetation, LAI and aboveground biomass. On the large end of the scale domain, naturally vegetated areas are separated from other land-use areas, and changes in land cover such as the expansion of agricultural areas are not considered as part of this project. The variability of the natural landscape and its geological and hydrological characteristics within the natural areas are an important focus of the research, because the interaction between the abiotic factors in the landscape and the vegetation provides important information about the mechanisms behind the vegetation development. The constraint in the spatial scale does not exclude any effects from global processes such as climate change, or small-scale processes like leaf physiology; but these processes are just considered as they are currently known.

The base vegetation descriptors also have their corresponding temporal scales on which changes can be measured and analysed. The LAI of a forest or shrub land typically shows a clear seasonality and because the studied vegetation is evergreen the leaves remain on the trees for an average of 1,5 to 2 years. Biomass has a larger lifespan, as the wood mass in a forest accumulated over a period of decades to centuries and therefore may be considered the integral of the growth since the last logging, fire, or change in vegetation type. The temporal scale of this project has a focus on the seasonal to the decadal period. It uses the daily processes for simulating the mechanisms of vegetation growth and makes projection for the coming six decennia.

3. Optimizing spatial image support for quantitative mapping of natural vegetation

This chapter was published as: Wiebe Nijland, Elisabeth A. Addink, Steven M. de Jong, & Freek D. Van der Meer, (2009). Optimizing spatial image support for quantitative mapping of natural vegetation. Remote Sensing of Environment 113 (4), 771–780.

Abstract

High-spatial-resolution images allow us to assess the spatial structure and variability of natural vegetation characteristics. In order to optimize quantitative image analysis, we looked for the optimal spatial resolution to map natural vegetation in a Mediterranean environment. The optimal spatial resolution was then related to the spatial characteristics of the scene and the mapped parameters. Based on the relation between airborne hyperspectral imagery and a field dataset consisting of 227 measured plots of Leaf Area Index (LAI) and aboveground biomass, we found an optimal pixel size of 55 and 95m for the mapping of LAI and aboveground biomass, respectively. The optimal spatial resolution we found is determined by the spatial structure of the mapped parameters on the one hand, and by the effects of shading patterns and gaps in the canopy on the other. The spatial properties of scene elements influencing the optimal spatial resolution can be detected effectively using average local variance functions and variograms, provided that these are studied at a wide spatial range. The use of an optimally sized mapping unit instead of the original 5m pixels resulted in an improvement of mapping accuracy of 7 to 17 percent. It is therefore recommended that the image support used is considered carefully in all quantitative mapping projects based on remotely sensed imagery.

3.1 Introduction

Vegetation is an important factor in environmental processes, such as erosion, carbon storage, and climate change, and parameters such as leaf area index (LAI) and biomass are widely used in environmental modelling (e.g. Brolsma and Bierkens, 2007; De Jong and Jetten, 2007; Running and Coughlan, 1988). Remote sensing is recognized as offering the most suitable tool to obtain spatially continuous data sets on these parameters (Cohen and Goward, 2004; Lu, 2006). The specifications of the imagery used largely determine the accuracy of the parameter estimates. Spectral resolution is particularly critical (Schlerf et al., 2005), but spatial resolution may also have important implications.

The spatial resolution of hyperspectral sensors has developed to a point that it is possible to derive quantitative data on natural vegetation in fragmented, and hence heterogeneous landscapes typical of the Mediterranean (Addink et al., 2007; De Jong et al., 2003). The Hymap airborne sensor (HyVista, 2003) is capable of collecting hyperspectral imagery with a 5m ground

resolution. At this resolution, individual tree crowns can often be identified, depending on their size and spacing. The benefits of fine resolution images are obvious: spatially continuous information of vegetation characteristics can be derived directly at hill-slope, forest-stand or even smaller scales.

The possibility of identifying individual tree crowns in very high spatial and spectral resolution imagery raises questions regarding the best scale to map stand-scale vegetation parameters. Careful consideration of the spatial scale of mapping is important because, as stated in the Modifiable Area Unit Problem (MAUP) (Openshaw, 1984), the choice for the spatial unit affects the outcome of the analysis, implicating the existence of an optimal unit for quantitative analysis. The common approach of analysing remote-sensing images per pixel is a specific case of the MAUP, because pixels represent artificial sampling units ignoring the spatial patterns on the earth surface (Marceau and Hay, 1999; Fisher, 1997). The optimal pixel size is influenced by the spatial structure of the investigated objects and the conditions required by the used techniques, e.g. spectral classification, regression, texture analysis. The spatial character of the study object must therefore be defined before an optimal resolution can be chosen.

Several techniques are available to summarize patterns in spatial data, of which variograms (Atkinson and Tate, 2000; Atkinson and Curran, 1997; Woodcock et al., 1988 a,b) and Average Local Variance (ALV) functions (Bøcher and McCloy, 2006 a,b; Woodcock and Strahler, 1987) are most commonly used. Both variograms and ALV functions provide the analyst with an indication of the object size in the investigated area.

Objects and their spatial characteristics can be interpreted using scene resolution models introduced by Strahler et al. (1986). They define two scene models: the H-resolution scene characterized by scene-elements larger than the image pixels, and the L-resolution scene characterized by scene-elements smaller than the image pixels. In this paper, we define a special case of an H-resolution scene characterized by scene elements so much larger than the pixel size that the hierarchical sub-elements of the scene objects can be detected. In image analysis, the required scene model depends on the goal and the specific technique used. Hard spectral classification requires homogeneous pixels with respect to the class definition and thus an H-resolution scene. An L-resolution scene cannot be classified in a hard way but may be analyzed using spectral unmixing or fuzzy classification (Atkinson and Aplin, 2004; Woodcock and Strahler, 1987). In the third case, the pixels are so much finer than the investigated objects that the defined classes consist of multiple, spectrally different pixels. In this case, the defined classes are invalid and have to be adjusted and possibly aggregated into larger units based on the spatial arrangement and density of the subunits (Sluiter et al., 2004; Barnsley and Barr, 1996). The third case can also be solved by first aggrading the pixels to a coarser grid making the classes spectrally homogeneous and then by treating the new image as a regular H-resolution scene (McCloy and Bøcher, 2007; Ju et al., 2005; Marceau et al., 1994). In the case of mapping natural vegetation parameters, objects are difficult to define or even non-existent, since their values show gradual transitions rather than abrupt boundaries. The lack of object definition makes the selection of a corresponding optimal pixel size problematic, but it should be small enough to capture the variation of interest in the vegetation (Atkinson and Curran, 1997; Woodcock and Strahler, 1987).

Retrieval of biophysical vegetation parameters from remotely sensed image spectra is done using either empirically determined models, or physically based radiative transfer models. One of the problems of biophysical parameter retrieval from spectral information is the ill-posed nature of this problem (Combal et al., 2003). This means that the solution to this problem is non-unique and different model parameterisations may lead to identical spectra. Uncertainties in the reflectance measurements may not simply result in uncertainties on the solution, but produce a leap in the solution space. Instead of being spread around the true solution, the solution found may spread in the whole parameter space (Atzberger, 2004). Therefore, eliminating measurement errors before application of the model is important when dealing with ill-posed problems. Optimizing the spatial support size may lead to significant improvement of the model results. The use of linear empirical models does not lead to ill-posed problems, because the used functions are well-posed by definition. In general, radiative transfer models have the advantage of better portability, but at this moment properly trained empirical models give more accurate results.

In this study, we used empirical models. With this approach, field and image data were combined in the analysis, showing the collective optimum without the addition of extra uncertainty and parameterisation choices introduced by a radiative transfer approach. The approach used to find the optimal resolution is to determine it empirically by seeking the smallest prediction error from a series of analyses using different spatial resolutions. A prerequisite of this method is the availability of sufficient field observations to reliably determine the prediction accuracy. We used a field dataset of 227 plots of LAI and aboveground biomass, combined with airborne hyperspectral imagery.

The objective of this study was to determine the optimal scale to map aboveground biomass and LAI in a Mediterranean study area. We used field data and imagery, and described the spatial characteristics of both datasets quantitatively. We combined field and image data to obtain the optimal pixel size from the combined data sets. Finally, we explored the relation between the optimal pixel size and the spatial characteristics of our data. Based on the analysis of imagery at a wide scale range, we explained the relation between the studied vegetation parameters and the optimal pixel size using the hierarchical scene model.

3.2 Methods

Study area

The study area is part of the Peyne catchment, situated in the Languedoc-Roussillon region in Southern France. The region has a Mediterranean sub-humid climate with long dry summers and maximum precipitation in early spring and autumn. Three sub areas were selected in the Peyne catchment to get a good representation of the natural vegetation types in the region. The vegetation of the natural areas of the Peyne catchment is sclerophyll and consists mostly of evergreen shrubs and trees, heath species, odorous herbs and grasses. Mixed deciduous-evergreen oak forests with dense undergrowth are considered the climax vegetation in the area (Tomaselli, 1981). On marginal soils, this vegetation type usually does not develop. Depending on substrate and disturbance regime (grazing, fire), low herbaceous vegetation, dense shrublands or

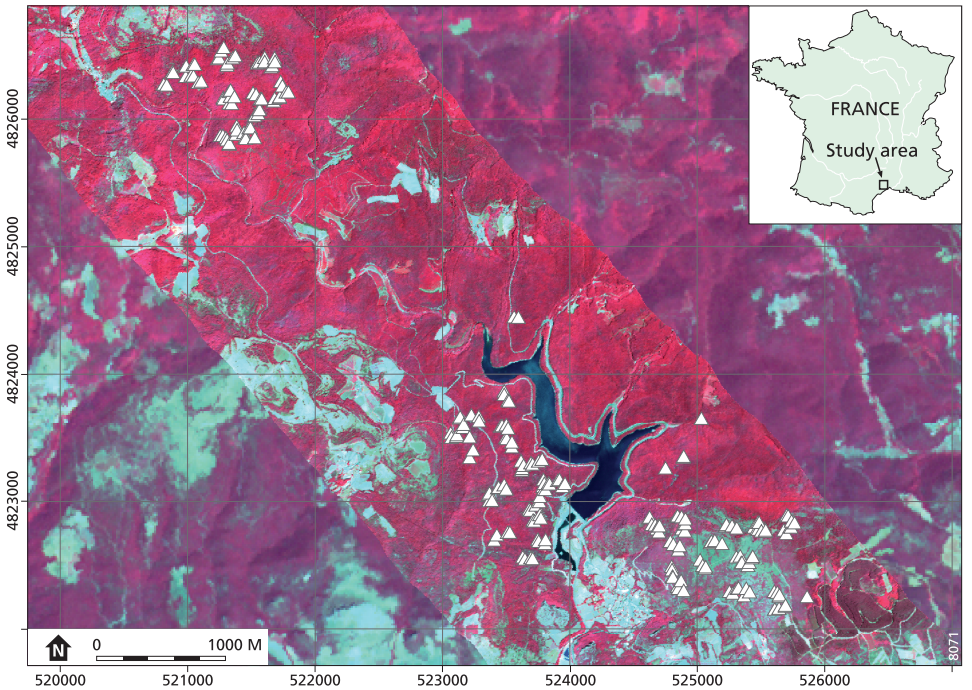

Figure 3.1: HyMap image (RGB = NIR (844nm), R (662nm), G(555nm)) projected on the ASTER image with field plot locations (Δ)

transitional types between these two occur (Sluiter and De Jong, 2007; Debussche et al., 1996). The three sub areas cover the full range of vegetation types in the region: 1) Well-developed mixed deciduous-evergreen oak forest, 2) Dense shrublands and low forest, and 3) Herbaceous vegetation and open shrubland (fig 3.1).

Field Data

Field data were collected in the late summer of 2005. The spatial distribution of sample plots was designed to get: 1) Representative coverage of the study area and its vegetation types, 2) Even representation of sample intervals with emphasis on the shorter distances to get accurate information on spatial variability in vegetation characteristics, 3) A random component in site selection in order to obtain a statistically unbiased representation of the measured parameters and their variability. The plots were located using a stratified-random-nested sampling scheme (Webster and Oliver, 2001). Within the three regions in the study area, the starting points of sample clusters were selected randomly. Each sample cluster consists of 8 points at 30, 60, 10, 90, 10, 60, 30m apart. From each plot, the next plot was selected at a fixed distance and a random direction (fig 3.2). The distances between the points are alternating shorter and longer to get an even distribution of points and lag distances over the area. Not all clusters are complete because of field logistics and weather; the total dataset consists of 227 plots (fig 3.1). At each field location, a detailed quantitative description of site and vegetation characteristics was made for a 5m square sample plot. LAI and aboveground biomass were used as the primary

vegetation descriptors. LAI is defined as the one sided leaf area per unit ground area (Watson, 1947). LAI was determined using a digital camera with a 180° fisheye lens and the Can-Eye software package for processing of the photographs (Jonckheere et al., 2004; Weiss et al., 2004). Can-Eye uses the gap fraction distribution to determine the LAI and corrects for leaf clumping. Jonckheere et al. (2004) concluded that the hemispherical photographs and LICOR-2000 yield consistent results for effective-LAI estimation, in addition Can-Eye calculates true LAI using a clumping correction factor. The photographs were taken up from the ground level to account for all the trees and the shrubs in the plots, grass understory is not present in the studied vegetation types. The aboveground biomass was estimated using allometric relations between stem diameter and biomass. Allometric relations for trees were available for *Arbutus unedo* and *Quercus ilex* (table 3.1) (Ogaya et al., 2003). The remaining tree species were subjected to either of the two relations, based on morphological similarity to either *A. unedo* or *Q. ilex*. Ogaya et al (2003) report the allometric relations to be highly significant and effective (*A. unedo* r^2: 0.99, $p < 0.0001$; *Q. ilex* r^2: 0.98, $p < 0.0001$). For shrub species a generic formula for Mediterranean shrubs was used based on the maximum diameter and height per individual (Pereira et al., 1994). The biomass values of all individuals were summed per plot and recalculated to Mg/ha. The field data were collected two years after the image data take, but in the same season. We expect that the data are representative. The studied vegetation is evergreen and develops slowly, therefore changes in biomass should be low, although LAI may show more change during and in between years. The spatial structure of the vegetation is not observed to show any significant changes either seasonally and annually. Weather conditions were similar for the two years, with just above average summer temperatures and below average summer (May – August) precipitation (2003: 97mm, 2005: 105mm, average: 137mm) (Meteo-France, 2008).

Imagery

The main image source in this study was a HyMap image acquired in July 2003 with a ground instantaneous field of view (GIFOV) of 5*5m. The HyMap sensor has 126 contiguous spectral bands in a spectral range from 0.45 to 2.48µm (HyVista, 2003). Band 1 and band 126 were excluded from the analyses because of their high noise content. The Hymap images were geocorrected and converted to surface reflectance at the German aerospace centre (DLR) using the PARGE software (Schläpfer and Richter, 2002) using a 25m DEM and ATCOR4 software using a standard atmosphere (Richter and Schläpfer, 2002).

Table 3.1: Allometric relations used in aboveground biomass calculations

Species	Formula	Source
Arbutus unedo	$\ln AB = 4.251 + 2.463 * \ln D50$	Ogaya et al., 2003
Quercus ilex	$\ln AB = 4.900 + 2.277 * \ln D50$	Ogaya et al., 2003
Shrubs (stem Ø < 3cm)	$AB = 642.0 * H^{0.0075} * Dmax^{2.4901}$	Pereira et al., 1994

AB : Aboveground biomass indvidual [g]

D : Diameter (D50: Stem diameter at 50cm [cm], Dmax : maximum projected shrub diameter [m])

H : Height [m]

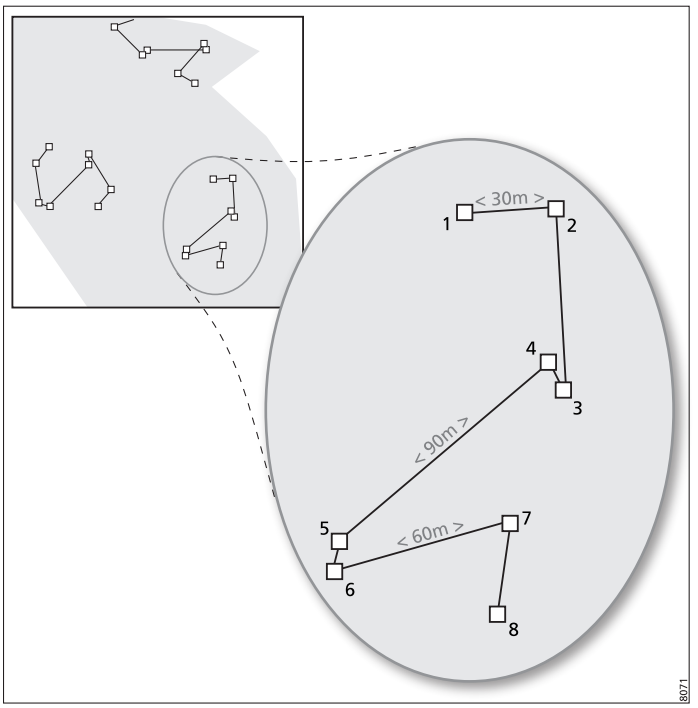

Figure 3.2: Example of the stratified-nested-random sampling pattern used for the collection of field data.

To extend the possible spatial range of the average local variance (ALV) functions, colour infrared (CIR) photographs and an ASTER image were added to the analysis. The CIR aerial photographs were taken in 1996, contain three spectral bands: green, red and near infrared and have a 70cm pixel size. The Advanced Spaceborne Thermal Emission and Reflection Radiometer (ASTER, 2005) scene was acquired in 2005 and only the visual and near infrared bands with a GIFOV of 15m were used. For all images the Normalized Difference Vegetation Index (NDVI) was calculated (Tucker, 1979). The NDVI of the HyMap image was calculated using the bands centred at 646nm for red and 844nm for near infrared.

The HyMap image was used because it was the most useful available image both spatially and spectrally. To produce the best regression results, we used all hymap wavelengths in the regression analysis. The spatial analyses were done using only the red reflectance and the NDVI, because the spatial techniques are not suitable for multispectral information.

The variogram

Variogram analysis is a common way to describe spatial properties of geographically distributed data, and has been widely applied within remote sensing studies (Atkinson and Aplin, 2004; Gamon et al., 1993; Cohen et al., 1990). The variogram summarizes the spatial dependency of

the data and is calculated as half the average squared distance between the paired data values (Isaaks and Srivastava, 1989) following equation 3.1:

$$\gamma(h) = \frac{1}{2m(h)} \sum_{i=1}^{m(h)} (x_i - x_{i+h})^2 \qquad \text{Equation 3.1}$$

where $\gamma(h)$ = the semivariance at lag distance h, $m(h)$ = the number of data pairs at distance h, and xi = the value of a data point, $xi+h$ = value of a point at distance h from i.

After calculation of the experimental variogram from the data, a mathematical model is fit through the points. Each variogram model can be described by two values, the sill and the range. The sill corresponds to the overall variance in the dataset, while the range is the maximum distance of spatial autocorrelation (Webster and Oliver, 2001; Curran, 1988). Often the function is offset from the origin to account for non-spatial errors like measurement uncertainties – this is called the nugget. The fitted variogram models were used to describe the spatial structure in the vegetation data and the HyMap imagery. A combined spherical and nugget variogram-model was fit to each of the variograms. The spherical model is the most commonly used model for experimental data (Webster and Oliver, 2001). Variograms of LAI, biomass and NDVI were made for all plots in each sub-area and for all plots together. Since the plots were situated only in vegetated locations, these variograms only summarize vegetated plots. Variograms of the NDVI were also made for all pixels in the individual sub areas and the three areas combined. These variograms also include non-vegetation pixels. Directional variograms were studied briefly, but no pronounced directionality was found.

The average local variance function

The Average Local Variance (ALV) function is a graph of the local variance in an image as a function of the pixel size of the image (Woodcock and Strahler, 1987). The ALV functions are calculated from an image in three steps: 1) Creating a series of images with increasing pixel size by linear averaging of the original pixels. 2) Calculating local variance images using a 3*3 pixel moving window. 3) Plotting the average local variance of the image against the degraded pixel size. To normalize the ALV functions between the three image sources, the ALV is presented as fraction of the global variance of that image. The concept behind the ALV function is that it shows a peak of maximal variance at a spatial resolution that is closely related to the dominant size of pattern elements in the image (Bøcher and McCloy 2006 a,b).

Woodcock and Strahler (1987) calculated the average local variance for a series of images with different resolutions and objects and found that the ALV function peaked at half or three quarter of the object size in the image. Bøcher and McCloy (2006 a,b) found the same peak based on synthetic images. The ALV functions were used to describe the local variability of the images in order to determine its source and to explain the effect of the different scene components on parameterisation accuracy and the optimal pixel size.

Regression

A regression model was fit between the field data and the spectral data for an image series with increasing spatial support size, to find the optimum resolution for determining biomass and LAI from hyperspectral imagery. Aboveground biomass values were log-transformed to correct for their strong non-normal distribution that does not meet the assumptions of our statistical analysis. The support of the reflectance data was increased by linear averaging of the reflectance of the pixels in a square window around the field plot location. The regression models were fit for all data and for the three areas apart. For the regression on the three separate areas only the odd numbered HyMap bands were used to make the number of variables lower than the number of observations. A common problem with fitting a regression model to hyperspectral images is the large correlation between spectral bands (multicollinearity). Partial least squares (PLS), principal component, lasso, and ridge regression are all linear methods that reduce the problem of multicollinearity (Hastie et al., 2001).

We used 'ridge regression' (Tichonov and Arsennin, 1977), because it does not discard any of the variables but stabilizes the result by penalizing the size of the coefficients (Equation 3.2) while fitting the model to all variables. Ridge regression minimizes the following criterion:

$$RSS(s) = \sum_{i=1}^{n} (y_i - \hat{y}_i)^2 + s \cdot \sum_{j=1}^{p} \beta_j^{\,2} \qquad \text{Equation 3.2}$$

where RSS = Residual Sum of Squares, s = shrinkage parameter, i = observation, n = number of observations, y = observed value, $\hat{y}$ = predicted value, j = predictor, p = number of predictors, β = regression coefficient.

In the formula, s is the ridge parameter that controls the amount of shrinkage that is applied to the coefficients. The optimal value of s was determined using a ten-fold cross validation, because an n-fold (leave-one-out) cross validation in some cases led to the selection of an over-fit linear model with too little shrinkage, which is an unstable solution. The regression analysis on the data was conducted using the R software (R-Team, 2006).

The variograms and ALV functions provide information on the spatial elements composing the scene and their representation in the used imagery. We compared the spatial scene elements to the optimal support size to map LAI and aboveground-biomass as shown by the regression root-mean-squared error. With the HyMap spectra resampled to the optimal spatial support using a moving linear average, we calculated maps of both LAI and biomass for the entire study area.

3.3 Results

Field data

The measured values for biomass and LAI (table 3.2) are similar to those of comparable areas in Spain and France (De Jong et al., 2003; Ibàñez et al., 1999; Pereira et al., 1994). The vegetation parameters and their variability differed between the three areas, with the highest values for LAI and biomass in the mixed forests and the lowest values in the mixed herb and shrublands. The dense shrublands have considerably less variability than the other two areas. The overall correlation between LAI and log-biomass was 0.44.

Variograms

Variograms of all plots and areas are shown in figure 3.3. The variogram models for the separate areas are summarized in table 3.3. The ranges of the variograms are larger for log-biomass than for LAI in all areas, meaning that the distance of spatial correlation is larger for biomass than for LAI. The variogram for the NDVI of the whole areas is significantly different from the other variograms which were calculated for the plots only. The difference in range can be explained by the effect of scene elements other than natural vegetation (roads, water bodies, vineyards) on the variogram. These elements were excluded from the sampling scheme and are thus not represented in the variograms of the plot locations only.

Table 3.2: Summary of the collected field data

	All		1: forest		2: dense shrub		3: herbs & shrub	
	mean	σ	mean	σ	mean	σ	mean	σ
Vegetation Height [m]	5.8	4.6	10.1	5.1	5	1.6	2.4	1.7
Vegetation Cover [%]	74%	13%	78%	9%	70%	13%	76%	15%
LAI [$m^2\ m^{-2}$]	3.17	0.8	3.51	0.6	3.3	0.4	2.7	1.1
Above.gr.Biomass [Mg ha^{-1}]	80.73	77.8	142.91	91.4	89.57	43.6	23.14	39.7
log-Biomass	1.53	0.76	2.05	0.35	1.88	0.28	0.79	0.72
Number of plots	227		67		76		84	

Table 3.3: Summary of the variogram models for the three sub-areas and all data

	LAI		log Biomass		NDVI plot loc.		NDVI all	
	sill	range	sill	range	sill	range	sill	range
All	1.02	475	2.22	750	0.014	630	0.0113	270
1: Forest	0.4	150	0.67	175	0.0009	530	0.002	130
2: Dense shrub	0.9	300	0.38	425	0.0052	480	0.0057	250
3: Herb & shrub	2.15	360	4.15	650	0.027	530	0.024	310

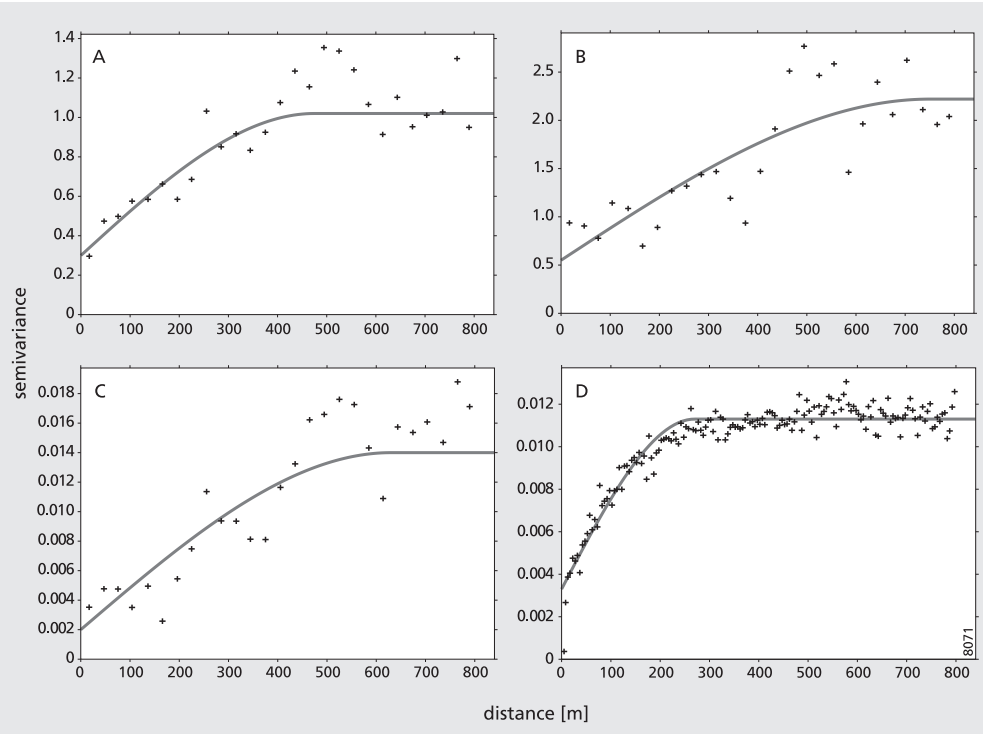

Figure 3.3: Variograms for all plots for A: LAI, B: log-Biomass, C: Hymap NDVI at plot locations, D: Hymap NDVI of whole area. A-C have a bin size of 30m; D has a bin size of 5m.

Average local variance functions

ALV-functions were made of the aerial photographs, the HyMap and the ASTER image, using the near-infrared band (HyMap ~ 844nm) and the NDVI (fig 3.4). The ALV functions are normalised between the different images displaying the local variance as a fraction of the global variance of the used image area. The left figure is based on all three areas with vegetation plots; the right figure is based on the whole extent of the ASTER image as shown in figure 3.1. The three images are used because the domain of an ALV function is limited by the pixel size and the extent of the used image. The width of the HyMap image is only 2.5km, which would limit the ALV domain too strongly. Two peaks of local variance are visible in the ALV functions, at 3.5m and 100m pixel size, indicated by the arrows in figure 3.3. According to Woodcock and Strahler (1987) and Bøcher and McCloy (2006 a,b) this means that the pattern elements in the images have a size of approximately 7m and 200m (2*peak resolution). The 3.5m peak is only slightly visible in the HyMap ALV function because the original pixel size of 5m is larger than this peak. The NDVI-based ALV functions are less pronounced than the NIR-based function. This is mainly due to the normalisation of brightness in the NDVI, which decreases the variability.

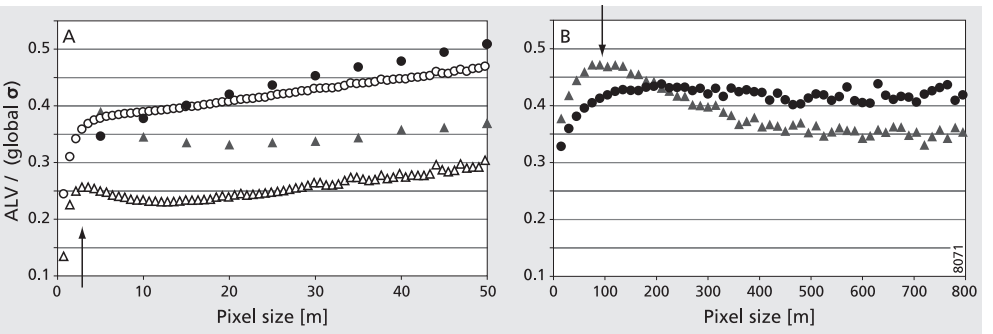

Figure 3.4: ALV functions normalised to global standard deviation of the study areas for A: CIR aerial photographs (△: NIR, ○: NDVI) and Hymap (▲: NIR, ●: NDVI) , and B: ASTER (▲: NIR, ●: NDVI)

As illustrated in figures 3.5a to 3.5d the ALV peaks can be related to the scene objects in the imagery, based on their size and local variance images. The 3.5m peak in the aerial photographs is caused by the canopy and vegetation structure (fig 3.5a, 3.5c): illumination differences and gaps in the canopy cause variability of the reflectance. The 100m peak in the ASTER image is related to the boundaries between natural vegetation and other scene elements, such as lakes, agricultural areas and built-up areas (fig 3.5b, 3.5d). The brightness differences in the images are an important source of local variability. This is illustrated by the ALV functions based on NDVI, since the NDVI normalises the brightness (Lillesand and Kiefer, 2004) and the peaks are thus reduced.

Regression

The cross-validation root-mean-squared error (RMSE) of a linear regression between HyMap spectra and field measured LAI and biomass were used as a direct measure of prediction accuracy. The regression models were fit between field data and a series of HyMap reflectance data with an increasing spatial support. Ridge regression was used to fit the models, because it overcomes the problems of multicollinearity in the Hymap data. In figure 3.6, the cross-validation RMSE are normalised to the RMSE of the original pixels and plotted against the size of the averaging window used in the Hymap image. The regression RMSE of LAI and log-biomass of all plots show a minimum at 55m and 95m respectively. The use of an optimally sized window results in an error reduction of 7 percent for LAI and 17 percent for log-biomass. The optimal support sizes for the three regions within the study area are variable, but show a close relation to the variogram ranges of the regions (Table 3.3). The optimal support size is between 1/6th and 1/10th of the variogram range. Scatterplots of observed and predicted values of LAI and biomass made for the selected optimal models for all plots (fig 3.7) show good model fits with some saturation at higher LAI values. The improvement of the model with optimal resolution compared to the original pixel size is significant for log-biomass and notable but not significant for LAI (biomass: $p < 0.001$, LAI: $p \approx 0.2$, single-sided students t-test). Consequently, maps with the biomass and LAI distributions were calculated from the HyMap image based on the regression models with the lowest RMSE for the complete dataset and image data resampled to the corresponding support size using a standard moving linear

filter of 55m for LAI and 95m for aboveground-biomass (fig 3.8). Note that the spatial support of the pixels changed while the number of pixels remained the same, producing a fine-scale map of the vegetation parameters. The vegetation patterns in the study area are clearly visible in the calculated maps.

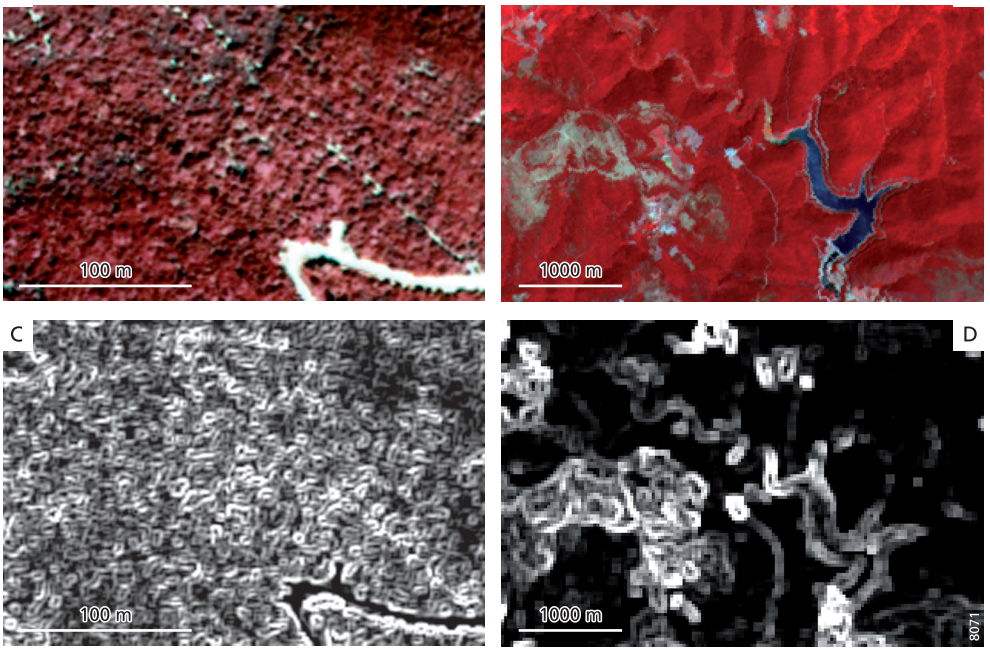

Figure 3.5: Original (A-B) and local variance images (C-D) of CIR aerial photographs (A) showing canopy structures and illumination patterns (C), and ASTER (B) showing Landuse boundaries and roads (D)

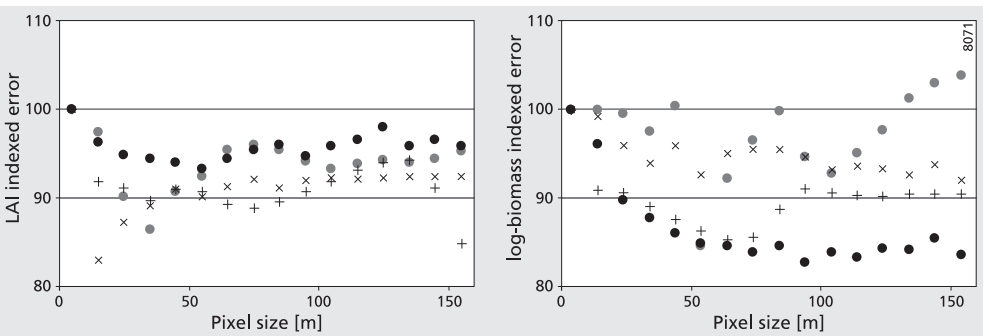

Figure 3.6: Indexed (original pixel RMSE = 100) prediction Root Mean Squared Error for LAI (left) and aboveground biomass (right) at different image support sizes. ●: All plots, × : Forest, ●: Dense shrub, +: Herb & shrub.

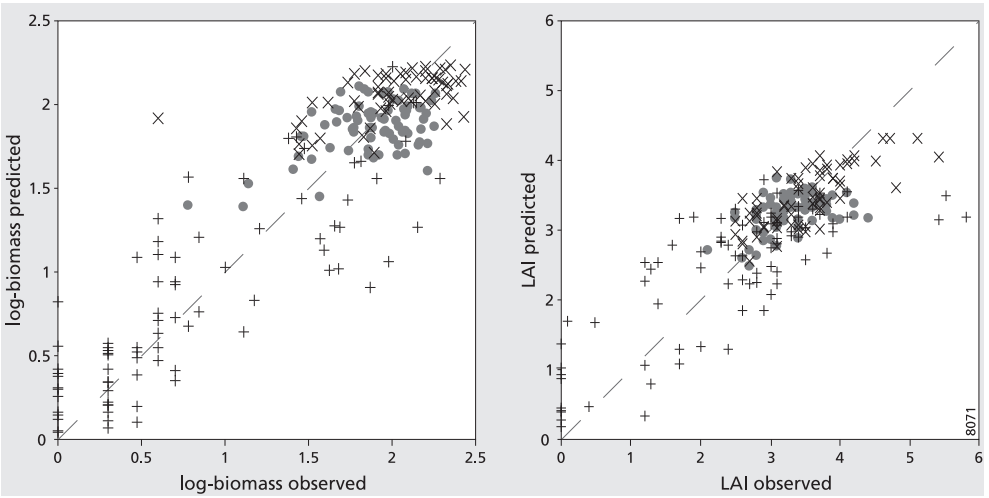

Figure 3.7: Scatterplots of observed vs. predicted values for LAI (left) and biomass (right) for plot covered with × : Forest, ●: Dense shrub, +: Herb & shrub. With dashed 1:1 line.

3.4 Discussion

This study investigated the effect of spatial scale on the quantitative mapping of vegetation parameters using hyperspectral images. We show a 7 to 17 percent reduction of prediction errors when a larger, optimally sized, window is used instead of the original pixels of 5m. The optimum window sizes lie between the two peaks in the ALV functions, and are between 1/6th and 1/10th of the sample-variogram ranges. The difference in optimal spatial resolution for LAI and biomass is closely related to the spatial structure and variability in both variables that shows in the sample variogram ranges. The mechanisms acting on this spatial structure are not completely understood, but a possible explanation is that historical factors such as land abandonment, wildfires and logging affect aboveground-biomass more than LAI. While LAI needs only a few years to reach a pre-disturbed state, aboveground-biomass requires decades.

Averaging the image spectra in a window centred on the field locations differs from using a larger original pixel. When combining field and image data the spatial registration of both datasets influences the optimal window: the location accuracy is ≈10m for the field plots and ≈1 pixel (5m) for the imagery. Linear averaging the pixel values over a window centred on the plot location decreases spatial registration errors, sensor noise, and removes part of the centre-bias produced by the sensor point spread function. Resampling an originally high-resolution image is therefore preferred over the use of coarse resolution imagery.

Using the hierarchi cal scene concept three scene components need to be considered when looking for the optimal spatial support:
1) The sub-elements composing the vegetation: individual trees and shrubs.

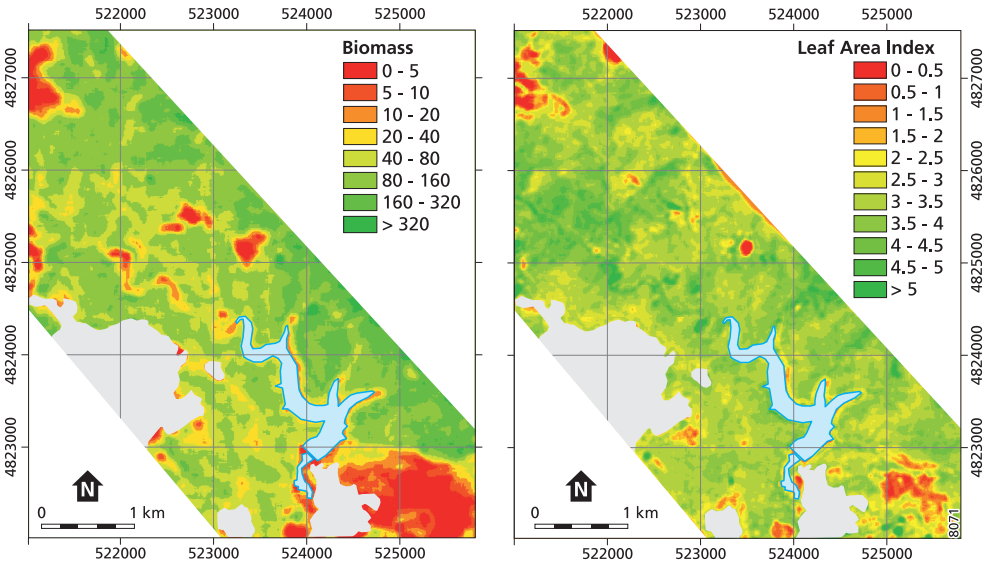

Figure 3.8: Biomass (left) and LAI (right) calculated from HyMap spectra using the regression equations with the least RMSE. Support size 95m for biomass and 55m for LAI.

2) The variability and spatial structure of the mapped parameters, LAI and biomass.
3) Other scene elements neighbouring or intersecting the study area, such as roads, water bodies and vineyards.

When using the scene components to find the optimal pixel size for analysis, the scene components have to be considered from a sensor viewpoint. Then the visual sub-elements composing the vegetation are parts of the canopy with different illumination conditions and gaps, while from a vegetation viewpoint the sub-elements would be the individual trees. The optimal pixel size of 55m and 95m we found for hyperspectral mapping of LAI and Biomass in a fragmented Mediterranean landscape is such that:

1) Scene sub-elements linked to canopy structure are blended within the pixel.
2) Effects of spatial mismatching between field and image data are minimized.
3) The spatial structure of the mapped parameter is well represented by the map.
4) Pixels are sufficiently small to separate the studied vegetation from other land cover units. This is especially important in complex scenes.

Known research on optimizing the spatial units for analysis focuses either on finding a maximum unit based on the demand of resolving certain objects (Atkinson and Aplin, 2004; Atkinson and Curran, 1997; Woodcock and Strahler, 1987) or on finding a minimum unit that solves interference problems with scene sub-elements (McCloy and Bøcher, 2007; Marceau et al., 1994). In this study, we analysed a broad spatial range to find an optimal unit that is constrained on both sides. The optimal support for any analysis is always the product of the studied object, the research goal and the chosen analysis method. The findings in our study are based on the quantitative spectral analysis of Mediterranean vegetation stands, requiring spatial

averaging of the spectra to decrease regression error. A study of He et al. (2006) about analysis of mixed grassland ecosystems using spectral indices also found that increasing the image support size improved mapping accuracy. For their ecosystem the optimal size to map LAI was found to be around 35m. High-resolution spatial patterns may also be used as a source of information towards stand characteristics (Cohen et al., 1990), or the spatial vegetation patterns may be the objective of the study itself (Rahman et al., 2003).

The optimal pixel sizes we found for our study area are specific for this area and are likely to differ for other areas or vegetation types. However, it should be noted that optimal pixel sizes exist. Vegetation parameters can be better estimated from spatially optimized remote sensing imagery then from the original pixels.

We used a regular square window to increase the support of the imagery and to investigate the optimal support for quantitative vegetation mapping. This rather crude method does not account for natural patterns. The use of image-based segmentation, as applied in Addink et al. (2007) makes it possible to optimize both the shape and size of the prediction units. The optimal size of segments will be close to the size found in this study or somewhat larger because the variable shape of the segments will eliminate the effects of mixing at the edges of scene elements. The downside of using segmentation is that it requires a much smaller original pixel size than the per-pixel approach.

3.5 Conclusions

Remote sensing offers the most suitable tool to obtain spatially continuous datasets on vegetation parameters for environmental monitoring and modelling. With the availability of hyperspectral sensors capable of resolving individual trees, it has become increasingly important to consider the spatial scale of the mapping process. In this study, we found an improvement in mapping accuracy of 7 to 17 percent for LAI and aboveground biomass, when an optimally sized prediction unit was used, instead of the original 5m pixel. The optimal resolution depends on the spatial character of the mapped parameter and is 55m for LAI and 95m for biomass in our Mediterranean study area.

ALV functions and variograms are useful aids in determining the optimal resolution. ALV functions are used to detect the size of scene pattern elements, while variograms provide information on parameter variability. Especially in situations with continuous variables as often in natural vegetation, it is necessary to assess the spatial structure of the studied scene, because it is difficult to determine object sizes beforehand. The hierarchical scene concept provides a framework to finding the optimal resolution for a mapping problem, provided that the scene elements are studied at a sufficiently wide spatial range. When relying on spectral information in the mapping process the pixel size should be such that:

1) Spectrally different scene sub-elements are averaged within the pixel to create a homogeneous spectrum at the studied scene scale.
2) The spatial variability of the mapped parameter is preserved through observation and mapping.

3) Neighbouring or intersecting scene elements are well separable from the study area.
The relative importance of the scene components will be different for each scene, depending on their size and spectral variability.

We recommend experimental determination of the optimal pixel size for all mapping studies, because it is more precise than any other method. However, in many cases this will be difficult because it requires extensive field data. In that case, the spatial unit for the analysis can be selected based on the hierarchical scene concept and the guidelines presented in this study. Whatever method is used, it is important to be aware of the effects of the spatial resolution on the mapping results, and to carefully consider the pixel size in every remote-sensing based mapping project.

Acknowledgments

The authors are grateful to Prof. Dr. E.J. Pebesma for his help with the spatial statistics for this paper. Rogier de Jong and Paul Hiemstra are acknowledged for their company and help during the field-data collection.

4. Detection of ecosystem functioning using object-based time-series analysis

This Chapter was published as: Wiebe Nijland, Elisabeth A. Addink, Steven M. de Jong, & Freek D. van der Meer, (2010). Detection of ecosystem functioning using object-based time-series analysis. In: Addink, E.A. and F.M.B. Van Coillie (Eds). GEOBIA 2010-Geographic Object-Based Image Analysis. Ghent University, Ghent, Belgium, 29 June – 2 July. ISPRS Vol.No. XXXVIII-4/C7

Abstract

Accurate detection of tree growth and ecosystem functioning in naturally vegetated areas is of interest to many applications, such as ecological and land degradation modelling, wildfire risk monitoring, carbon budgeting, and climate science. However, the changes are often small when compared to normal spatial and seasonal variability, or occur gradually in time. We use object-based image analysis (OBIA) for time-series analysis of vegetation functioning because objects coincide better with ecological units in the field than pixels. For this study, we combine 12 ASTER images recorded between 2002 and 2008 with information from 75 field sites that were visited multiple times to provide field reference. A single segmentation of multi-temporal data is used to align all available data to a single object framework. The images are recorded before, during, and after the dry summer season, and thus show the effect of summer drought on the vegetation in our study area. The object-based method of creating time series from imagery allows for a reliable detection of small changes in NDVI and TIR. Using this approach, we show a differentiation in vegetation response to drought that can be related to the underlying lithological substrate and its water holding capacity. The presented method is especially valuable in fragmented landscapes which are common to areas in the Mediterranean basin.

4.1 Introduction

Changes in vegetation functioning are of great interest to many applications, such as ecological and land degradation modelling (Hoff and Rambal, 2003; Chiesi et al., 2002), wildfire risk monitoring (Maselli et al., 2000), carbon cycling (Pastor and Post, 1986), and climate science (Walther et al., 2002). In this study we consider vegetation parameters at a canopy or ecosystem level, such as aboveground biomass, Leaf Area Index (LAI), light use and transpiration. These parameters represent vegetation functioning at different timescales: Biomass accumulates the growth over several decades; LAI changes at seasonal or yearly basis (Chason et al., 1991); while transpiration and light use have considerable variations depending on weather conditions and even the time of day (Gratani and Varone, 2004; Sala and Tenhunen, 1996).

Earth observation is a valuable tool for the monitoring of vegetation functioning and is the only feasible method to obtain spatially continuous data over large areas at regular intervals (Cohen and Goward, 2004). In the Peyne study area in Mediterranean France, we use earth observation to obtain detailed information on vegetation functioning on seasonal to yearly time scales to study the interaction of vegetation with the climate and landscape. The availability of multiple images acquired between 2002 and 2008 allows us to combine spatial, spectral, and temporal information in our analyses.

The changes of vegetation parameters due to stress or due to growth are often small when compared to the cyclic variations that occur at seasonal or daily timescales (Xiao et al., 2004; Richard and Poccard, 1998). We use object-based image analysis (OBIA) for time-series analysis because objects better represent the ecological units in the field than pixels. The subtle changes in vegetation parameters are difficult to identify using traditional pixel based image analysis, because the pixel grid is an artificial regularization that is different for each image and therefore introduces additional unwanted variations to the data (Fisher, 1997). Therefore we use image segmentation to create a stationary object framework for our images to improve coupling between field and image data and to decrease the unwanted effects of pixel regularization and georectification errors.

For this study, we combine 12 images from the Advanced Spaceborne Thermal Emission and Reflectance radiometer (ASTER) (Yamaguchi et al., 1998) with information from 75 field sites that were visited multiple times to provide a field reference. At the field sites we measured aboveground biomass and LAI as principal vegetation parameters. LAI was measured both at the onset and near the end of the dry summer period in 2008, to record changes in leaf area. From the imagery we use NDVI as principal parameter, because of its relation to leaf area and light use (Tucker, 1979; Fensholt et al., 2004). As a second parameter we use thermal brightness, which is related to the surface energy balance and transpiration.

Within the extent of our study area in Mediterranean France, the natural vegetation cover is differentiated mainly by the variability in geological substrates. The focus of this paper is therefore on the relation between vegetation functioning and the geology at seasonal and inter annual timescales. The field sites were distributed over five common substrates which are used to stratify the data for further analyses. In this paper we aim at gaining new insights in Mediterranean vegetation functioning and its relation with the geological substrates. We use the temporal patterns in LAI, NDVI, and thermal brightness as key parameters on vegetation functioning. The application of OBIA is an important factor in this process, because it allows detection of small changes in thermal radiance and NDVI, and provides a reliable coupling between field and image data.

4.2 Methods

Study Area

The study area is part of the Peyne catchment, situated in Mediterranean France. The region has a Mediterranean sub-humid climate with annual average precipitation of 800–1000 mm

and a dry summer season. The catchment is situated at the edge of the 'Montagne Noir' and is characterized by a high spatial variation of bedrock material because the formations were tilted and heavily deformed during the Hercynian orogenesis (Alabouvette, 1982). Common types of bedrock are limestone, basalt, flysch, calcareous sandstone, and dolomite. Soils in the area are shallow and are poorly developed with often only an AC or AR profile. Soil characteristics are differentiated mainly upon the nature of the geological substrate (Bonfils, 1993).

Part of the study area is used for agriculture, mostly vineyards and pasture. The steep hills, remote areas, and poorest soils are covered with (semi)natural vegetation ranging between low (< 0.5m) herbs and shrub, and moderate (< 10m) evergreen forests. The dominant tree and shrub species are *Quercus ilex*, *Arbutus unedo*, *Erica arborea*, and *Buxus sempervirens*; these are all evergreen and sclerophyllous. Much of the area has been cultivated as coppices in the past (Mather et al., 1999), which has resulted in many small stems sprouting from a shared root system. Tree height varies between 1 to 10m with little or no understory vegetation.

Imagery

For this study we use 12 ASTER scenes recorded between 2002 and 2008. The images were prepossessed by JPL into surface reflectance for the Visual and Near InfraRed (VNIR) sensor and into surface radiance for the Thermal InfraRed (TIR) sensor (Abrams and Hook, 2008). The pixel size is 15m for VNIR and 90m for TIR. The VNIR bands are used to obtain the NDVI which is related to vegetation cover, LAI, and the photosynthetic activity of the vegetation. The TIR information is closely related to the surface temperature which is influenced by the cooling effect of transpiration of the vegetation, and by the emissivity of the surface (Schmugge et al., 2002). The SWIR bands were not used because they are unavailable for 2008 as a result of a sensor defect.

To ensure a good geographical correspondence between the field locations and the imagery, the image of 2007.08.14 was georeferenced using 70 ground control points. All other images are corrected using image-to-image registration to this reference image based on > 300 evenly spread tie-points. The location accuracy of all images is close to 1 pixel (15m). All images were cropped to a size of 1550 by 1250 pixels and cover the area between 0512083–4836478 and 0535333–4817728 (UTM31N, WGS84). The TIR bands were resampled to the 15m grid using the nearest-neighbour method to preserve the original values without smoothing.

Image Segmentation:

To improve the coupling between the field data and the images and because objects coincide better with ecological units in the field than pixels, we used object-based image analysis (OBIA) for the stacked time-series of images. OBIA strengthens the signal and reduces errors due to spatial mismatches and canopy illumination differences. A single multi-scale segmentation was applied to the multi-temporal data to align all data to a single object-based framework. Because the VNIR and TIR bands have different spatial sampling resolutions, we use hierarchical multi-scale image segmentation with two levels. The first level is optimized for the VNIR bands and in the second level the segments are aggraded into larger units optimized for the TIR bands. Further analyses of the spectral data and temporal dynamics were based on the spatially averaged spectral values of the objects obtained by image segmentation.

The multi-scale hierarchical segmentation was applied to the stacked ASTER images using the eCognition Developer 8 (Definiens, 2009) software package. Three images with partial cloud cover were excluded from the segmentation because the clouds would interfere with the segmentation. The remaining images got equal weights in the segmentation.

The segmentation parameters were chosen with two main objectives: 1) To obtain one common spatial framework for the analysis of multitemporal data, minimizing then effects of the regularization imposed by the sensor and faults in the image geographical registration. 2) To create spectrally homogeneous objects that represent the spatial structure of the landscape and more specifically the variability within the naturally vegetated areas.

In previous research in the Peyne area, we determined the optimal support size for spectral studies on natural vegetation. The size was found to be between 1300 and 2500m² for square pixels (Nijland et al., 2009) and between 6300 and 8500m² for image based segments (Addink et al., 2007). Based on these results we aimed at an average segment size of 7500m² for the areas with full forest cover (NDVI > 0.8). The selection of the forest area only was done because the optimum in these studies was found for natural vegetation which mainly covers the more homogeneous parts of the landscape.

For the TIR bands, the 7500m² segments were too small because they cover less than one original 90m pixel. To get a stable statistical description of a segment it needs to be several times the size of an original pixel (Strahler et al., 1986). We took 10 TIR pixels (81000m²) as the modal segment size to assure that all segments would be large enough. The segments in the more homogeneous, forested areas are generally larger, with an average size of 162000m² for segments with NDVI > 0.8.

In both segmentation levels the weight of the segment shape was set to 0.2 using compactness only. The spectral information gets the largest weight to obtain homogeneous segments, but compactness is included because compact segments are more robust with respect to variability at the edges of the segments which is introduced spatial misalignment of the images.

Field data

Field data were collected in 2008. For this study, we have 75 field plots which were all visited twice: in June, at the onset of the dry summer period; and in September, near the end of the dry season. At each site we measured the diameter of all tree stems in a 5 by 5 meter sample plot and made a series of five hemispherical photographs for the calculation of LAI. At the second visit, only the LAI was determined because the changes in stem diameter over one season are not significant

LAI is defined as the one-sided leaf-area per unit ground area (Watson, 1947). The hemispherical photographs were taken at the four corners and in the centre of each field plot and the LAI was determined using Can-Eye software (Weiss et al., 2004; Jonckheere et al., 2004). Aboveground biomass was estimated using allometric relations between stem diameter and biomass. Allometric relations for trees were available for *A. unedo* and *Q. ilex* (Ogaya et al., 2003).

Table 4.1: Allometric relations for aboveground biomass calculations

Species	Formula	Source
Arbutus unedo	ln AB = 4.251 + 2.463 * ln D50	Ogaya et al., 2003
Quercus ilex	ln AB = 4.900 + 2.277 * ln D50	Ogaya et al., 2003
Shrubs (stem Ø < 3cm)	$AB = 642.0 * H^{0.0075} * Dmax^{2.4901}$	Pereira et al., 1994

AB : Aboveground biomass indvidual [g]

D : Diameter (D50: Stem diameter at 50cm [cm], Dmax : maximum projected shrub diameter [m])

H : Height [m]

The other tree species were divided into two groups, based on morphological similarity to either *A. unedo* or *Q. ilex*. Biomass was estimated using the respective relation (table 4.1). For the shrub species a generic formula for Mediterranean shrubs was used based on the maximum diameter and height per individual (Pereira et al., 1994). The biomass of all individuals were summed per plot and recalculated to kg m^{-2}.

4.3 Results

The field plots were situated in five of the most important substrates of the study area. The substrates are the basic units for further analyses and the average values and standard deviations of LAI and aboveground biomass are shown in figure 4.1. The Limestone has a low shrub type vegetation and therefore considerably lower aboveground biomass than the other substrates that have a forest cover. The Calcareous Sandstone and Flysch substrate have a dense forest cover with a closed canopy. Since the trees were coppiced in the past they have no real stems. Instead they branch out from stools resulting in thin stems only resulting in relatively low values for aboveground biomass.

Image spectra were collected at all field plot locations. As a reference we added a bare dolomite mine, and an area with grass cover to the plots of NDVI and TIR over time (fig 4.2). To emphasize the thermal differences within the study area and to reduce the effect of large temperature fluctuations, the TIR data is presented as a percentage of the water thermal radiance. The thermal brightness of the lake area is plot in the graph and set by definition at 100%. The year, month and day of image acquisitions are noted at the horizontal axis of the graphs.

The most striking feature is the strong reduction of NDVI and rise of temperature of the grass area over the course of summer. The mine is completely bare and has a low NDVI and strong thermal radiance, although not as strong as the grass area because of its high albedo. The naturally vegetated areas have similar behaviour at first sight, but at closer look the limestone and basalt have stronger reduction in NDVI and temperature rise then the other substrates.

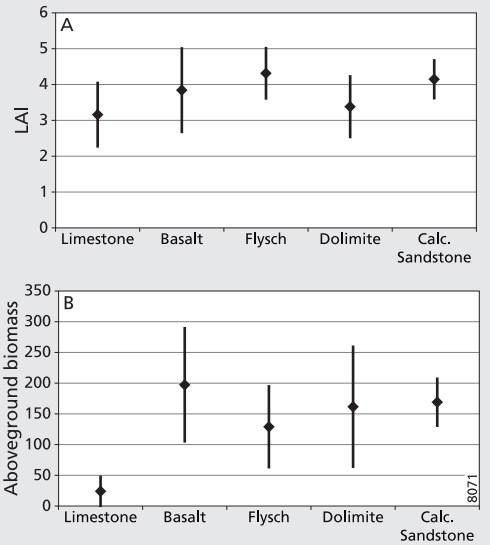

Figure 4.1: Average values and one sd of top: aboveground biomass and bottom: LAI of the five main substrates.

Dry season

In 2008 we had two field campaigns, one in June and one in September. In each campaign we visited the same 75 plots to record changes in LAI during the dry summer season. The vegetation is evergreen, but in dry circumstances part of the leaves may be shed. In 2008, the dry season started at the end of June, and lasted three months. During this period there was very little rainfall, and the trees depended entirely on water extracted from the ground. The type of substrate determines the water-holding capacity and the depth of fissures that allow tree roots to reach this water. The changes of LAI determined in the field, and NDVI and TIR derived from ASTER from June to September are shown in figure 4.3.

The Limestone and Basalt area show a reduction in LAI and NDVI and an increase in TIR. These areas show clear signs of stress, and shedded part of their leaves. This results in a reduction of NDVI and in a reduced transpiration, leading to higher surface temperatures. The Calcareous Sandstone and Dolomite areas show no reduction in LAI and Dolomite even an increase in LAI. This is consistent with a smaller reduction in NDVI and lower TIR values indicate that vegetation on these substrates was less stressed and had less reduction in transpiration. The Flysch area is indifferent and shows a mixed signature with little reduction in LAI and NDVI, but an increase in TIR. This could mean that transpiration is already reduced because of water shortage, but leaf shedding has not yet occurred.

4.4 Discussion

With the combination of spectral and temporal information from earth observation we investigate the vegetation functioning at different lithological substrates in the Peyne study area. The use of multi-temporal data introduces a number of issues regarding the spatial and spectral correction of the used images. Although all images were acquired by the same sensor and were processed in a standardized, validated manner by JPL, still some differences between the images need to be considered when interpreting the data. The VNIR reflectance of the open and active dolomite mine should be constant, but small variability is still present.

To reduce the effects of small scale (~pixel size) variability and spatial misalignment of the images, we use image segmentation to create a stationary object framework for the time series analyses. The use of one object framework derived from the stacked image time-series also improves the coupling between field and image data, because the support of the image data is enlarged and more constant through time when compared to a pixel-based approach.

The spectral corrections of the VNIR reflectance images were effective as is shown by the NDVI of the dolomite mine (fig 4.2 top). The mine is actively exploited and has a constant bare

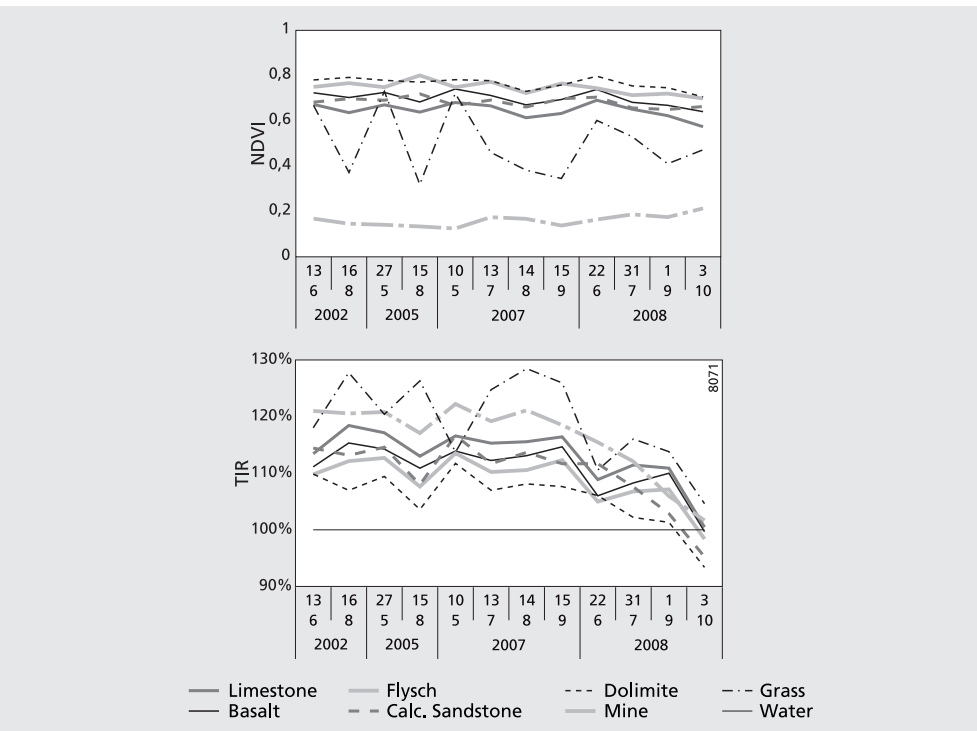

Figure 4.2: Average values of ASTER images for vegetated segments and an active open dolomite mine through time for top: NDVI and bottom: TIR surface rightness relative to the lake area.

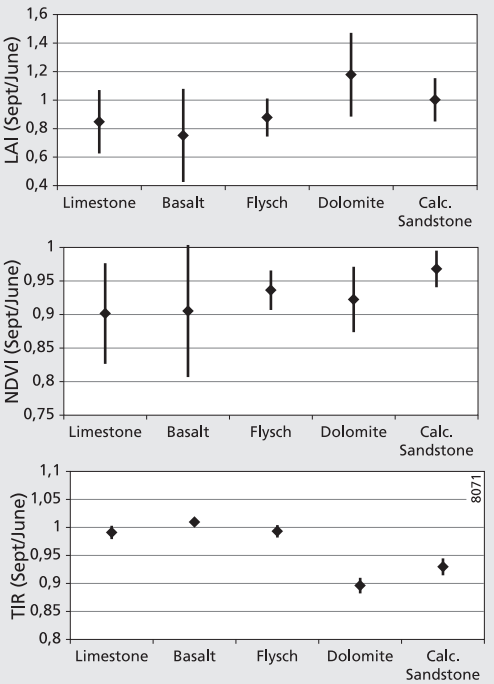

Figure 4.3: Differences between June and September values for top: LAI, middle: NDVI and bottom: TIR for 2008 with the bars indicating the standard deviation of the plots.

dolomite surface. The temporal stability of this surface can be used as a reference and shows a reasonably stationary signal. The remaining signal might be noise in the NDVI values, because the dolomite mine has a spectral flat response throughout the spectrum and hence very low NDVI values.

We normalized the TIR information to the radiance taken from two artificial lakes in the study area. The water temperature of the lakes is not constant and shows a delayed change compared to temperature changes over land. However, by comparing the vegetated areas to the water, we obtain information about the transpiration of the vegetation and its difference with an ideal open-water, evaporating surface. On a wet area or healthy vegetation, much of the incoming energy is used to evaporate water which will have a cooling effect on the surface. Vegetation with water shortage has less transpiration leading to higher surface temperatures. Apart from temperature, the TIR radiance depends also on the emissivity of the surface. There was no need to correct for emissivity changes, because they can be considered constant through the year for a closed forest cover (Schmugge et al., 2002). The emissivity of the pasture may decrease when the grass dries, therefore temperature changes may be somewhat larger than already shown here.

The main focus of this study was on the shrub and forest vegetations in our study area but it is difficult to separate the effects of stress on evergreen vegetation from the seasonality of grasses and annuals. In the Flysch and Calcareous Sandstone, the canopy cover is almost continuous and herb cover is absent, but in the Dolomite and even more at the Basalt and Limestone there is considerable grass cover between or under the trees. In these locations, the seasonal change of the grass cover influences the temporal patterns of NDVI and transpiration and partly obscures the changes in the trees and shrubs.

4.5 Conclusions

In this paper we presented an object-based analysis of multi-temporal remotely sensed and field data aimed at monitoring vegetation functioning and especially the effects of drought stress during the summer. Looking at five substrates in our study area, we found differences in our key indicators for vegetation health -LAI, NDVI, and TIR- that can be related to the resilience of the vegetation against summer drought. The relation between these vegetation patterns and the geological substrates in our study area indicates the importance of soil water storage on vegetation growth.

In this study we used an object-based method of creating temporal units from imagery because it allows for a stable coupling between field and image data. The object-based analysis decreases the effects of edge, and image misalignment. The presented method using object-based analysis of high resolution images is especially valuable in fragmented landscapes with a high spatial variability of the environmental conditions, which is common in Mediterranean areas.

5. Detection of soil moisture and vegetation water abstraction in a Mediterranean natural area using electrical resistivity tomography

This Chapter was published as: Wiebe Nijland, Mark van der Meijde, Elisabeth A. Addink, & Steven M. de Jong, (2010). Detection of soil moisture and vegetation water abstraction in a Mediterranean natural area using electrical resistivity tomography. CATENA 81 (3), 209-216.

Abstract

Vegetation growth in semiarid, Mediterranean ecosystems is greatly dependent on moisture availability in the soil, as little precipitation is available during the growing season. Predicting the effects of climate change on vegetation development requires understanding of the exact relation between climate, moisture availability, and plant growth. Accurate moisture measurements in naturally vegetated areas are difficult because of high spatial variability and because of the coarse, shallow soils. In this study, we evaluated the possibilities of using Electrical Resistivity Tomography (ERT) to measure soil moisture availability and plant water use in a Mediterranean natural area. We found that ERT is a useful tool for measuring soil conditions, providing information on the spatial patterns within the soil and reaching depths otherwise inaccessible. In heterogeneous soils, we differentiated between lithological and moisture effects in the measurements using multi-temporal data. Absolute calibration to moisture content was sometimes possible, but strongly location dependent. Based on the ERT measurements, we found that although the soils in the study area are shallow and rocky, plant roots penetrate deeply into the fractured and weathered bedrock, and vegetation subtracts water from depths down to 6m and below. This information is important for understanding the plant–soil relations and modelling vegetation development. We conclude that ERT provides crucial information on soil moisture processes unavailable using any other currently available measurement method.

5.1 Introduction

Water availability is an important constraint on tree and shrub development in Mediterranean ecosystems, but in practice it is difficult to quantify the dynamics and spatial distribution of soil moisture in shallow and stony soils. Precipitation during the growing season is usually low, causing primary production of biomass to be water limited (Poole et al., 1981; Sala and Tenhunen, 1996; Gracia et al., 1999). During prolonged periods of summer drought, water stored in the soil column is the only available water source for plants and trees. If the soil

moisture content drops below a certain level, stomatal closure is induced to reduce water loss, prohibiting photosynthesis (Damesin and Rambal, 1995; Hoff et al., 2002). A drought-induced growth stop is common in Mediterranean regions and this limits ecosystem productivity. Miller and Hajek (1981) estimated the sensitivity of the length of the ecosystem growing season to soil moisture; they concluded that the length of the Mediterranean growing season is fairly sensitive to soil moisture retention. The season extends by 10 days per 10cm of soil depth and shortens by about 12 days per 10% increase of soil rockiness.

Hoff and Rambal (2003) find similar results based on Forest-BGC (Running and Coughlan, 1988; Running and Gower, 1991) simulations of Mediterranean woodlands. The simulations illustrate that Leaf Area Index (LAI) development and net photosynthesis is sensitive to the effective soil water availability, which is highly correlated to rooting depth. Some Mediterranean tree species are known to have extensive root systems penetrating deeply into fractured bedrock (Kummerow, 1981). Accurate characterization of the soil and the ability of trees to extract water from the soil profile are crucial for the understanding of Mediterranean ecosystems and the modelling of primary production.

Regional climate simulations of the Mediterranean area predict increased temperatures and decreased summer rainfall for 2070 (Gao and Giorgi, 2008). Annual average precipitation will not change much, but the distribution of precipitation over the year will shift to a stronger seasonal character with dry summers and wet winters. For vegetation growth, these climate changes will cause decreased water availability during the summer growing season. The dependence of vegetation on soil water storage will therefore increase.

Measurements of soil hydrological processes are commonly either point based, or integrated over large areas. Point-scale measurement includes gravimetric methods (Van Reeuwijk, 2002) or electrical soil probes (Robinson et al., 2003; Muñoz-Carpena et al., 2004) integrating over a volume < 1.0dm3. Moisture detection at regional and continental scales has recently advanced by using satellite imagery (Robinson et al., 2008). A gap in measurement data exists between the two scale levels: point and regional. Where little information is available on soil moisture distribution and on water redistribution processes at hill slope or at small catchment scale, a spatial scale is important for ecosystem models. These typically simulate processes at the stand scale or down to a cell size of ~20m (Running and Coughlan, 1988; Aber and Federer, 1992; Landsberg and Waring, 1997; Gracia et al., 1999; Mouillot et al., 2002).

Besides information on the spatial distribution of soil moisture in the landscape, information is also required on the vertical distribution of water, i.e. in the soil profile. Available area-based soil moisture methods, e.g. mobile Time Domain Reflectometry (TDR) arrays or airborne remote sensing, have a depth resolution of only a few centimeters. Gravimetrical or TDR measurements of deeper soil layers require coring or excavation and therefore are very laborious. As a result, these methods are of limited use for the study of deeper soil moisture storage and for water availability to plant growth.

Apart from that, they are generally unsuitable for use in forested areas and stony soils as the tree roots find their way through cracks in the bedrock (fig. 5.1). In conclusion, the study of soil water use and of water availability in Mediterranean ecosystems is hampered by a lack of suitable methods to determine water content with a sufficient spatial support, depth, and usability on rocky, forested terrain.

Figure 5.1: Field photo showing *Q. ilex* roots growing deep into fractures of the bedrock material. The section was exposed at a road cut.

Electrical resistivity measurements of the soil could fill the gap at a spatial and vertical scale and yield valuable information suitable for ecological models. In-situ experiments already showed the value of resistivity measurements for monitoring root-zone moisture distribution in precision agriculture (Michot et al., 2003; Srayeddin and Doussan, 2009) and on a grassland – forest transition (Jayawickreme, 2008). Electrical resistivity measurements yield information over transects of tens of meters and down into the profile for several meters. The electrical resistivity of a soil or rock is controlled by two components: the solid particles and the pore fillings (Friedman, 2005). Anomalies in electrical resistivity arise when a contrast in resistivity is present through differences in material, density, or water content. For example, due to the good conductivity of groundwater, the resistivity of a sedimentary rock or soil is much lower when it is wet rather than in a dry state. Electrical Resistivity Tomography (ERT) is a method that uses a multielectrode array measuring soil electrical resistivity of many electrode combinations to derive a 2D cross-section of earth resistivity along the electrode array. Field measurements of soil electrical resistivity are possible using battery powered, portable equipment. After installing the electrodes, a modern automated setup for resistivity measurements needs less than one hour to deliver a total set of resistivity measurements required to derive a 2D cross-section. The electrodes connect to the soil through 1cm-diameter steel pins that are inserted in the ground and these can be used in rocky soils without damage to the equipment.

In this study, we present the use of ERT to detect spatial and temporal patterns of moisture in variable shallow soils and weathered bedrock. We made ERT profiles for four substrates in our study area, combined with detailed descriptions of soil pits, soil moisture content, and vegetation. We visited each site twice; both at the onset of the dry season, and near the end of the dry summer period. Some of the locations were visited a third time after high intensity rainfall events. The objective of this paper is to evaluate the use of ERT measurements to study water availability, and soil-water use by vegetation in a natural Mediterranean area.

5.2 Study Area

The test locations for this study are situated in the Peyne catchment in Mediterranean southern France. Annual average precipitation is 800–1000mm and is concentrated in the spring and fall. The catchment is situated at the edge of the 'Montagne Noir' and is characterized by a high spatial variation of geological bedrock. Four lithologies were used for the ERT experiments: Flysch, Basalt, Calcareous Sandstone, and Dolomite (Alabouvette, 1982). The formation characteristics, as well as the dry electrical resistivity of the bedrock, vary considerably (Table 5.1). The soils in the area are shallow and are poorly developed with often only an AC or AR profile. They are classified as regosols, lithosols, or luvisols according to the FAO soil classification system (Driessen et al., 2001). Soil characteristics and vegetation types are differentiated mainly upon the nature of the geological substrate (Bonfils, 1993). The downward transition of soil into weathered rock often has an indistinct boundary and tree roots often penetrate deeply into weathered, fractured, or faulted rock. The study area is covered with (semi) natural and agricultural vegetation, mostly vineyards and pasture. Our ERT measurement sites were all located in areas with natural growth. The vegetation mainly consists of evergreen shrubs and trees and is sclerophyll. Tree height varies from 1 to 10m with little or no understory

vegetation. Much of the area has been cultivated as coppices in the past (Mather et al., 1999), which has resulted in many small stems sprouting from a shared root system. The distribution of land cover and vegetation types is highly correlated with the lithology. The Flysch has dense shrub vegetation with a mix of *Arbutus unedo*, *Quercus ilex*, and *Erica arborea*. The Basalt plateaus are mainly used for pasture, and naturally vegetated areas show signs of land abandonment with Q. ilex trees clustered around former stone heaps and walls. The Calcareous Sandstones are covered with a well-developed mixed oak forest with *Q. ilex*, *Q. pubescens*, and *A. unedo* 5–10m in height. A second vegetation layer is present with *Buxus sempervirens* and *Hedera helix* up to 5m tall. Land cover in the Dolomite area is highly variable, with bare rock outcrops, mixed herbs and shrubs, and low shrub-like forests.

5.3 Methods

In our Mediterranean southern France study area, we used ERT to detect spatial and temporal patterns of soil moisture in variable shallow soils and weathered bedrock. In 2007, we made ERT profiles for 14 sites on four different geological substrates in June, at the onset of the dry season, and again in September, near the end of a three-month dry period (Table 5.2). Five locations were visited a third time in autumn (column 5 of Table 5.1) after a series of high intensity rainfall events with a total precipitation of ~120 mm. At each site, we also registered detailed descriptions of soil pits, surface soil moisture measurements along the ERT transect using Frequency Domain Reflectometry (FDR), and gravimetric soil moisture samples. During the first visit (week 24 and 25), we measured aboveground biomass and LAI as reference vegetation characteristics (Table 5.2). The profile sites were chosen in naturally vegetated areas with no recent disturbance.

Table 5.1: Location, time, substrate, and vegetation of the ERT profiles

Site number	Location (UTM 31N WGS84)		Lithology	Measured week nr. (2007)	LAI	Above gr. biomass (kg m–2)
	X	Y				
1	0523387	4822769	Flysch	24, 38, 41	5.3	153.2
2	0523800	4823060	Flysch	24, 38	6.3	70.1
3	0523152	4823879	Flysch	24, 38	5.1	225.2
4	0517297	4831095	Dolomite	24, 37, 41	2.4	2.3
5	0516603	4831416	Dolomite	24, 37	4.5	130.3
6	0520895	4826668	Basalt	24, 38	4.6	205.4
8	0523180	4823877	Flysch	24, 38	5.7	117.9
9	0523434	4823386	Flysch	24, 38, 41	5.6	140.4
10	0517397	4831347	Dolomite	25, 37, 41	3.3	68.0
11	0519008	4829779	Calc Sandstone	25, 38, 41	4.1	182.3
12	0519220	4829389	Calc Sandstone	25, 38	3.3	90.2
13	0522621	4826342	Flysch	25, 39	3.3	242.5
14	0522681	4823337	Basalt	25, 39	1.9	111.3

Table 5.2: Lithological characteristics of the substrates (Alabouvette, 1982; Bonfils, 1993) and their resistivity in dry conditions (Lowrie, 2007)

Subsurface lithology	Dry resistivity
Flysch/Schist: Layered mix of highly fractured, carboniferous low-grade metamorphic sandstone and argillite. Soil development is shallow, with mostly loose pellets of bedrock and poor water-holding capacity.	10^2 to 10^3 Ω m^{-1}
Basalt: Quaternary volcanic flows. The flows are now plateaus due to differential erosion. Shallow, acid soils with many boulders.	~10^2 Ω m^{-1}
Calcareous Sandstones: Eocene lacustrine deposits deformed and highly fractured. Shallow rocky soils with high clay content.	~10^3 Ω m^{-1}
Dolomite: Gray Jurassic dolomite with extensive karst development. In low areas, loose sand of up to 2 m depth occurs and has low wter retention capacity.	~10^4 Ω m^{-1}

Electrical Resistivity Tomography

ERT is based on the insertion of a controlled direct electrical current (DC) into the ground through electrodes. The electrical current flow adapts to the subsurface resistivity pattern so that the potential difference at a certain distance away from the source, as a function of the subsurface structure, can be measured using a second pair of electrodes (fig. 5.2). In the idealized case of a uniform conducting half-space, the current flow resembles a perfect dipole pattern and the resistivity determined using a four-electrode configuration is the true resistivity of the half-space. When the electrode spacing is varied, or the spacing remains fixed while the whole array is moved, then the apparent resistivity will, in general, change. Depending on the variable small or large distance between the electrodes, the derived apparent resistivity will be a property for a shallow or deep volume, respectively. Combining measurements of many different electrode combinations along a line allows the calculation of the actual 2D distribution of electrical resistivity at this transect. The 2D graph represents the bulk properties of a three dimensional space around the electrodes because the electrical current flows in a sphere-like pattern, rather than along a plane. The patterns of resistivity in the soil result from lithology, porosity, structure, temperature, root density and water content (Lowrie, 2007). We used an array of 28 electrodes with 1m spacing, which provides reliable resistivity information to a depth of approximately 6m. Electrical currents were inserted and measured according to the Schlumberger configuration (Telford et al., 1990). Inversion of the data was done with EarthImager2D (for more details on the software and used algorithms see: AGI, http://www.agiusa.com/agi2dimg.shtml). We used the time lapse inversion module to create difference images of the various resistivity sections.

Relation of resistivity and groundwater

The resistivity of the subsurface is strongly influenced by the presence of groundwater, which acts as an electrolyte. This is especially important in porous sediments and sedimentary rocks. Their minerals are normally less conductive than groundwater, so the resistivity of sediment decreases with a greater amount of contained groundwater. This is also dependent upon the proportion of the rock volume that consists of pore space (the porosity), the connectivity of pore space, and the fraction of this pore volume that is water filled (Friedman, 2005). The resistivity of a rock is proportional to the resistivity of the dry material and the resistivity of the pore space. These

observations are summarized in an empirical formula, called Archie's law, for resistivity [Ω m^{-1}] of the rock, Equation 5.1 (Archie, 1942; Lowrie, 2007).

$$\rho = \frac{a}{\phi^m S^n} \rho_w \qquad \text{Equation 5.1}$$

Where ρ(porosity) and S (saturation factor) are fractions between 0 and 1, ρ [Ω m^{-2}] is the resistivity of the groundwater, and the parameters a (tortuosity), m (cementation factor), and n (saturation exponent) are empirical constants that need to be determined for each case. Generally, 0.5 ≤ a ≤ 2.5, 1.3 ≤ m ≤ 2.5, and n ≈ 2.0 (Lowrie, 2007). Archie's law is only valid in clean porous media, without considerable amounts of clay (Friedman, 2005).

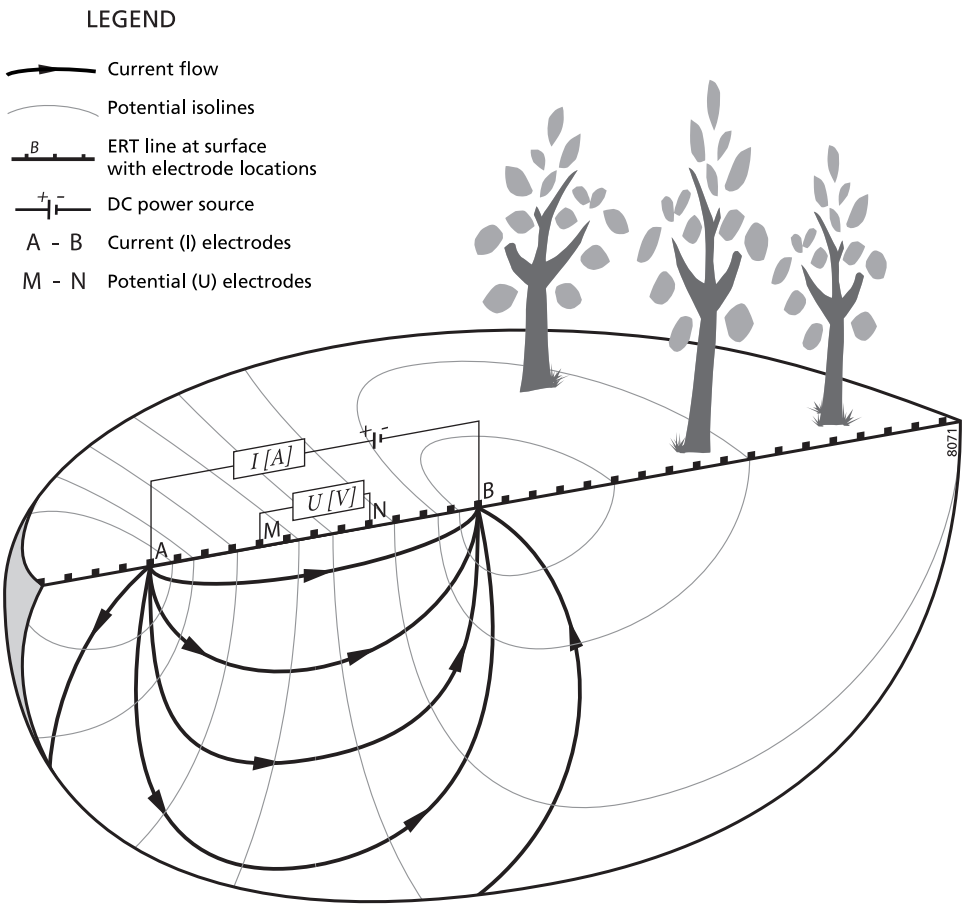

Figure 5.2: Schematic diagram of resistivity measurement in a uniform medium. By combining measurements of many electrode combinations using computer tomography, a spatial earth resistivity section is made.

Time-lapse ERT

The sensitivity of earth resistivity to differences in soil density and lithology poses a difficulty on moisture detection, because many soils show much spatial variability. A comparison of resistivity measurements at different moments allows filtering of the ERT signal by the stationary characteristics of the soil and therefore highlights changes in soil moisture content. From the variables influencing earth resistivity, moisture is the only one significantly varying on a sub-year timescale and consequently ERT measurements at different times in the year yield the basis for soil water content mapping. On the investigated timescale, earth resistivity may also vary due to temperature changes; the effect is about 2% per 1˚C (Friedman, 2005). In our case the temperature difference between June and September was 2˚C (16 to 18 ˚C) at 40cm depth, resulting in resistivity changes less than 5%. As the temperature differences, and hence the resistivity changes, at larger depths will have been even smaller, we neglected this effect in further analysis because it is very small compared to moisture induced changes.

Additional soil measurements

In each of the resistivity profiles of 28m length, a soil pit was dug as deep as possible using a hand shovel and pickaxe. The depths of the pits were constrained by bedrock and reached 40–200cm. The locations of the pits were selected in a homogeneous and representative part of the profile, based on analysis of the ERT data. Soil pits were used to make a description of the soil profile, and to take soil samples for gravimetric determination of soil moisture content. Soil samples were taken at 10 cm depth intervals, weighed, oven dried, and weighed again. Gravimetric moisture content was calculated as:

$$\theta_g = M_{wet} - M_{dry} \big/ M_{dry} \qquad \text{Equation 5.2}$$

where θ_g: gravimetric moisture content, M_{wet}: fresh sample weight (kg), and M_{dry}: oven dry sample weight (kg).

In addition to the gravimetric moisture samples, we used an FDR soil moisture probe to determine the moisture content in the soil pits at 10cm intervals and at the surface along the resistivity profile at 1m intervals. The FDR readings are known to have a good linear relation with moisture content. The relation is influenced by clay and organic content, therefore an onsite calibration is advised (Miller and Gaskin, 2008). We fitted site-specific calibration lines between the gravimetric moisture and FDR values for each of the tested substrates (fig. 5.3).

5.4 Results

ERT measurements were made at 14 sites located on four geological substrates to determine soil moisture content and the dynamics of soil moisture content over the summer. ERT was selected because it provides information on soil water content at a local scale and over vertical profiles, and because other methods fail in these stony soils. The absolute resistivity values and patterns were greatly dependent on the type of substrate and are related to the typical resistivity of the bedrock (Table 5.2). The resistivity data was of very good quality with high S/N ratio (>3500 at the top of the model and >50 at the bottom), and repeat measurement errors below 1%. The data

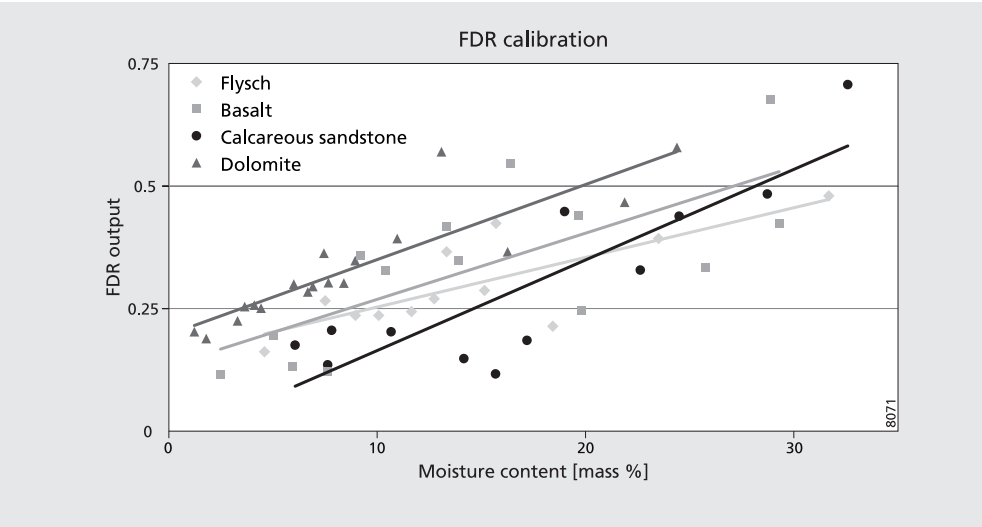

Figure 5.3: FDR calibration lines for the tested soil types. r^2 Flysch: 0.61, Basalt: 0.46, Calcareous Sandstone: 0.70, Dolomite 0.79.

inversion models gave consistently low error statistics with RMS < 1.5% and L_2 < 1. The time lapse images showed high similarity in areas not affected by changing water content in the soil indicating high reproducibility of the data.

The upper part of all the soil profiles is cracked and loose with dense roots and has a resistivity between 100 and 1000Ω m–1. This first layer is 60–150 cm thick as shown in Fig. 5.4. and has a higher variability and clearly different resistivity values from the underlying base. Flysch and Basalt have a lower base resistivity than the values in the top layer as shown in Fig. 5.4 a and b, respectively. Calcareous Sandstone and Dolomite have a much higher base resistivity than the values at the top as shown in Fig. 5.4 c and d, respectively.

Moisture profiles

The gravimetrical moisture content measured from the soil pits was generally between 5% and 15% as shown in Fig. 5.5. In the top 10cm, which was high in organic material, moisture contents reached 25%. Minor rain events before and during the field campaign also caused high top soil moisture content. The moisture profiles for Flysch and Dolomite (fig. 5.5) show a decrease of moisture with depth. For the Basalt and Calcareous Sandstone, the maximum pit depths were 40cm. Profiles are not shown, but moisture contents decrease with depth as on the other substrates.

A direct relation between soil resistivity and moisture, fitted by applying Archie's law (Equation 5.1), could only be made for the Dolomite substrate (fig 5.6). For the other substrates it is possible to derive qualitative information on soil moisture patters, but because of the presence of clay, Archie's law is not valid and calculations of actual moisture contents cannot be made.

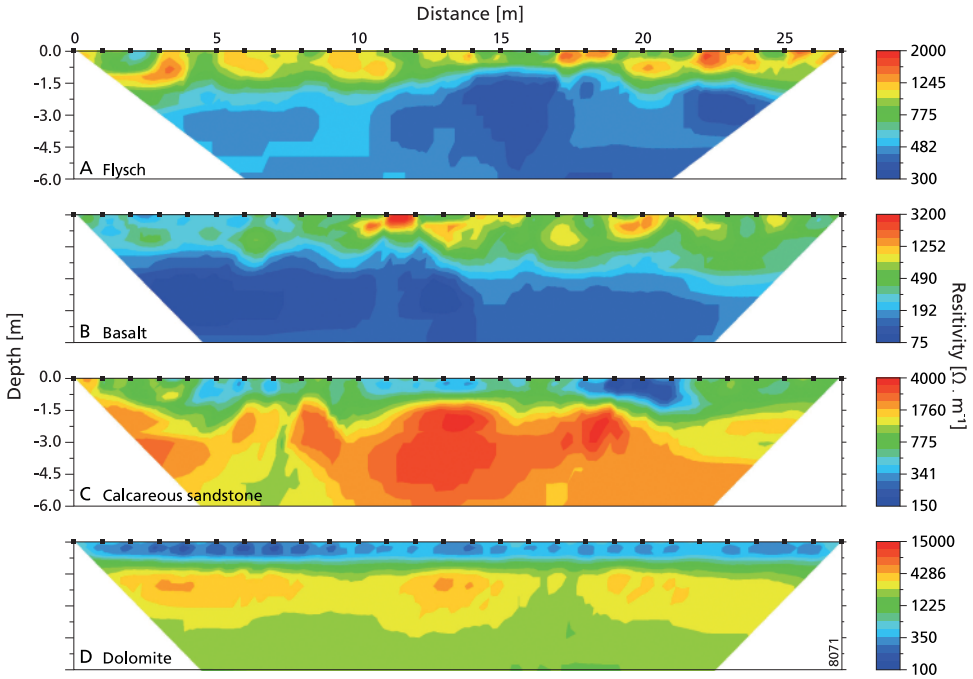

Figure 5.4: Example resistivity profiles for all four substrates (location nr.): A, Flysch (1); B, Basalt (6); C, Calcareous Sandstone (12); D, Dolomite (10). Color scales are optimized to the individual profiles. Inversion RMS-errors [%]: A 1.02, B 1.30, C 1.44, D 1.04

To apply Archie's law, we converted the gravimetrical soil moisture measurements to volumetric content using average bulk density (1.6) and porosity (0.3) values for the whole soil profile. The obtained fit for Archie's law in the Dolomite is good (r^2 = 0.83) except for water contents exceeding 8%. These high water contents were only found close to the soil surface where porosity may be higher, and the sensitivity of the ERT measurements is poor in the uppermost part of the profile. The parameters used to fit Archie's law were: porosity: 0.3, m: 1.5, n: 1.88, ρ : 26 (Ω m^{-1}), and a: 0.5.

Time-lapse ERT

It is difficult to separate lithological variability from soil moisture content using a single ERT profile. To separate between these two, we used time-lapse ERT. This approach uses two profiles at the exact same location to determine the difference in resistivity over time. In our case, we took profiles at the start of the summer and near the end of the dry season. We assumed that the lithology remained unchanged during this period and that all observed resistivity changes could be attributed to moisture and temperature changes. The resistivity effect of the temperature change is less than 5%, while the observed changes ranged between 40 and 1000%. Hence we neglected the temperature effect in further analysis. Fig. 5.7 shows the Flysch substrate ERT profile for June, the profile for September, and the 'difference profile' between June and September. All the difference profiles show an increase of resistivity in the zone down to 4m,

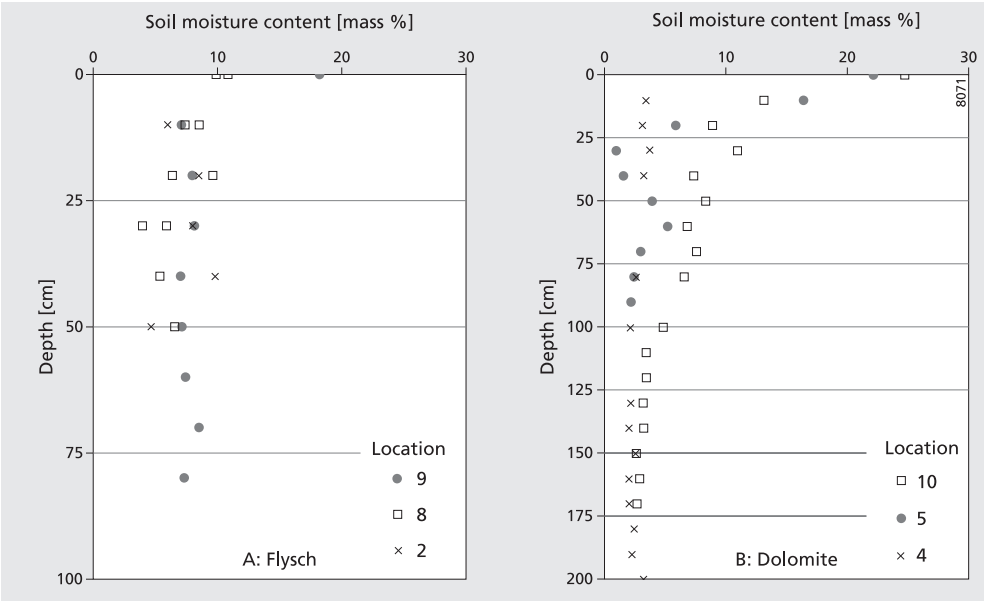

Figure 5.5: Depth profiles of measured gravimetrical moisture content in June of A: Flysch and B: Dolomite.

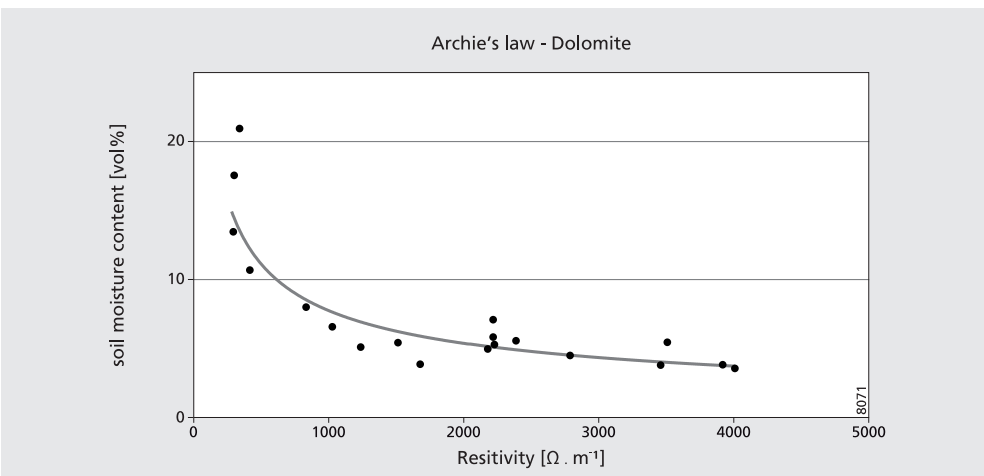

Figure 5.6: Relation between soil moisture and resistivity fitted with Archie's law for Dolomite.

but only the Flysch is shown here as an example. This increase can be contributed to water abstraction by vegetation.

Depth average profiles of resistivity change from June to September (fig. 5.8) showing the distribution of water abstraction from the soil. The top layer shows little difference, because some early September rainfall wetted the top part of the soil profile. The common pattern now shows a three-layer profile: a top layer with a high lateral variability, a second layer with water abstraction by trees during the summer, and a base with no change at all. The depth of each zone is very different for the geological substrates in the study area (fig. 5.8). In the Flysch and Basalt, the vegetation uses water from the soil down to 4m, with maximum extraction around 2m deep. On the Calcareous Sandstone, water is used from below 6m, the maximum depth of our measurements. On the Dolomite, water is used down to 5m. The resistivity change profiles are also related to the vegetation at the measurement locations. The Flysch and Basalt areas are covered with low shrub-type forest, whereas on the Calcareous Sandstones and Dolomite the trees are generally larger, as is the water abstraction zone.

5.5 Discussion

ERT enables the spatial imaging of soil characteristics down to a depth of over 5m. The ERT approach currently fills a gap in the detection methods for soil moisture characteristics and is applicable where other methods fail for logistic reasons. The spatial range of ERT makes it very useful for the detection of root zone processes in forests. The translation of ERT measurements into soil moisture content is not straightforward, because resistivity is also sensitive to the lithology and density of the substrate. The latter resulted in large differences between the measured resistivity values for the different geological substrates in our study area with large variability and anomalies occurring within the profiles. These short range variances and anomalies may be caused by the presence of solid rock fragments or fractures. In some cases, we can directly relate electrical resistivity to soil water content using Archie's law. This may only be used with great care, because many other soil characteristics influence the resistivity. Calibration parameters for Archie's law are very site specific, and a relation based on topsoil measurements may even be invalid for the underlying bedrock because of possible differences in material compaction and organic content (Friedman, 2005).

The use of time-lapse ERT is very effective in separating the soil moisture signal from lithological variability in the profile. ERT measurements for soil moisture detection are therefore especially useful when applied in a monitoring setting, because by comparing the measurements at different times it is possible to separate the effects of moisture and lithology. In most locations, it is difficult to get absolute measurements of soil moisture, but the benefit of using ERT is seen as obtaining spatial data from otherwise unreachable depths.

ERT was used in a naturally vegetated area with shallow heterogeneous soils. The natural vegetation in the study area has deep root systems penetrating fractured bedrock to access stored water during the long dry summer period. The depth of root systems and shallow soils make soil moisture measurement very difficult, because most of the commonly used methods are confined

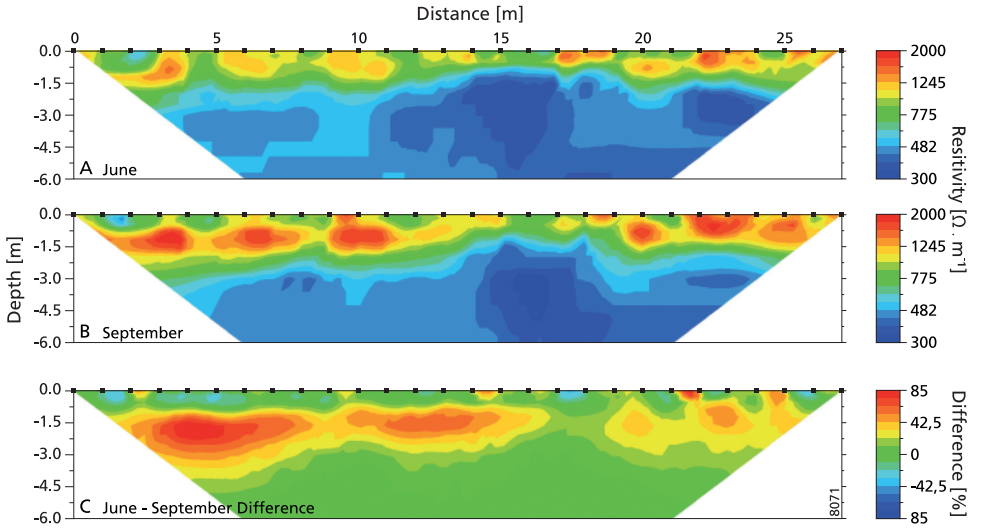

Figure 5.7: ERT profile on Flysch (1) of A: June and B: September, and C: Resistivity difference between A and B. Inversion RMS-errors [%]: A 1.02, B 1.05 C 1.47.

to the surface. For ERT profiles made in June and in September, we assume no changes in lithology, only in the soil water content. The difference profiles show a clear division into three soil layers: a top layer of 60–150cm that can also be accessed in most soil pits, a second layer reaching a depth of 300–600cm, and a third invariable base layer. The top layer hosts dense roots that can take up water during the wet seasons or directly after rainfall events. The two bottom layers are not accessible for additional measurements, but from the difference in resistivity over the summer season, it can be concluded that the vegetation uses water from the second layer. This conclusion is supported by observations of fresh road cuts in the study area that show large roots penetrating several meters into the fractured rock (fig. 5.1). Besides, the main species in our study area (*Q. ilex* and *A. unedo*) also are known to have deep root systems (Canadell et al., 1996; Kummerow, 1981).The difference profiles also show the effect of the different geological units on water availability for the vegetation, improving our knowledge on soil characteristics and vegetation water use. The spatial component in the measurements allows estimation of the small-scale spatial variability in the soil, which is impossible using point-based methods.

5.6 Conclusions

In this paper, we introduce and evaluate the use of Electrical Resistivity Tomography to measure soil characteristics and moisture availability in forested areas on four different geological substrates. ERT is shown to be a useful technique for the detection of soil moisture, filling a spatial gap in available measurement techniques, and providing data at otherwise unreachable depths. Using ERT, we show that vegetation extracts water from below the soil zone from the weathered rock layers to depths of 3-6m. Hence, water storage in weathered bedrock is important for the vegetation in our area to bridge the dry, hot summer. Soil development in

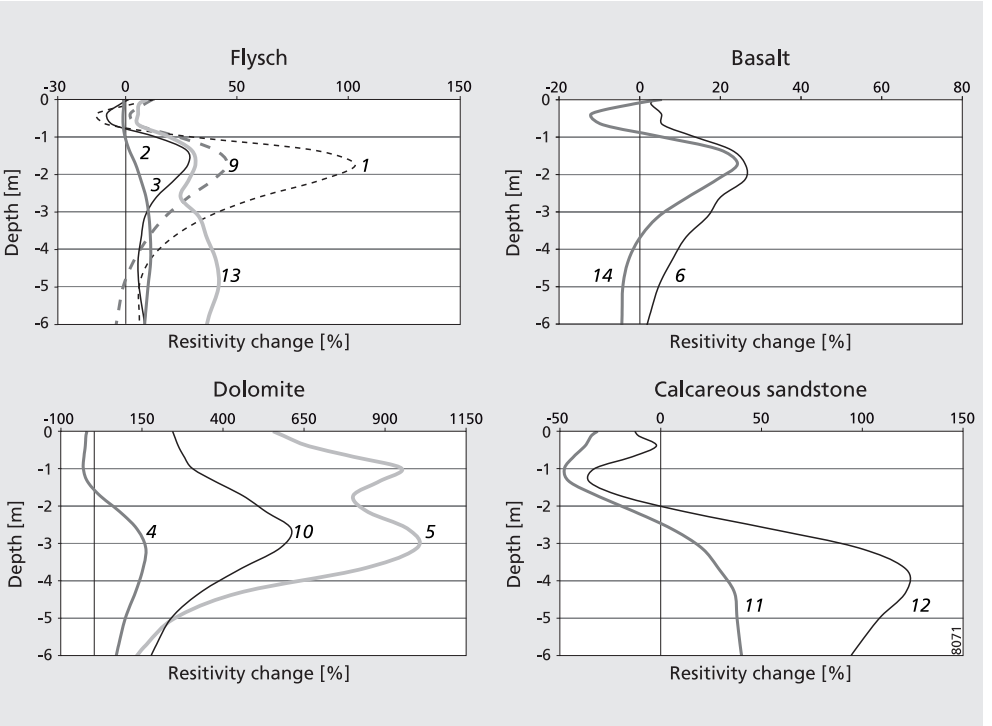

Figure 5.8: Depth averaged relative resistivity changes between June and September as a percentage of June resistivity on the four tested substrates. Each graph is marked with the profile location number (Table 5.1).

the study area is shallow, with bedrock close to the surface. The vegetation has deep roots, but due to the stoniness of the soil it is extremely complicated to observe the actual rooting depth and moisture abstraction. ERT is therefore a useful addition to other soil moisture estimating techniques, allowing measurement at depths over 5m, and providing information on the spatial variability of the soil. Combining ERT measurements with Archie's law is a promising technique to obtain actual spatial moisture data on deep soil layers, but the relation is only valid in absence of clay. Although the method yields valuable insight in the spatial and temporal dynamics of soil moisture in rocky substrates, the absolute values obtained by applying Archie's law should be interpreted with care as they are based on calibrated parameters that are site- or even soil-layer-specific. In heterogeneous soils, multitemporal information is needed to separate stationary, lithological variability from more dynamic differences in moisture content.

Our study of water use by Mediterranean vegetation shows that lithology is an important factor controlling water availability, water storage capacity, and maximum root penetration depth. This information improves our knowledge of soil–vegetation interactions, and may be used to improve vegetation development and productivity modelling. We conclude that ERT measurements, although laborious, provide crucial information in the study of soil moisture

content, soil moisture redistribution processes, and water availability to plant growth, even in shallow and rocky soils.

Acknowledgments

The authors would like to thank Peter Gill and Mark de Leeuw for their contribution on the FDR calibration, and Peter also for his help in the field campaign.

6. Relating ring width of Mediterranean evergreen species to seasonal and annual variations of precipitation and temperature

This chapter was published as: Wiebe Nijland, Esther Jansma, Elisabeth A. Addink, Marta Domínguez-Delmás, & Steven M. de Jong, (2011). Relating ring width of Mediterranean evergreen species to seasonal and annual variations of precipitation and temperature. Biogeosciences 8, 1141-1152.

Abstract

Plant growth in Mediterranean landscapes is limited by the typical summer-dry climate. Forests in these areas are only marginally productive and may be quite susceptible to modern climate change. To improve our understanding of forest sensitivity to annual and seasonal climatic variability, we use tree-ring measurements of two Mediterranean evergreen tree species: *Quercus ilex* L. and *Arbutus unedo* L.. We sampled 34 stems of these species on three different types of substrates in the Peyne study area in southern France. The resulting chronologies were analysed in combination with 38 years of monthly precipitation and temperature data to reconstruct the response of stem growth to climatic variability. Results indicate a strong positive response to May and June precipitation, as well as a significant positive influence of early-spring temperatures and a negative growth response to summer heat. Comparison of the data with more detailed productivity measurements in two contrasting years confirms these observations and shows a strong productivity limiting effect of low early-summer precipitation. The results show that tree-ring data from *Q. ilex* and *A. unedo* can provide valuable information about the response of these tree species to climate variability, improving our ability to predict the effects of climate change in Mediterranean ecosystems.

6.1 Introduction

Mediterranean regions are regarded as an outstandingly rich area with respect to history, geography and biodiversity. Mediterranean areas are species-rich and form original bio-geographic regions due to a unique combination of climate, relief, soil and long-term human use of the landscape (Naveh and Kutiel, 1990). The Mediterranean is also a very attractive place for living and recreation. Pressure on the Mediterranean environment and water resources is therefore high and generally increasing (Grenon and Batisse, 1989; UNEP, 2009).

Forest growth in Mediterranean environments is mostly water limited because of the warm, dry summers. This strong limitation results in slow succession rates and climax vegetations characterized by moderate or low above-ground biomass (Di Castri and Mooney, 1973;

Rambal, 2001). The predicted climate change for the Mediterranean countries consists of an increase of the extreme character, including longer periods of drought, more concentrated rainfall, and increased mean temperatures (Hertig and Jacobeit, 2008; Gao and Giorgi, 2008; Gibelin and Déqué, 2003). This will promote drought stress and may lead to a decrease in vegetation productivity and possible a loss of species (biodiversity) and ultimately desert-like conditions. Mediterranean ecosystems are very sensitive to climate change, because growth is already strongly limited and forests are only marginally productive. Small changes in water availability and temperature may have considerable impacts on the resilience of the present natural vegetation types. Mediterranean landscapes have a worldwide significance because their ecosystems are widely recognized as biodiversity hotspots, with a species density surpassed only in tropical forests (Gómez-Campo, 1985; Médail and Quezél, 1999; Vogiatzakis et al., 2006). Apart from its ecological value, vegetation cover also protects against soil erosion, provides food for livestock and decreases flooding risks by interception and retention of precipitation. Because vegetation has so many functions and effects on the landscape, any changes in vegetation cover or productivity will have a large impact on the ecology as well as for the human inhabitants.

To accurately predict the possible effects of climate change on Mediterranean forest ecosystems it is important to understand the relationship between plant growth and the most important climate variables. The main question in this context is: "which climatic variables most strongly affect vegetation productivity?" This study investigates the local relationship between annual vegetation productivity of Mediterranean trees and meteorological variables (i.e. annual and seasonal variations of rainfall and temperature).

Climate-productivity relations have been studied extensively for agricultural crops (e.g. Van Keulen and Wolf, 1986) and to a lesser extent for production forests, but are largely unknown for many natural vegetation types. Good progress is being made using computer-modelling experiments (Reichstein et al., 2003; Hoff et al., 2002; Landsberg and Waring, 1997; Running and Coughlan, 1988) and global or regional studies using satellite observation (Field et al. 1995; Nemani et al., 2003; Reichstein et al., 2007), but besides flux-tower measurements and small-scale laboratory tests, little validation data is available (Pereira et al., 2007; Chiesie et al., 2005; Hanson et al., 2004; Baldochhi and Xu, 2007).

Relating stem growth to seasonal and annual records of rainfall and temperatures using absolutely dated annual tree-ring width may result in new information about the effects of climate change on tree growth in the Mediterranean region. Stem-growth increments as recorded in annual tree rings are an accurate record of past stem growth and more generally of past forest productivity. Productivity and stem growth are influenced by both regional and local processes. Local factors like soil depth, nutrient and mineral availability, slope exposition, and competition between individuals causes stem growth to show significant local variations. This study however focuses on the impact of the overall regional variation of precipitation and temperature on stem growth.

Tree rings are also used as a climate proxy for reconstructing past climates beyond the available instrumental records (dendroclimatology) (Briffa, 2000; Jones et al., 1998; Fritts, 1976). Dendroclimatic reconstructions in general focus on high latitude or high altitude sites where

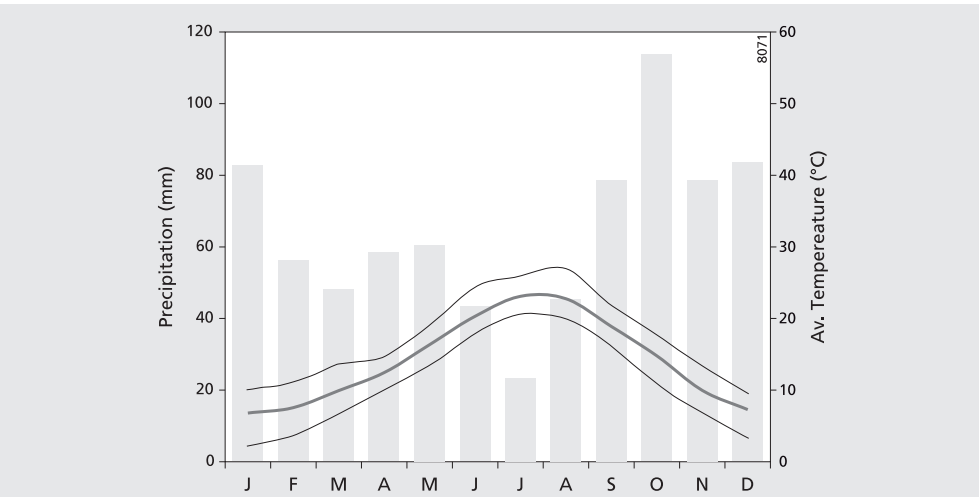

Figure 6.1: Yearly average climate diagram of the study area for 1970-2008. Bars: precipitation, gray line: average temperature, thin lines: monthly average minimum and maximum temperature.

temperature is the main growth-limiting factor and as a result are mainly representative for temperature (Martinelli, 2004; Grudd et al., 2002; Briffa et al., 2004; Büntgen et al., 2005; Büntgen et al., 2010). Mediterranean climates are characterised by a significantly uneven distribution of rainfall over the year with concentrations of precipitation in autumn and spring, and by a regular occurrence of severe moisture deficits in the summer months (fig 6.1). These climatic characteristics cause tree growth to be mainly limited by water availability. Therefore annual tree growth in this region most likely reflects water availability or drought rather than temperature.

The comparison of Mediterranean tree-ring chronologies of needle-leaf and deciduous species to climate data shows a positive growth response to winter and spring precipitation, and a negative response to summer temperature (Martin-Benito et al., 2008; Campelo Nabais et al., 2007; Tessier et al., 1994). Longer chronologies of needle-leaf trees have been successfully used to reconstruct precipitation and drought fluctuations in the Mediterranean basin and Canadian prairies for time intervals of 500 years and longer (Nicault et al., 2008; Touchan et al., 2005; Case and MacDonald., 1995). Evergreen trees do not always show a clear winter stop in their growth because they have leaves all year around. In addition their growth may halt during summer because of water shortage. These phenomena cause a lack of well-defined annual rings in their wood. Mediterranean species are therefore difficult to date accurately, and few dendrochronological studies are available from Mediterranean ecosystems. Cherubini et al. (2003), however, point out that if sufficient care is taken with the selection, sampling and counting, it is possible to use these species for tree-ring analysis. They further claim that such analyses would provide valuable insights in tree-growth processes and sensitivity of evergreen Mediterranean species to anticipated climate change.

Recent studies on holm oak (*Quercus ilex*) tree-ring chronologies from Portugal and Spain illustrate the possibility of using this evergreen species for dendroclimatologic analyses and show good correspondence between tree growth and precipitation (Campelo et al., 2009) as well as temperature (Paton et al., 2009) in and before the growing season. Holm oak often shows a double growing season around a period of drought-induced rest (Paton et al., 2009; Campelo et

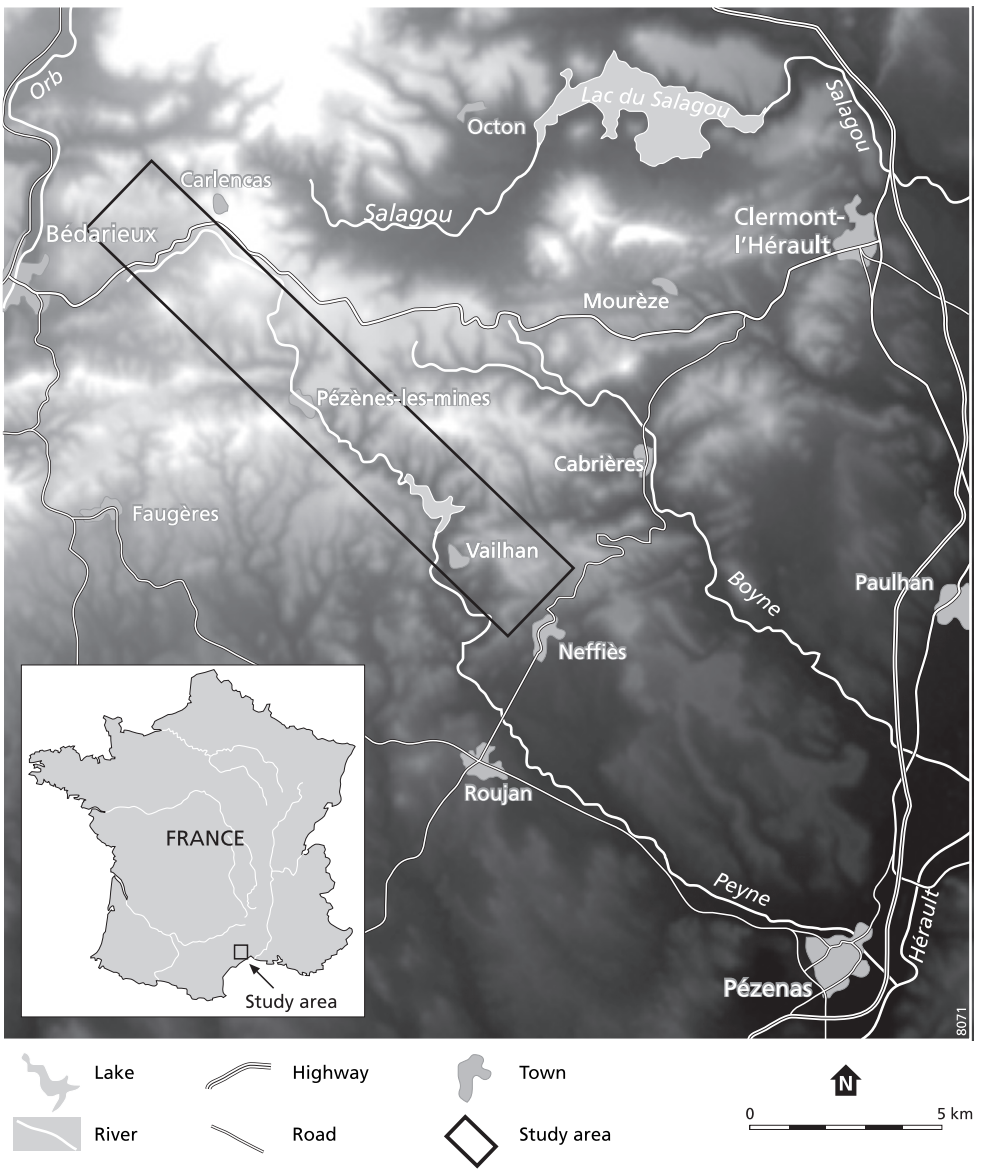

Figure 6.2: Location of the study area in Southern France.

al., 2007). Their conclusions are that spring is the most important growing season and that high precipitation in late summer or early autumn triggers the formation of wide double rings.

As part of a larger study of the effects of climatic change on ecosystem productivity in the Mediterranean we were keen to know which meteorological variables steer biomass production most. The common approach in this case is to apply computer models, which can also be used to evaluate the effects of different climate-change scenarios. However, validation of model performance is limited by data availability from small-scale experiments or indirect data from satellite imagery. In this context tree-ring analysis may provide additional information on past forest productivity and its sensitivity to climate variability. The advantage of ring-width data is that they are available over extended periods of time and are archived in existing forests. Our study area contains different geological substrates which have different water-holding capacities (Nijland et al., 2010) and we would like to know if biomass production on different substrates responds differently to climatic variables. The two dominant tree species in the area are strawberry tree (*Arbutus unedo* L.) and holm oak (*Quercus ilex* L.) and we would also like to know if they show the same growth response to climatic variations. The research questions of this study therefore are:

1) Which meteorological variables have the strongest effect on forest productivity of the evergreen Mediterranean species *Q. ilex* and *A unedo* as expressed in annual stem-growth increments?
2) Is there a difference in the climate sensitivity of *A.unedo* and *Q.ilex* co-existing in the same area?
3) Is there a difference in the climate sensitivity of these species growing on different geological substrates?

6.2 Methods

Study Area

The study area is situated in the catchment basin of the Peyne river, a tributary to the Hérault in southern France (fig 6.2). The region has a Mediterranean sub-humid climate with dry summers and maximum precipitation in autumn (fig 6.1). The annual precipitation sum is very variable, ranging from 400 to 1200 mm with a long-term average just below 800 mm. The mean annual temperature is around 14 °C with monthly average summer temperatures between 20 and 27 °C and monthly average winter temperatures between 2 and 10 °C. The vegetation on the natural sites of the study area is sclerophyll and consists mostly of evergreen shrubs and trees, heath species, odorous herbs and grasses. Dominant species in the area are *Q. ilex* (holm oak), *A. unedo* (strawberry tree), *Quercus pubescens* Wild. (downy oak) and *Erica arborea* L. (tree heath). Mixed deciduous-evergreen oak forests with dense undergrowth are considered the climax vegetation in the area (Tomaselli, 1981), but on the marginal soils this vegetation type usually does not develop. Depending on substrate and history, all types ranging from open scrublands to low dense forests with sparse understory occur (Sluiter and De Jong, 2007; Debussche et al., 1996). The catchment basin is situated at the edge of the 'Montagne Noir' and is characterized by a high spatial variation of geological substrates. These substrates vary with respect to soil type, soil depth and moisture storage capacity, which also might influence the vegetation productivity. Trees were sampled on three types of substrate: Dolomite, Calcareous Sandstone, and Flysch

(Alabouvette, 1982). Soils are shallow and poorly developed and classify as regosols or lithosols according to the FAO soil classification system (Driessen et al., 2001).

Trees

The two dominant tree species of the Peyne area are considered in this study: *Q. ilex* and *A. unedo*. Both species are evergreen and tree heights in our study area range between 3 and 12m.

Quercus ilex L. family: *Fagaceae*. (FR: chêne vert) is a sclerophyllous oak species abundant in large parts of the Mediterranean basin. The leaves are persistent, leather like and variable in form and size. They are mostly elliptical (dimensions: 2 to 7cm long and 1 to 3cm wide) and sometimes have a spiny edge. Flowering is in spring and the acorns ripen in one year (Blamey and Gray-Wilson, 2004). *Q.ilex* wood is semi-ring-porous with larger vessels formed in spring and generally smaller vessels spread throughout the summer wood. The wood has pronounced radial rays (Schweingruber, 1993).

Arbutus unedo L. family: *Ericaceae*. (FR: arbousier) is a tree-like shrub of the heather family growing up to 10m tall. Leafs are dark green and glossy (dimensions: 5 to10cm long and 2 to 3cm wide), with a serrated margin. It flowers in autumn with panicles of bell shaped flowers and has a red rough-surfaced berry (diameter: 1 to 2cm) which ripens during the next summer season (Blamey and Gray-Wilson, 2004). The wood of *A. unedo* is diffuse-porous with most of the vessels formed in spring with often a denser ring of vessels formed at the onset of the growing season

Most forests in the Peyne area have been managed in the past as coppices for charcoal production (Mather et al., 1999). When the forests were cleared, the root systems remained intact and the forests recovered quickly through resprouting. This is still recognizable in the current forest morphology, many smaller stems being grouped in stools that share a common root system.

Data collection:

To obtain ring-width samples, live tree stems were felled and disks were cut from a straight section of the stems at 50 to 100 cm from ground level. A first test series of disks was collected in September 2007. During this field campaign we also sampled a number of trees using an increment corer. After preparation of the cores it proved impossible to obtain accurate ring counts based on the narrow cores, for three reasons: 1) both species show only weak seasonality, 2) some annual rings are locally missing, and 3) *Q. ilex* has pronounced rays which interfere with the rings in sections of little annual growth. For these reasons the core samples were omitted from this study and we focussed on the disks. To increase the number of samples we collected a second series of tree disks in June 2009. In total 34 trees were sampled: 19 *Q. ilex* and 15 *A. unedo*. All disks were prepared by first sanding them and then polishing them using silicon carbide abrasive. The prepared disks were digitized on a 2400dpi flatbed scanner and their images were enhanced for increased contrast and sharpness. The rings were counted along two radial sections following the growth direction of wood. The location of the sections was chosen visually in order to avoid sections with strongly compressed rings and reaction wood as much as possible. The rings were measured manually on screen using CooRecorder (Larsson, 2010)

and while doing this we verified our observations by looking at the original wood through a stereomicroscope with magnification of 8x to 32x. The on-screen method allowed for accuracy assessment and correction of false and missing rings. For the dating and comparison of tree-ring curves we used the program Past4 (Knibbe, 2010). The steps were:

Cross dating the series:

1) Detrending measurement series using logarithms of first differences between adjacent ring widths ($x_i - x_{i-1}$) (Hollstein, 1980).
2) Calculating Student's t-values based on Pearson's cross-correlation coefficients between the series (Wonnacott and Wonnacott, 1990; Jansma, 1995).
3) Calculating percentage of parallel variation between the series 'Gleichlaufichkeit' (Hollstein, 1980).

Verification of results:

to verify results and check for measuring mistakes and missing rings we used: 1) COFECHA (Holmes, 1983). 2) Visual verification of anomalous growth, possible missing rings and measuring mistakes by on-screen comparison of undetrended (raw) ring-width curves and microscope observations of the colour and cell structure of the wood.

Meteorological data

Monthly rainfall sums and temperature averages were obtained from the Meteo France observation station in Gignac (43°39'48"N; 3°33'48"E, altitude 58m), which is about 30km from the study site and at a similar distance to the Mediterranean Sea. Data is available from 1970 to 2008 (38 years). Fig 6.1 shows the monthly averages over the whole period of observation.

Detailed carbon flux data

Gross-Primary-Productivity (GPP) data derived from flux-tower measurements from 2000 to 2008 are used in this study as source of temporally detailed reference data to complement the yearly tree-ring widths. The CarboEuropeIP site Puechabon (FRpue) is situated at approximately 35km from our research area in an evergreen forest dominated by *Q. ilex*. A detailed analysis of the flux data is published in Allard et al. (2008) and the data is publicly available (Rambal et al., 2010). From the available variables in the flux data, we used the GPP because it is most closely related to photosynthesis and includes all of the different influences like water availability, incoming solar radiation, and temperature.

Chronologies

The common signal of the individual measurement series was checked using Cofecha (Holmes, 1983; Grissino-Mayer, 2002). The series were averaged into three chronology types: (a) one single chronology representing all series regardless of tree species and substrate; (b) two species-specific chronologies; and (c) three substrate-related chronologies. For each of the chronologies we only used samples with a high common signal as expressed by the series intercorrelation calculated with Cofecha. Samples with a low common signal caused by reaction wood, local processes or suspected misdating were excluded from the chronologies in order to strengthen the common regional signal in the data. Before combining the measurements in the chronologies, the individual ring-width series were normalised and detrended using a smoothing-spline

function with 50% frequency response for a period of 32 years (Bunn, 2008). The normalised series are expressed as ring-width index (rwi), which is the actual ring width divided by the expected (trend) ring width. The average rwi equals 1 by definition. The chronologies were compared to monthly precipitation sums and average monthly temperatures, using cross-correlation coefficients (Pearson's R). In addition we used Precon (Fritts, 1991) to create bootstrapped response functions. Bootstrapped response functions are a statistically more robust way to compare dendrochronological and meteorological time series and in addition they allow for significance testing (Guiot, 1991).

6.3 Results

Cross-sections were taken from 34 trees in total (19 *Q. ilex* and 15 *A. unedo*). Stem diameters were between 8 and 16cm, which is representative for the tree population in the area.

Annual ring boundaries were difficult to discern in the samples of both species since clear colour signature was absent, average ring widths were below 1mm, and false rings were often present due to summer dormancy. However, we managed to obtain reliable ring-width measurements and dates for most tree sections, by closely examining the cell structure and colour of the wood.

Q. ilex in a productive growth phase shows wide rings, with the vessel and cell sizes steadily decreasing within the year (fig 6.3a). In less productive years its rings are narrow and contain few vessels that decrease in size in a more irregular manner. The annual boundaries of narrow rings are characterized by a jump in vessel size that occurs over a wider section of the wood and usually coincides with a transition from a darker to a lighter wood colour (fig 6.3b).

A. unedo has fine rays in the wood and is diffuse porous, but pore density is mostly highest in the earliest-formed part of the ring (fig 6.3c). False rings frequently occurred within the annual rings and are most probably caused by different growing phases and dormancy within the growing season. These 'rings' can be differentiated from true annual rings because they have vague boundaries rather than the sharp delineation characteristic for winter dormancy (fig 6.3d).

The trees in the study area mostly grow from stools and therefore have skewed or crooked growth forms. As a result the samples contain abundant reaction wood, which to some extent is also reflected by the ring measurements. The resprouting can also be recognised in the wood section, as anomalously large first rings (fig 6.4). The root mass is large compared to the shoot and leaf biomass in this first growth phase, and competition for light and water is greatly reduced (Floret et al., 1992; Khatouri, 1992). In recent clear-cuts, the canopy is observed to close in around five years after logging, this is visible in the samples as a decrease and stabilisation of ring widths.

The longest ring record is 78 years long and the average age for all sampled trees is 55 years. For the analysis we restricted the time series to the maximum length of available meteorological data, i.e. 1970 to 2008, which gives a total of 38 years. By analysing the data for 38 years while average tree age dates back to 55 years we excluded the anomalously large rings formed in the

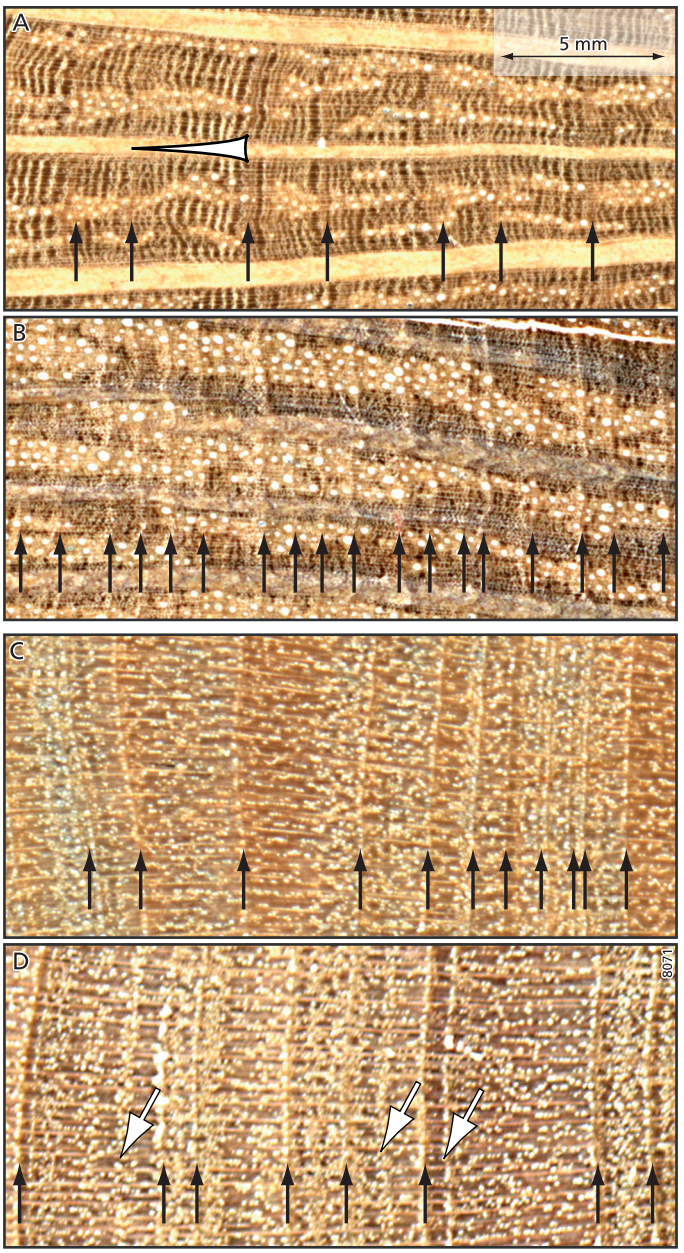

Figure 6.3: Example wood sections of A,B: *Q. ilex* and C,D: *A. unedo* with true (black arrows) and false (white arrows) rings marked. The white marking in A indicates the decreasing vessel size within one year. All sections have the same scale.

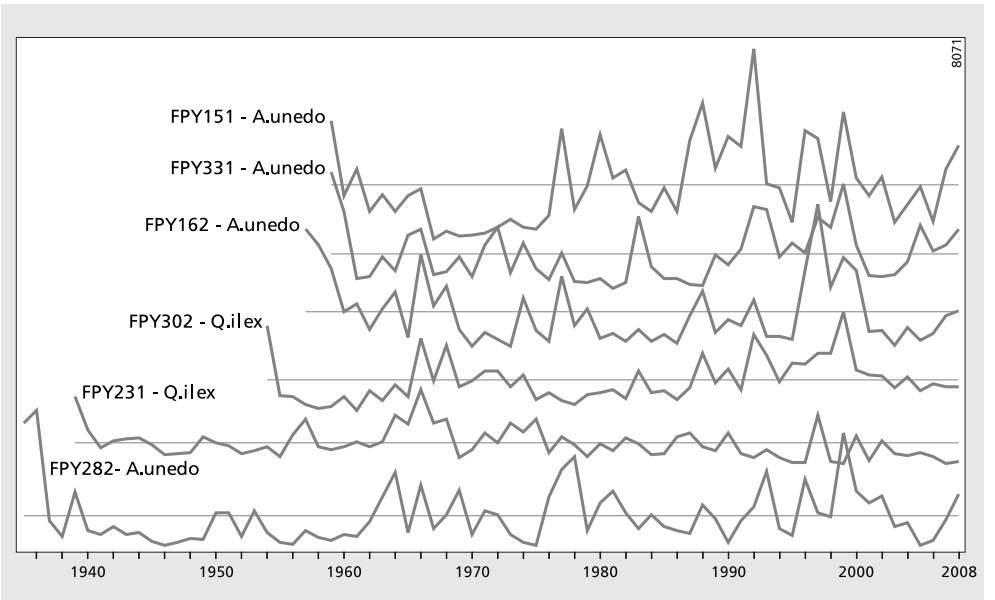

Figure 6.4: : Example ring-width series with characteristically large first rings reflecting coppice and resprouting growth of the forest.

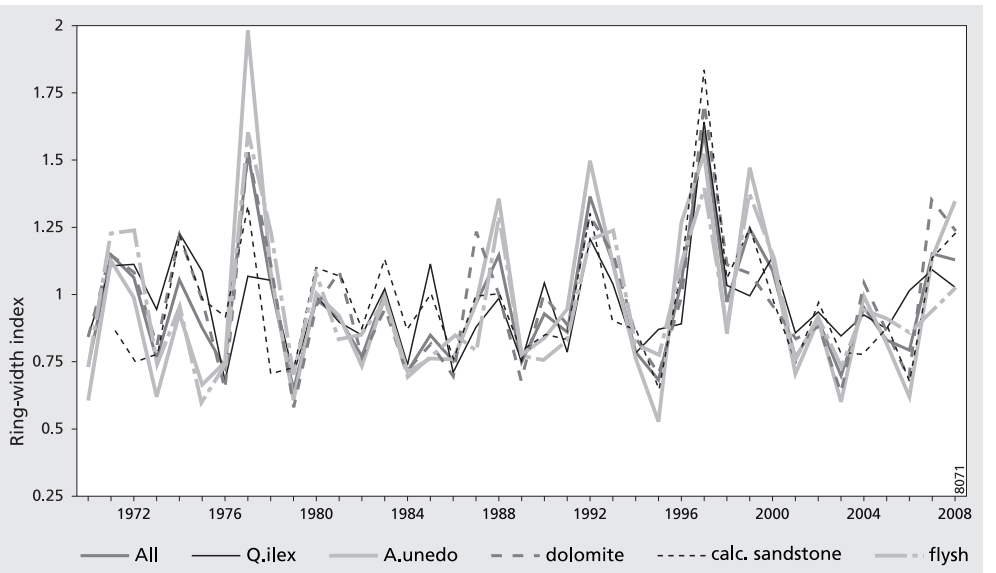

Figure 6.5: Normalized and detrended average ring width chronologies.

first growth years as a result of re-sprouting. For further analysis, ring width chronologies were created from the total pool of ring samples (34 trees * 2 samples), and for subsets based on the two tree species and the three different substrates. The species-specific chronologies each include all substrates, and the substrate-specific chronologies equally represent both species growing on that substrate. Table 6.1 lists the different chronologies and their descriptive statistics. The correlation and sensitivity of the *A. unedo* chronology are higher than those of *Q. ilex*, indicating a stronger common forcing on *A. unedo*. The substrate-specific chronologies show a less clear signal with the highest correlation for Dolomite and the highest sensitivity for Flysch. The number of samples included in the substrate chronologies is limited, but correlations and sensitivity of the series are adequate (above the critical level of 0.32 for p = 0.05 and n = 38) for further analysis (Table 6.1).

The normalised ring-width chronologies show very similar patterns throughout the analyzed range, indicating a strong common forcing and accurate relative dating (fig 6.5). Positive pointer years are visible in 1977, 1992, and 1997 and negative pointer years are 1995, 2003 and 2006 (Schweingruber et al., 1990).

Table 6.1: Base statistics of the ring-width chronologies. [1]) minimum\maximum of yearly averaged ring widhts in each chronolology. [2]) Average correlation between the radii in each chronology over 38 years.

	Total	*Q.ilex*	*A.unedo*	Dolomite	Calc. Sandstone	Flysch
No. trees sampled	34	19	15	8	9	17
Min. age [years]	34	44	34	34	51	44
Max. age [years]	78	76	78	76	60	78
No. trees used	23	12	11	8	7	12
No. radiï	41	19	22	13	12	19
Average ring width [mm]	1.02	0.94	1.06	1.22	0.81	0.91
Min year-av ring width[1] [mm]	0.60	0.57	0.53	0.70	0.43	0.58
Max year-av ring width[1] [mm]	1.64	1.74	1.93	2.02	1.58	1.50
Normalized & detrended series						
Min ring width index	0.65	0.68	0.53	0.58	0.65	0.60
Max ring width index	1.61	1.64	1.98	1.70	1.83	1.59
Average Correlation[2]	0.42	0.35	0.51	0.50	0.33	0.39
Sensitivity	0.46	0.36	0.55	0.38	0.45	0.49
Correlations between chronologies						
all		0.76	0.93	0.84	0.77	0.85
Q.ilex	0.76		0.50	0.79	0.59	0.56
A.unedo	0.93	0.50		0.69	0.71	0.86
Dolomite	0.84	0.79	0.69		0.64	0.58
Calc. Sandstone	0.77	0.59	0.71	0.64		0.50
Flysch	0.85	0.56	0.86	0.58	0.50	

Climate response

Next we analyzed the relationship between ring width and weather conditions. The correlation coefficients and response functions between the annual ring widths and monthly average temperatures and precipitation sums over the period from 1970 to 2008 (38 years) show a consistent and significant climatic forcing on tree growth (fig 6.6).

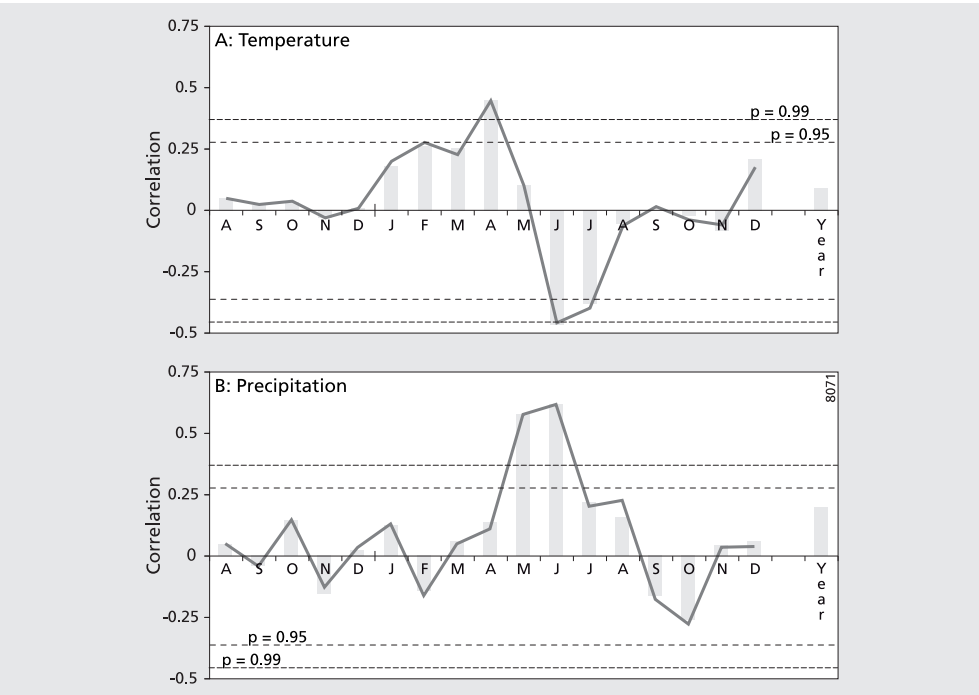

Figure 6.6: Correlations (bars) and response functions of monthly average temperatures (A) and precipitation sums (B) with yearly growth indices of the all tree chronology.

The temperature graph shows two main features: a positive temperature/growth relationship in January to April, and a negative one in June and July (fig 6.6a). This means that tree growth benefits from high temperatures at the beginning of the vegetation period and that growth is reduced if summer temperatures are high. The precipitation graph shows a strong positive tree-growth response in May and June, indicating a high dependence of the trees on rainfall in these months (fig 6.6b). May and June are the most productive months of the growing season in the area and the clear correlation with precipitation in these months shows that productivity is strongly drought limited. A second feature in the precipitation graph is a small negative growth response in September and October. The negative response is likely to be caused by the correlation between warm summers and high precipitation in these months and shows that the trees in this area do not benefit from the large amounts of precipitation falling in September and

October. The growth potential in autumn is low because of the declining temperatures and day length at the end of the vegetation period.

The last bar in each graph shows the relationship between ring width and yearly averaged temperature and precipitation. The correlation with the yearly variables is low and insignificant, showing that analysis of yearly averages does not reveal the actual sensitivity of the trees to climate variability. Both graphs also show little correlation with conditions in the preceding year (August to December), indicating that there is no memory effect in this ecosystem.

Comparison of the climate response functions of *Q. ilex* and *A. unedo* (fig 6.7) shows a slight temporal difference between their growth responses, with *A. unedo* having it strongest response a bit earlier in the season than *Q. ilex*. Apart from this their response is very similar, which is to be expected because they belong to the same plant-functional type of evergreen broadleaf trees/ shrubs. *Q. ilex* and *A. unedo* can be found in mixed stands throughout our study area and other parts of the Mediterranean basin.

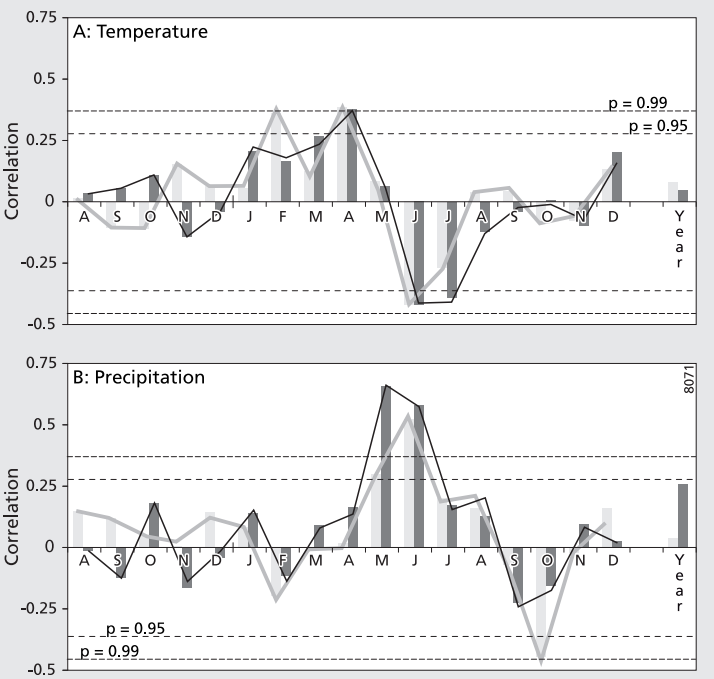

Figure 6.7: Correlations (bars) and response functions of monthly average temperatures (A) and precipitation sums (B) with yearly ring widths of the *Q. ilex* (white) and *A. unedo* (black) chronology

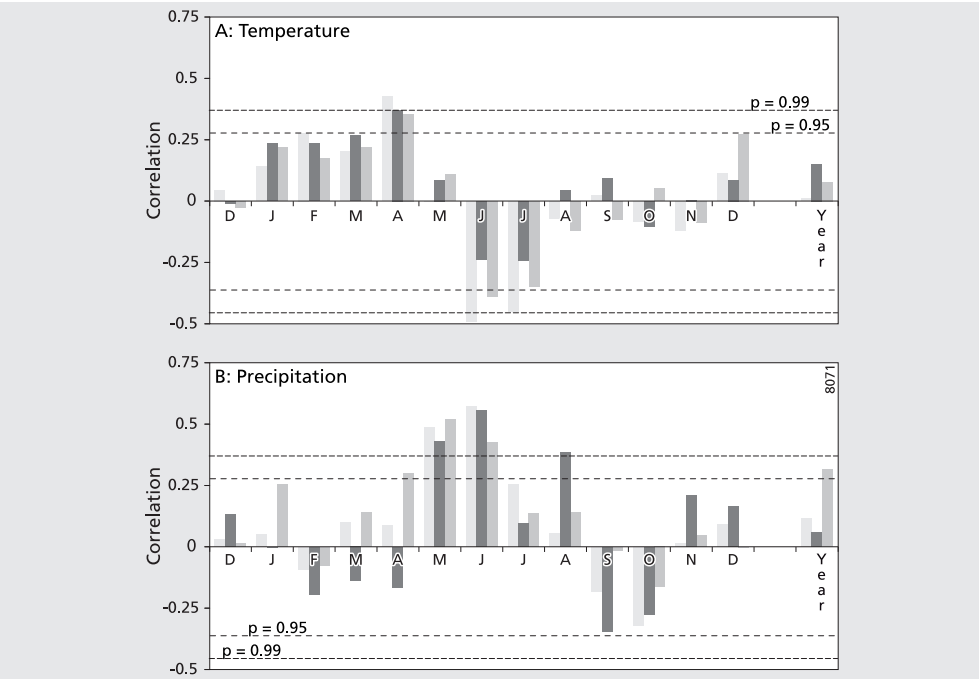

Figure 6.8: Correlations of monthly average temperatures (A) and precipitation sums (B) with yearly ring widths of the Dolomite (white), Calc. Sandstone (gray), and Flysch (black) chronologies.

The differences of the response functions for the three substrate-based chronologies are small (fig 6.8). Conclusive interpretations based on these response functions are necessarily limited due to the low number of samples in each class. The most notable difference occurs between the Calcareous Sandstone chronology and those of both other substrates, the Sandstone chronology showing lower sensitivity to summer temperatures and a high response to August precipitation whereas both other substrate chronologies show no response to precipitation in August.

To examine the processes underlying the yearly wood production in more detail we compared our data to GPP data from flux tower measurements. We specifically looked at 2004 and 2006 as examples of a typical high productive (2004) and low productive (2006) year (fig 6.9). The difference between these two years shows a high correspondence with climate response we found in the tree-ring analysis and therefore provides confirmation of the climate/growth responses we inferred for Peyne. Two important differences are visible in the GPP curves of 2004 and 2006. The most striking difference is the large dip in productivity in May to August of 2006 where only a narrow dip is present in July and August of 2004. The second difference is a generally higher productivity during the first half of 2004 than during the first half of 2006. The large reduction in 2006 summer productivity is caused by low spring and summer rainfall in combination with high summer temperatures. In 2004 the productivity is also reduced during the warmest part of the summer, but the decline starts much later because of higher spring

precipitation. The high productivity in the first half of 2004 is caused by higher early spring temperatures resulting in an early start of the growing season.

6.4 Discussion & Conclusions

In this study we present the combined analysis of tree-ring chronologies of two Mediterranean evergreen tree species and 38 years of monthly temperature and precipitation data from the same area. Despite the difficulties in measuring and dating the annual rings we found consistent ring-width patterns and a strong response of tree growth to climate variability. The analyses prove a significant statistical relation between annual stem increments and monthly meteorological variables and the patterns we found provide valuable insights regarding the mechanisms behind tree growth and the sensitivity of the ecosystem to climate variability. The inferred physiological processes are confirmed by a more detailed temporal look at the ecosystem based on flux-tower measurements.

In our study area, tree growth is purely dependent on the conditions during the growing season, most importantly rainfall in May and June. This is in contrast to the results of four independent studies of *Q. ilex* ring chronologies established in Portugal and Spain. These studies show a stronger sensitivity to winter and early-spring precipitation, most likely because of greater water retention in the soil (Campelo et al., 2009; Paton et al., 2009; Gea-Izquierdo et al., 2009; Nabais et al., 1998). A study on young *Q. ilex* trees grown from acorns in Montpellier (60km from our site) shows a response that is similar to the Peyne response, with high climate sensitivity during the current growing season and no response to the conditions during the preceding year (Zhang and Romane, 1991). The response functions for both temperature and precipitation (fig. 6.6) show no significant growth response to weather conditions in August, while this month is in the

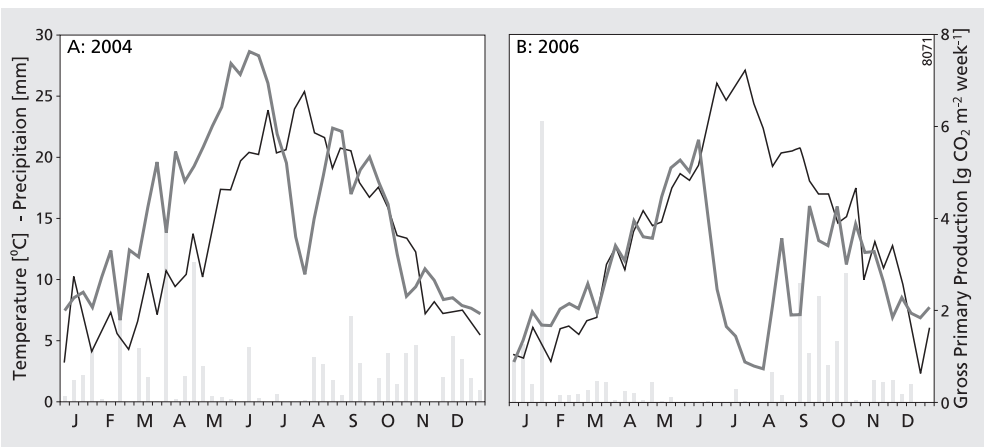

Figure 6.9: Weekly ecosystem gross productivity (gray line), average temperatures (thin black line), and precipitation (bars), derived from flux measurements at Puechabon CarboEuropeIP test site.

middle of summer season. A possible explanation of this phenomenon is that even in wetter or cooler years both trees species show very little growth in August because growth is still limited by drought and/or heat. The difference we found between the Calcareous Sandstone and both other substrate chronologies indicates that the vegetation on the former substrate maintains a better growth potential throughout the dry season. Trees on Calcareous Sandstone show a stronger positive response to August rainfall, which fits with the higher clay content and the deep water retention that is found on this substrate (Nijland et al., 2010).

Modern climate change is expected to intensify the typical characteristics of the Mediterranean climate. Temperatures will increase throughout the year, and rainfall will concentrate more in autumn and winter, leaving a more persistent dry period in summer (Hertig and Jacobeit, 2008; Gao and Girogi, 2008; Geblin and Déqué, 2003). Our results show that especially an intensification of summer drought may have serious deteriorating effects on tree growth.

The results of a combined analysis of monthly meteorological records and annual tree-ring widths can provide valuable insights in ecosystem functioning and its sensitivity to climate variability and possible climate change. As ring widths from the past are archived in living trees and are readily available for at least the past five decades in most standing forests, they are an important information source for the prediction and modelling of vegetation development. This source at present is underused in Mediterranean climates (Cherubini et al ., 2003).

Accurate parameterisation of productivity models is complicated by the scarcity of field data, for example from detailed gas exchange or sap-flow measurements. In absence of other data, ring widths may be used to determine the relative importance of different limiting factors (e.g. water, temperature) on productivity throughout the year. Integration of model results and ring measurements may aim at reproduction of ring width chronologies using forest simulation models, but can also aim at matching the seasonal sensitivity of the models to climatic variability to the response function derived from the analysis of tree ring and meteorological data. By calibrating the models using the seasonal patterns of limiting factors in addition to the total annual productivity or resulting leaf area, the model results are greatly improved especially towards the assessment of climate-change vulnerability. If climate-related stem growth is representative for the overall growth of trees (with other biotic and abiotic factors having a relatively weak impact), and if stem growth during a period of already increased temperature can be compared to growth before increased greenhouse gas concentrations, then the conclusion would be justified that the growth-climate relations we established will be valid in the future. However, the Mediterranean climate is very variable and predicted changes are smaller than the current year to year variability contributing to the likeliness of the relation remaining valid in a future changed climate. Although detailed plant-physiological studies remain very important for the understanding of plant growth and ecosystem functioning, tree-ring analysis seems to be a very promising tool for expanding both the temporal scale as well as the geographical coverage of field-validation data.

In this study we focussed on ring width data only, but other studies in Mediterranean areas suggest that more detailed measurements of wood anatomy (Campelo et al., 2010) or including

double ring data (Campelo et al., 2007; Zhang and Romane, 1991) may also provide information on the sensitivity of trees to climate.

In conclusion, we found that the evergreens *Q. ilex* and *A. unedo* in the Peyne area in southern France are very sensitive to precipitation in the months from April to July and are also sensitive to spring and summer temperatures. The trees hardly benefit from the precipitation surplus in autumn and winter. Both species effectively show a very similar pattern in their climate response. There are little differences between the substrate-related responses, with the examined substrates all being shallow but characterized by different water-retention capacities. Trees growing on the Calcareous Sandstone are more sensitive to August rainfall than on the other substrates which indicates a larger growth potential during the driest and warmest part of the summer.

Tree-ring analysis of Mediterranean evergreen species is not easy because of frequent false rings and unclear ring boundaries, but accurate measurement and dating is possible if enough care is taken during the preparation and measurement of the samples. Combining ring-width chronologies with meteorological records provides useful information on vegetation functioning and climate sensitivity. Tree stems contain much information that is of great interest to productivity modelling and climate-impact predictions. This information is archived and readily available in every forest.

Acknowledgements
The authors thank Rogier de Jong, Wilco Klutman and 'Boomwerk Bilthoven' for their cooperation in felling and sampling the tree stems and Emma Daniëls is kindly acknowledged for her help in the ring-width measurements.

7. Modelling vegetation growth for past and future climates using Forest-BGC

7.1 Introduction

Vegetation growth in Mediterranean climates is generally slow and limited by the warm, dry climate. The same climate makes the region an attractive place to live and work and for leisure activities. Furthermore, the Mediterranean region is an interesting settlement location for high-tech companies resulting in increasing population numbers and environmental pressure: traffic, transport, recreation, and water consumption (UNEP, 2009). Next to the increasing human pressure on the Mediterranean region, the anticipated climate change for the upcoming century will intensify the warm and dry character of the climate which may lead to decreased water availability and changes in vegetation growth (Gao and Giorgi, 2008; Hertig and Jacobeit, 2008). The changes in vegetation growth and biodiversity may have adverse effects on the attractiveness of the area and it is therefore important to consider these changes in long-term economic planning.

Present knowledge about interactions between the landscape, climate and vegetation is insufficient to make reliable predictions about the impact of climate change on the region. Climate change with shifting patterns of rainfall and generally increasing temperatures may result in higher or lower vegetation productivity, or changes in species composition. In this study I focus on changing productivity of the natural vegetation. To improve the future projections of vegetation development the dynamical vegetation model Forest-BGC (Running and Coughlan, 1988; Running and Gower, 1991) is used and its performance is analysed using field data and tree-ring analysis. Dynamical modelling of vegetation productivity is an important tool in assessing the effects of change scenarios on the landscape. In this chapter, knowledge obtained from field observations, remote-sensing image analysis, and tree-ring chronologies as described in chapters 3 to 6 are used to parameterize and validate the Forest-BGC model for the forests in the Peyne area. Next, the model is used to evaluate the effects of the expected climate changes on tree growth in the area.

Forest-BGC is selected for this modelling exercise, because it has a good balance between model process complexity and the number of parameters needed. Forest-BGC has been successfully adapted to run in a variety of forest environments, including Mediterranean broadleaved evergreen forests like in our study area (Hoff et al., 2002). Modelling forests in a Mediterranean climate sets specific demands on the model principles because vegetation is mostly limited in its growth by the typical climate with long dry periods during the summer, therefore the vegetation is only marginally productive. Anticipated climate change may further increase these limitations because of higher temperatures and increasing aridity during summer (Gao and Giorgi, 2008; Hertig and Jacobeit, 2008). It is therefore crucial to use a model with an accurate process

description with respect to water shortage and able to capture the seasonal variability in rainfall and the resulting water stress.

The modelling exercise is applied in two steps. First, the model is used with true meteorological data for the past 60 years to validate the model results against field data and tree rings. Second, the model is used with meteorological records adapted such that they fit climate projections for 2070 (Gao and Giorgi, 2008) to evaluate the sensitivity of vegetation growth to anticipated climate change and to create projections of future vegetation development.

In the validation step the model results are compared with both the state of the current ecosystem and variability in the productivity during the past four decades. The use of field observations over the last four years, and tree ring data for the last four decades allows the evaluation of the model performance on decadal/centennial as well as on a monthly/seasonal timescale. In the Peyne study area in southern France, we collected extensive reference data to test the model results. The data consist of vegetation surveys (Chapter 3 and 4), soil water availability measurements (Chapter 5) and tree-ring data (Chapter 6). In the vegetation surveys, Leaf Area Index (LAI) and aboveground biomass were measured as principal vegetation variables. The studied forests were used for coppicing in the past, but the last harvest was at least 60 years ago. Soils in the area are very shallow, but the vegetation is able to use deeper sources of water stored in the fissured bedrock. The profiles have a very high rock fraction and roots are found to penetrate down to 6m or deeper into the rock (Chapter 5; Nijland et al., 2010). Tree-ring measurements are an accurate source of information on stem growth over the past 40 years. By analysing the relation between stem growth and monthly meteorological variables, I also derived information about the monthly sensitivity of the trees to temperature and precipitation (Chapter 6; Nijland et al., 2011).

In the scenario runs, the effect of changes in temperature and precipitation are evaluated. Changes are used both constant over the year, and with a stronger change in the summer season as predicted by Gao and Giorgi (2008). The main research question of this chapter is:
What will be the effect of regional climate change on the growth of Mediterranean evergreen broadleaved forests?

To answer this question, Forest-BGC is parameterized for the specific vegetation and soils in the study area to evaluate the model performance at both decadal and seasonal timescales. Field observations and tree-ring records are used as reference data for the model validation.

7.2 Methods

Model Principles

Forest-BGC (Bio Geochemical Cycles) (Running and Coughlan, 1988; Running and Gower, 1991) is an ecosystem productivity model that simulates the carbon, nutrient and water cycles for a homogeneous forest stand. The primary productivity and photosynthesis run at a daily time step and require daily inputs of meteorology (minimum and maximum temperatures, precipitation, humidity, and incident shortwave radiation). Production is accumulated and

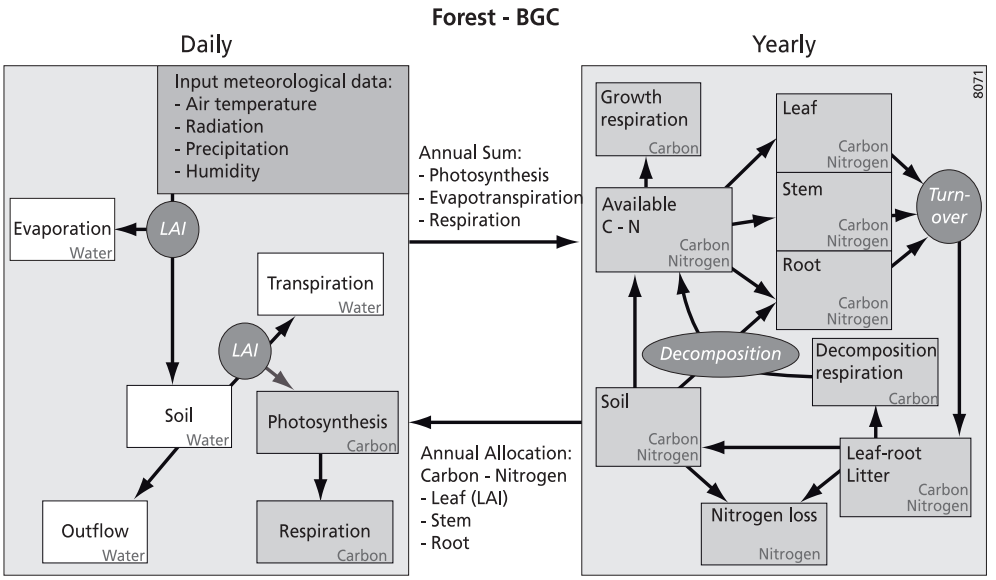

Figure 7.1: Model scheme of forest BGC, after Running and Coughlan (1988).

dynamically allocated to leaves, roots and wood once a year (fig 7.1). Forest-BGC was originally developed for cool climate needle-leaf forests, but it was successfully adapted for Mediterranean deciduous forests (Chiesi et al., 2002) and broadleaf evergreen forests (Hoff et al., 2002).

A prerequisite for using a model to make predictions is that the model performs well on both the decadal/centennial as monthly/seasonal timescales. The monthly or seasonal timescales provide guidance to how realistic the model processes are. Most climate scenarios based on regional climate simulations predict that the changes will not be uniform over the year. A reliable representation of monthly/seasonal processes is therefore important to avoid bias in the outcomes of the vegetation model. If the model performs well on both temporal scales, it is reasonable to assume that the predictions are also reliable.

For this study Forest-BGC was coded in the PCRaster Python modelling framework based on the original publications of Running and Coughlan (1988) and Running and Gower (1991) and their Turbo Pascal source code. The model has two components: a daily and a yearly cycle.

The daily model calculates the water balance, transpiration, photosynthesis and maintenance respiration based on daily inputs of temperature, precipitation, radiation and humidity. In the water balance, the soil is modelled as a single layer without lateral interaction. Soil water recharge is calculated from precipitation minus the interception by the canopy. Any water exceeding the soil water-holding capacity is considered to be drainage and leaves the system. Potential transpiration is calculated according to Penman-Monteith (Monteith, 1965). The relation between soil-water content and soil-water potential [Pa] is adapted according to Hoff

Table 7.1: Parameter values for the Forest-BGC model. source: Hoff et al. (2002).

Parameter	Value	unit
Air CO_2 concentration	0,0006	molCO_2 / mol air
Leaf CO_2 concentration	0,00007	molCO_2 / mol air
Air entry soil water potential	-0,004	MPa
Empirical value for soil water potential exponent	5,05	-
Specific leaf area	0,01169	m^2 / gC
Canopy light extinction coeff	0,72	-
Soil field capacity	130	mm
Rainfall interception	0,5	mm / LAI / day
Surface albedo	0,12	-
Minimum leaf water stress (no water restriction)	-0,2	MPa
Half maximum radiation level	3000	kJ / m^2 / day
Maximum canopy water conductance	0,0025	m / s
Cuticular conductance	0,000031	m / s
Maximum leaf water stress (inducing stomatal closure)	-3,5	MPa
Slope of canopy conductance vs. absolute humidity deficit	0,05	m / s / g / m^3
Photosynthesis light compensation point	432	kJ / m^2 / day
Photosynthesis response coefficient	9720	kJ / m^2 / day
Maximum Leaf CO_2 conductance	0,0005	m / s
Low temperature photosynthesis compensation point	0	°C
High temperature photosynthesis compensation point	40	°C
Leaf maintenance respiration coefficient	0,00012	gC / °C / day
Wood maintenance respiration coefficient	0,000012	gC / °C / day
Root maintenance respiration coefficient	0,00033	gC / °C / day
Temperature effect on mesophyll conductance adjustment scalar	4	-
Respiration coefficient Q_{10}	2,3	-
Maximum leaf nitrogen concentration	0,0396	gN / gC
Minimum leaf nitrogen concentration	0,0242	gN / gC
Leaf nitrogen retranslocation fraction	0,27	-
Nitrogen/carbon decomposition factor	0,5	-
Maximum LAI	6	m^2 / m^2
Average leaf lifespan	1,5	year
Leaf lignin fraction	0,158	-
Mobile nitrogen retention time	20	Years
Atmospheric nitrogen deposition	2,8	gN / m^2 / year
Wood turnover coefficient	0,01	- /year
Root turnover coefficient	0,9	- /year
Growth respiration coefficient (leaf, root and wood)	0,22	-
Optimal decomposition temperature	20	°C
Fractional constant of soil/litter carbon decomposition rates	0,0005	-
Decomposition rate scalar	0,85	-

et al. (2002), using an exponential relation between the soil-water content and the soil-water potential instead of the originally proposed linear equation. The Hoff relation better simulates the highly negative soil water potentials occurring under Mediterranean forests. Photosynthesis carbon fixation is calculated per day using biochemical principles. The most important variables influencing photosynthesis are the leaf area, canopy water availability and canopy CO_2 conductance. This last variable is the product of a species specific maximum and limitation indices for shortwave solar radiation, N availability and temperature. From this potential productivity the maintenance respiration, which is a function of temperature and the carbon pools, is subtracted to calculate the Net Primary Productivity (NPP).

On a yearly basis the totally produced carbon is allocated to the leaves, roots, and wood. The leaf growth is limited by water and nitrogen availability. The root growth is calculated as a ratio of the leaf growth. The ratio is influenced by water and nitrogen limitation. Wood allocation is calculated as the excess carbon after leaf and root growths are satisfied. The availability of nitrogen is calculated using the soil and litter pools of nitrogen, and decomposition which is a function of yearly average temperatures. The litter pools are refilled by leaf turnover. The new pools of carbon and nitrogen are calculated in the yearly time step as the product of a fixed turnover and the new allocation. The leaf carbon pool is hereby essential because it is translated to Leaf Area Index (LAI) for the next year using the leaf mass per area parameter.

Model parameterization

Species specific model parameters were set to the values reported by Hoff et al. (2002) and are summarized in Table 7.1. This parameterization was originally made for a coppiced *Q. ilex* stand in the Puechabon, located approximately 35km east of the Peyne field site. The Peyne forests are mixed *Q. ilex* and *A. unedo*, but both species are broadleaved evergreens and the *Q. ilex* parameterization is therefore assumed to be valid for this mixed stand. To account for the differences in forest characteristics between the Puechabon and Peyne areas, Forest-BGC was calibrated by adapting the values for maximum canopy CO_2 conductance and cuticular conductance. These parameters regulate the productivity of the vegetation and the resistance to summer drought. (Chiesi et al., 2007). The Peyne area has similar leaf-area values to the Puechabon, but considerably lower wood biomass. To simulate this, the maximum canopy CO_2 conductance was lowered from 8.0 $*10^{-4}$ to 5.0 $*10^{-4}$m s^{-1} and the cuticular conductance was lowered proportionally (from 5.0 $*10^{-5}$ to 3.1$*10^{-5}$m s^{-1}).

Input meteorology

Meteorological input data for the Forest-BGC model were based on the European Climate Assessment and Dataset (ECA&D) (Klein Tank et al., 2002) station Sète (Station ID: 797, Location: 43.2°N; 3.4°E, Elevation 80m). The meteorological station is located 40km south of the field site. This dataset was used because it was the only available dataset with a sufficiently long daily record. From direct measurements only daily minimum, maximum, and average temperatures, and precipitation are available. To create complete series of meteo data required by the Forest-BGC model, we used MT CLIM (version 4.3 for Excel) (Thornton and Running, 1999; Kimball et al., 1997; Glassy and Running, 1994). MT CLIM estimates daily values for vapour pressure deficit and incident radiation from temperature and precipitation inputs. Soil temperatures were calculated using an empirical relation derived from daily observations of soil

and air temperatures on the Puechabon CarboEurope-IP site from 2000 to 2008 (Rambal et al., 2008) and is based on 10 day running average air temperatures.

$$SoilT = 0.84 + AirT_{10day} \times 1.73 \qquad \text{Equation 7.1}$$

where: $SoilT$ = average soil temperature, $AirT_{10day}$ = 10 day average air temperature. The r^2 for this function is 0.96.

Reference data

The reference data used to validate the model outcome are field plots of aboveground biomass and LAI, and tree-ring data. From the model results,

NPP [gC m^{-2} $year^{-1}$], LAI [m^2 m^{-2}], and wood biomass [gC m^{-2}] are used. Wood biomass has the most direct relation to the tree-ring reference data and field measurement of aboveground biomass. NPP is used to evaluate the productivity part of the model that is run at a daily time-step, without considering the effects of the yearly allocation routine. LAI is chosen as an additional variable because leaf area is one of the primary indicators of ecosystem functioning and is directly related to photosynthetically active surface and plant evapotranspiration.

All reference data on the current forest state and the development in the past were collected in the Peyne area. In the naturally forested areas aboveground biomass and Leaf Area Index (LAI) were measured in 5 by 5m square plots, and wood samples were collected for tree ring analysis. The aboveground biomass was calculated based on stem diameters and an allometric relation reported by Ogaya et al. (2003) (Table 7.2).The LAI was determined using digital hemispherical photographs of the canopy that were analysed using the Can-Eye software (Jonckheere et al., 2004; Weiss et al., 2004) which is also explained in more detail in Chapter 3 (Addink et al., 2007; Nijland et al., 2009).

In 55 field plots I measured an average LAI of 3.9 (sd: 0.6) and an aboveground biomass of 1,4kgDM m^{-2} (sd: 0.7) (Table 7.3). For this area I assume that the ratio between aboveground and belowground biomass is 1, and 45% of the dry matter consists of carbon (Hoff et al., 2002) which results in a woody biomass of 1.3kgC m^{-2} (sd = 0.6). For the Puechabon area the reported values are 2.9 for the LAI and 7.3kgDM m^{-2} for aboveground biomass (Hoff et al., 2002).

To obtain data on the past productivity of the forest I use stem-growth increments stored in living trees as annual tree rings. A total of 34 tree stems of *A. unedo* and *Q. ilex* were sampled

Table 7.2: Allometric relations for aboveground biomass (Ogaya et al.,2003).

Species	Formula	Source
Arbutus unedo	ln AB = 4.251 + 2.463 * ln D50	Ogaya et al., 2003
Quercus ilex	ln AB = 4.900 + 2.277 * ln D50	Ogaya et al., 2003

AB : Aboveground biomass indvidual [g]

D50: : Stem diameter at 50cm above ground level [cm]

Table 7.3: Basis statistics of the field plots for aboveground biomass and Leaf Area Index.

	aboveground biomass [kgDM m^{-2}]		LAI [-]	
	average	sd	average	sd
Total	1,43	0,70	3,96	0,59
Flysch	1,30	0,65	4,05	0,57
Dolomite	1,63	1,03	3,51	0,60
Calcareous Sandstone	1,70	0,42	4,02	0,54

and analysed for annual tree rings as presented in chapter 6 (Nijland et al., 2011). The tree-ring analysis yielded two variables that can be compared with modelled growth predictions: 1) time series from 1968 to 2008 of yearly stem-growth increments, 2) response functions of stem growth to monthly variability in temperature and precipitation. Comparison between the yearly records is straightforward, the direct relation between the modelled productivity and the stem increments from the tree rings indicates the validity of the model. For a comparison of the tree ring data and model outcomes on a monthly basis, I use the sensitivity of both time series to the monthly variability in the meteorological input data. The method of creating these monthly response functions of these series is commonly used in tree-ring analysis and is described for the used tree-ring data in chapter 6. The series are correlated to the temperature and precipitation in each of the months within the year to assess the importance of each month to the total growth. The yearly model outcomes of NPP, LAI, and woody biomass are subjected to the same process to create the response functions that can be directly compared to the tree-ring based response functions.

Scenario Simulations

Forest-BGC was fed with eight different scenarios to study possible future changes in forest productivity. To create meteorological inputs for scenario simulations, the original meteorological time series of 1950 to 2010 is used as a basis. The data was altered by shifting the temperature or decreasing the precipitation with a percentage. The change scenarios are based on the climate simulations of Gao & Giorgi (2008). They used a regional climate model (RCM) for the Mediterranean basin and worked out the IPCC A2 and B2 scenarios (IPCC, 2007). Their results for Mediterranean France in 2070 predict a temperature rise between 3 and 6°C for the summer and between 1 and 3°C for the winter plus a decrease in precipitation of 20% to 50% during the summer with winter precipitation remaining the same or even showing a slight increase. Based on Gao & Giorgi (2008) the "most probable" scenario has a 2°C increased temperature in winter and 5°C increased temperature in summer with a decrease in summer precipitation of 40%. The seasonal temperature change is applied as a cosine function with +2°C at the first day of the year and +5°C at day 183. The decrease in summer precipitation is applied for the months May to August. The following eight scenarios were defined (Table 7.4):

1. Normal run with unaltered meteorological data of 1950 to 2009
2. An increase of the average annual temperature of 3°C.
3. A decrease of the annual precipitation of 10%.

4. Combined effect of an increase of the average annual temperature of 3°C and a decrease of precipitation of 10%
5. An increase of the temperature with seasonality: winter +2°C and summer +5°C.
6. A decrease of summer precipitation with 40%.
7. A 'most probable' scenario of climate change for the next decennia with a combined seasonal increase of the temperature (winter +2 °C and summer +5 °C) and a decrease of summer precipitation with 40%.
8. An extreme scenario simulating a completely dry four month summer combined with an increase of the temperature with 2 °C in winter and 5 °C in summer

7.3 Results:

Normal run: 1951 - 2008

The model run is initialized with values for LAI of 1,5 and for wood biomass of 250 gC m^{-2} to simulate the situation of quick resprouting after coppicing in which the trees quickly recover an initial leaf area and the remaining stumps are the basis for regrowth. The model is run for 60 years (1950 – 2009) for both the original (Puechabon) and Peyne calibrated parameter settings (fig 7.2). The model shows a very quick recovery of the leaf area (within 5 years) to values between 3 and 4 with some years showing values over 5 as some sort of outlier which fall back to the base level in the next year (fig 7.2b). The wood biomass increases steadily for the first three decades and then stabilizes (fig 7.2c). The main difference between the calibrated and original model runs are visible in the wood biomass which is considerably lower in the calibrated runs, fitting the observed values in the study area. The primary productivity is slightly lower, while the leaf area is almost the same resulting in a decreased allocation of carbon to wood production. The average values of both biomass and LAI are within the standard deviation of the measured field values and the general pattern looks reasonable except from the high spikes in the LAI graph. The spikes are the result of years with high rainfall, in these years there is no water limitation to leaf growth and all available carbon is allocated to the leaf and root compartments causing very high LAI and no allocation to wood.

Table 7.4: Climate Scenarios used in Forest-BGC to assess the effect of climate change.

	Scenario	Temperature Change		Precipitation Change	
		winter	summer	winter	summer
1	normal	-	-	-	-
2	year temperature	+ 3		-	
3	year precipitation	-		-10%	
4	year temperature & precipitation	+3		-10%	
5	seasonal temperature	+ 2	+ 5	-	-
6	seasonal precipitation	-	-	-	- 40%
7	seasonal temperature & precipitation	+ 2	+ 5	-	- 40%
8	seasonal temperature & dry summer	+ 2	+ 5	-	- 100%

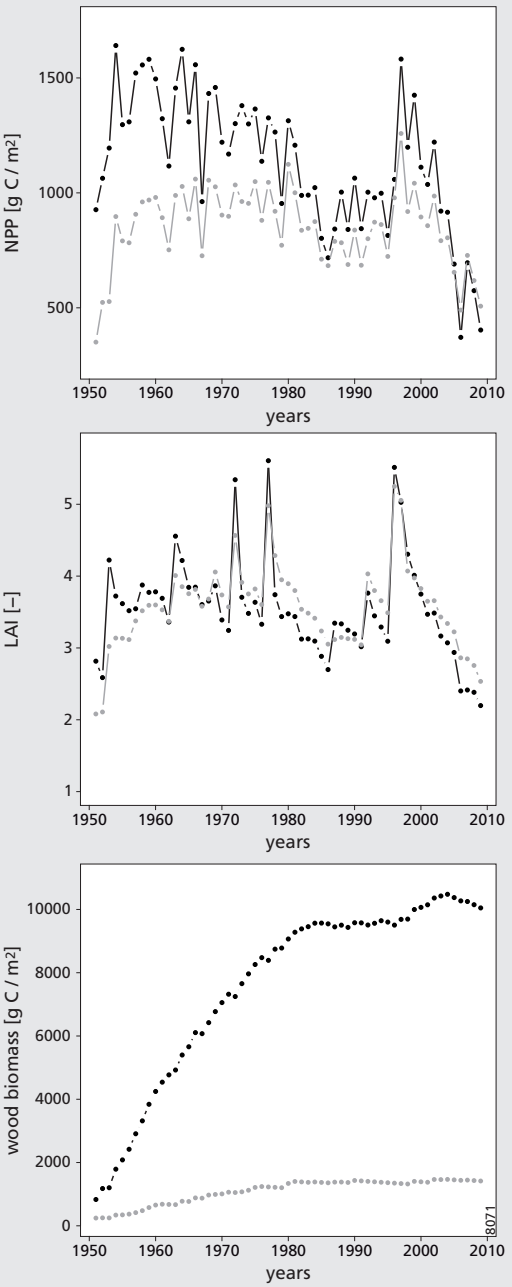

Figure 7.2: Yearly values of NPP, LAI, and wood biomass from the original (●) and calibrated (●) Forest-BGC model runs 1950-2009.

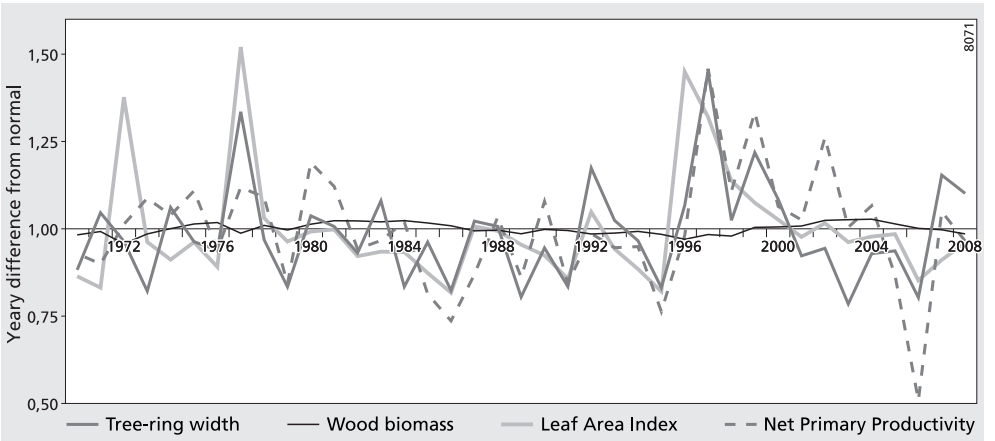

Figure 7.3: Normalized and detrended model time series compared to tree-ring chronology for 1970-2008.

Yearly variability in productivity

The normal run of the model resulted in overall values of LAI and biomass in range with the observed values. The next step in validating the model results was to compare the model outcomes with the tree-ring record and evaluate the performance on a yearly basis as shown in fig 7.3. To normalise the data, each series is shown as its deviation of a cubic-spline (50% response, period 32 years) trend line. The average ring-width curve from our tree-ring data is considered as ground truth data and compared to the wood biomass, LAI and Net Primary Productivity of each year. The wood biomass has very little variability and no significant correlation (r = -0.08) with the tree-ring data. The lack of correlation between the wood carbon and the tree rings is caused by the way biomass is allocated to the wood in the model. Carbon is only allocated to the wood as the other demands (maintenance respiration, leaves and roots) are satisfied. In a productive year with low stress levels, more carbon is allocated to leaf growth and therefore less carbon remains for the wood. By this principle the relation between productivity and wood growth is dampened or even reversed. The series of LAI and NPP show a much better correspondence with the tree-ring data (correlations r=0.62 and r=0.68 respectively), indicating that the model does perform well in general and the model reproduces the between-year variability well.

Monthly sensitivity to the climate

For the evaluation of model performance on a monthly timescale, the sensitivity of the model outputs to monthly average meteorological inputs is used. The resulting response functions are used to compare the model results to the tree-data on a monthly basis (fig 7.4). As in the yearly evaluation, woody biomass has low sensitivity and a poor correspondence to our field data and therefore the wood biomass data is not included in the figures. The correlation between the yearly model results and monthly temperature is positive during the months January to April, and negative during the summer, June to August (fig 7.4a). The correlation with precipitation is clearly positive during May, June and August, is less strong in July and is unclear during the other months of the year (fig 7.4b). The patterns agree well with the results obtained from the

tree-ring analysis. These results confirm that growth mainly takes place in the spring and early summer months and that the model can fairly well account for this temporal behaviour.

Scenario Simulations

The Forest-BGC model is now parameterized and validated against field measurements and past records of tree growth from tree rings. Next, the model is used to evaluate the effect of climate change on vegetation growth in the study area. The climate scenarios are tested with

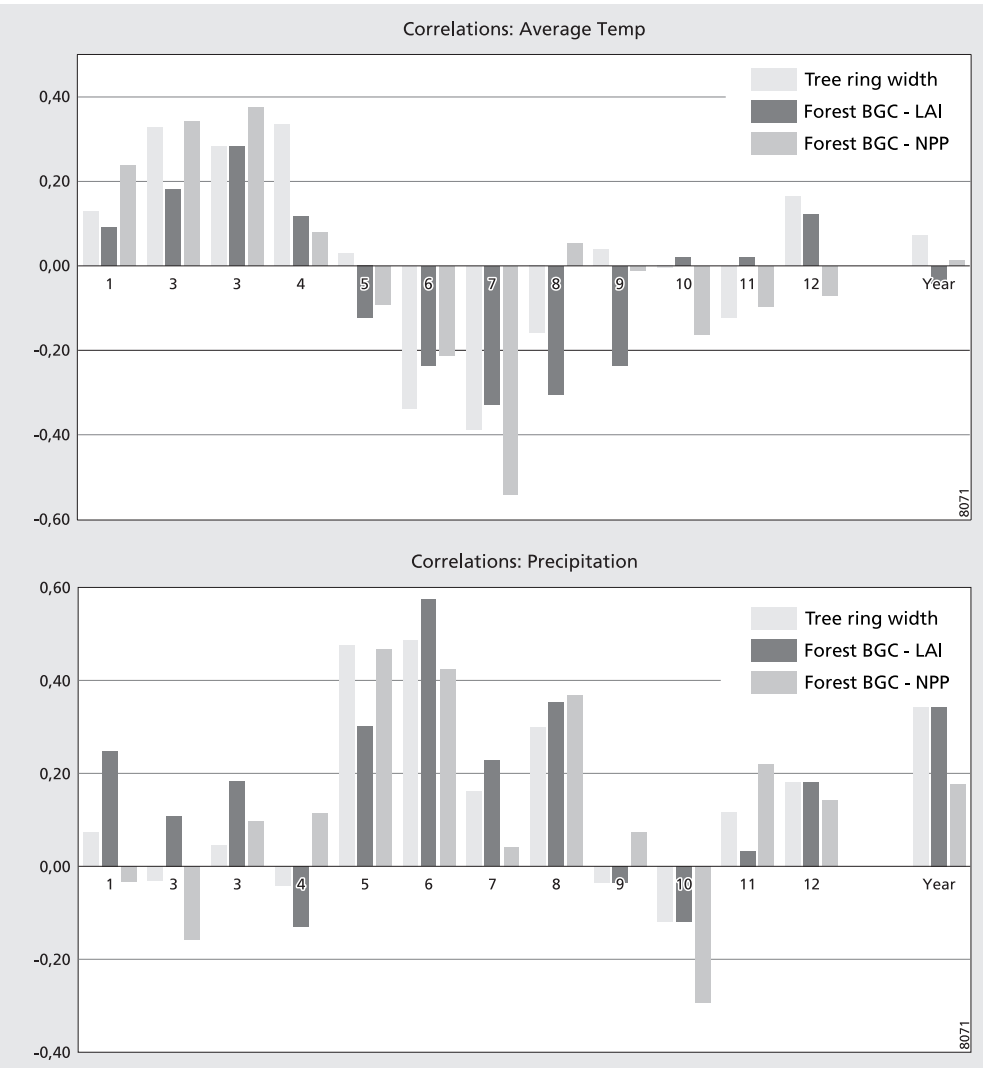

Figure 7.4: Monthly sensitivity of tree ring width and model results (LAI and NPP) to variability in temperature (top) and precipitation (bottom) for 1970-2008.

Table 7.5: Forest-BGC climate scenario results for the Puechabon Forest.

Scenario		Temp	Precip	LAI	Wood Biomass	NPP
1	normal	-	-	3,54	9,59	1134
2	year temperature	+ 3	-	3,33	7,51	988
3	year precipitation	-	- 10%	3,50	9,07	1103
4	year temperature & precipitation	+ 3	- 10%	3,28	6,95	962
5	seasonal temperature	+2\+5	-	3,20	6,10	903
6	seasonal precipitation	+ 2	0\- 40%	3,13	8,39	980
7	seasonal temperature & precipitation	+2\+5	0\- 40%	2,69	4,72	752
8	seasonal temperature & dry summer	+2\+5	0\- 100%	1,83	2,12	480

Table 7.6: Forest-BGC climate scenario results for the Peyne Forest.

Scenario		Temp	Precip	LAI	Wood Biomass	NPP
1	normal	-	-	3,56	1,39	851
2	year temperature	+ 3	-	3,32	0,84	750
3	year precipitation	-	- 10%	3,48	1,21	824
4	year temperature & precipitation	+ 3	- 10%	3,22	0,72	722
5	seasonal temperature	+2\+5	-	3,15	0,46	680
6	seasonal precipitation	+ 2	0\- 40%	3,25	1,07	758
7	seasonal temperature & precipitation	+2\+5	0\- 40%	2,74	0,25	580
8	seasonal temperature & dry summer	+2\+5	0\- 100%	1,87	0,22	363

both the original (Puechabon) and the calibrated (Peyne) parameter settings, because of the large difference in wood production between the Peyne and Puechabon forest. The scenario runs (Table 7.5 and 7.6) confirm that the vegetation growth is limited by the warm and dry weather in the area because any increase in temperature or decrease in rainfall leads to lower values for productivity, LAI and woody biomass. Temperature has a large effect on NPP and wood biomass, by increasing the respiration. LAI is somewhat stronger influenced by precipitation, specifically summer precipitation because the leaf area is limited by water stress which occurs during the dry period in the summer. The combination of both leads to the lowest productivity. The runs also show that the vegetation is more sensitive to concentrated changes during the summer season (fig 7.6) than to a constant change during the entire year (fig 7.5). The effect of the most probable climate scenario (nr. 7) in the Puechabon is a halving of the supported wood biomass and a decrease in LAI of 0.8. In the Peyne area, the most probable scenario decreases the LAI by 0.9 with little or no allocation to the woody biomass. The results indicate strong deterioration of the forest now growing on most naturally vegetated areas as the woody biomass is expected to halve or even to completely disappear. The extreme scenario with no precipitation during the whole summer results in even lower biomass and a halving of the LAI. With these values the vegetation cover would be discontinuous and will probably result in a significant change in species composition (Vennetier and Ripert, 2009).

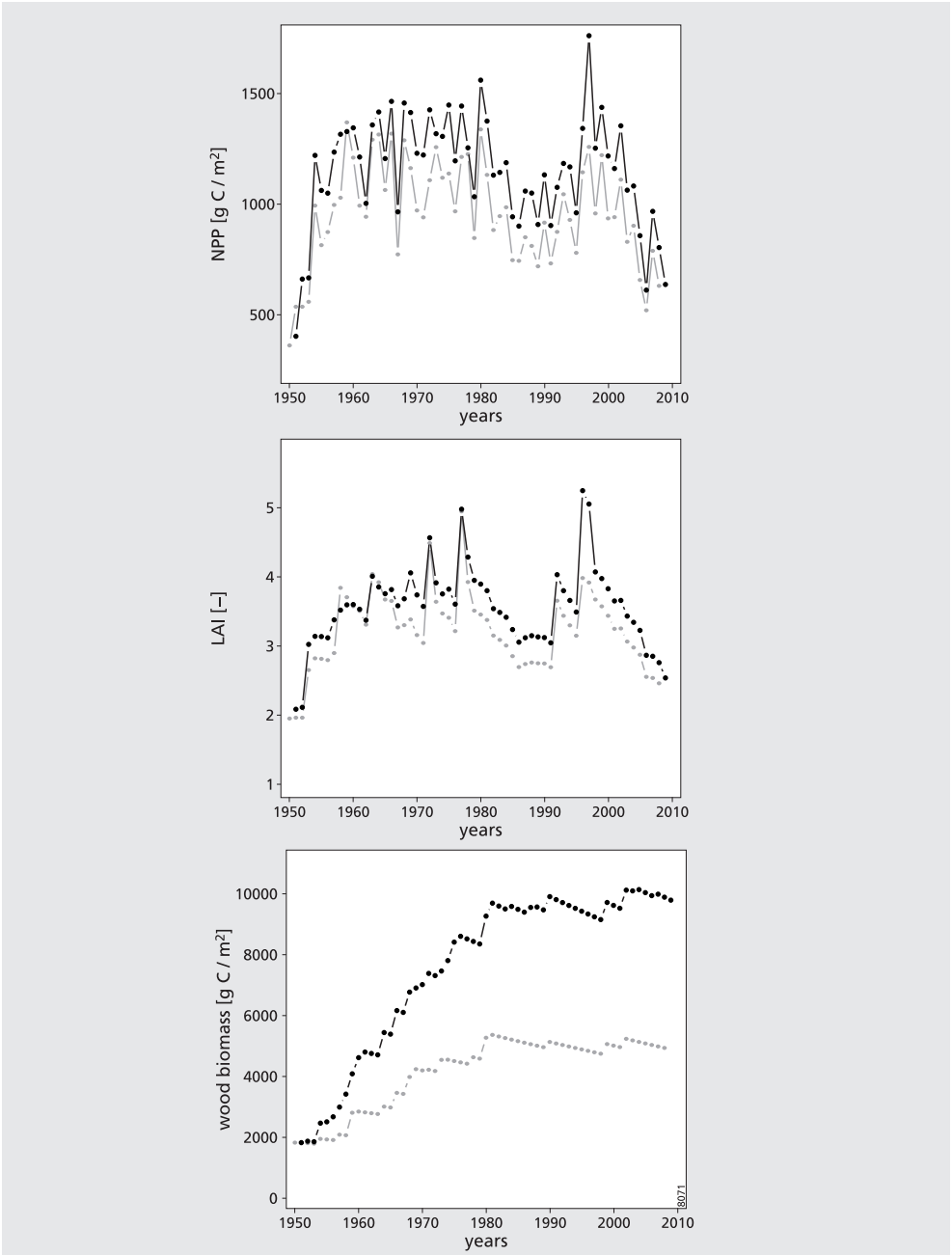

Figure 7.5: LAI, NPP and wood biomass for normal, scenario 1 (●) and year average temperature and precipitation change, scenario 4 (●) runs.

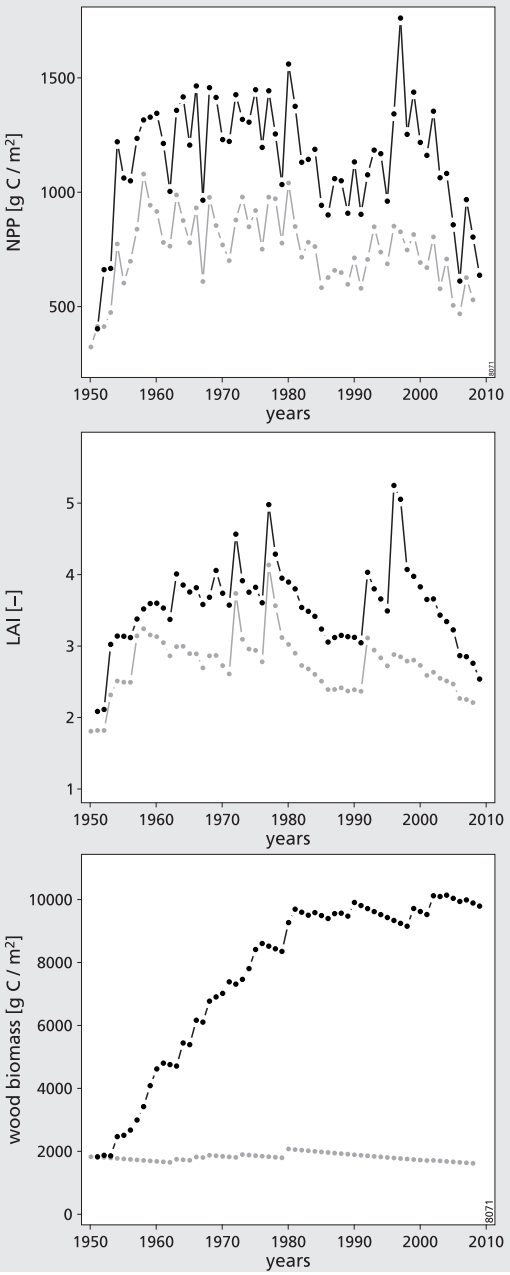

Figure 7.6: LAI, NPP and wood biomass for normal, scenario 1 (●) and seasonal temperature and precipitation change, scenario 7 (●), runs.

7.4 Discussion:

The forest-BGC model was used to simulate vegetation growth in the Peyne area for the past 60 years and for the future with a changing climate. The normal model runs simulating the past are used to evaluate the model performance against field data and result of tree ring analysis. The model runs of future developments use RCM based climate change scenarios to predict the effects of the projected climate changes on vegetation growth.

Projected vegetation changes

The Forest-BGC runs show that the 'most probable' projected climate change (scenario 7) has a significant impact on the vegetation productivity. Specifically the increased summer temperatures and the decrease in summer rainfall have a large deteriorating effect on the growth of Mediterranean evergreen species. During the summer the vegetation growth is limited by drought and heat. If drought and heat are more severe, they cause a large decrease of the growth. The runs with either precipitation or temperature change show less change, indicating that specifically the combination of a warmer climate with less rainfall has the strongest impact on vegetation growth. This may be explained by the heat increasing the water demand while, because of decreased precipitation, there is less water available during the growing season. The heat itself increases the maintenance respiration leading to a lower amount of biomass that can be supported for a given primary productivity. The most probable scenario (nr. 7) results in a halving of the aboveground biomass in the Puechabon area. In the Peyne area, where wood productivity is already very low under current conditions, the model predicts no growth of the woody biomass at all. Because the growth in this area is already marginal, the effects of climate change in this area may be severe and result in a serious decrease of biomass and vegetation cover, or a change in the vegetation type and species. A change in vegetation type and species composition may be expected to adapt to warmer and drier conditions (Vennetier and Ripert, 2009) and can possibly cause completely different growth patterns and productivity.

Model Validation

The reliability and validity of the Forest-BGC model was evaluated using field data of aboveground biomass, LAI and tree-ring data. The model performed well on both decadal and monthly timescales. The predicted NPP and LAI closely resemble the values and variability observed in the field. The yearly variability in wood biomass as calculated by the model shows little agreement with the measured data from tree rings. This is caused by the allocation function treating wood biomass as a rest pool to store remaining biomass once the demands for leaves and roots are satisfied. Adjustment of this function to a more conservative allocation to leaves in wet years could yield better results for both the wood and the leaf compartments, because in highly productive years, too much leaf growth is allocated at this moment.

The good agreement between the tree-ring data and model results on a monthly basis indicate the reliability of the model, and make the model suitable for predicting the response of the vegetation to expected changes in precipitation and temperature. The method of validating the model results relies partially on vegetation variables that can be detected using remote-sensing imagery (Nijland et al., 2009; De Jong et al., 2003). Tree-ring data is somewhat more laborious to obtain, but readily available in any live forest. This method of model validation in a

specific area requires less effort in data collection than currently common practice which relies on detailed plant physiological measurements or flux data. Comparison of seasonal-sensitivity patterns to tree ring data does allow evaluation of the model performance on monthly timescales. Such monthly basis is important to climate-scenario predictions, especially when the expected changes are variable within the year as in the study area.

The climate scenarios for the future model runs were created by adding changes onto an existing time-series. An advantage of this method is that the different scenario runs can be directly compared. A disadvantage is that by using this method it is not possible to influence for example the distribution and number of rainfall events in the year. Based on the climate-change prediction it is expected that there will be fewer rainfall events and that the amount of rain per event might increase. More violent rainfall events will lead to lower water availability to the vegetation because more water will leave the area as surface runoff.

7.5 Conclusions

In this study I used the Forest-BGC vegetation model to evaluate the effect of climate change on the broadleaf evergreen forests in the Mediterranean Peyne catchment. The model is first parameterized and validated against past tree-growth records from annual tree rings and current field measurements of leaf area and aboveground biomass. The normal model runs for 1950 to 2009 past runs agree well with the field data and show the same monthly sensitivity patterns to climate variability as the tree-ring records. The model results based on unaltered past climate data give confidence in the model performance and for evaluation of future climate change scenarios.

This chapter presents a reliable method of model validation using tree-ring data that does not need detailed plant physiological measurements or flux data. The tree-ring based validation is, although laborious, more portable to different regions than other methods of model evaluation because it needs less infrastructure to obtain usable validation data. Using a detailed comparison of the monthly sensitivity of the model results and tree rings to variability in the climate, we were able to validate the model for use with predictive climate scenarios.

The scenario runs show that both a decrease of precipitation and an increase in temperature by themselves will lead to less tree growth and lower leaf area and biomass. The combined effect of temperature and vegetation change, specifically during the summer season may cause a reduction of the biomass of 50% or more and a decrease of the leaf area by 25%. The model results described in this chapter should be interpreted with care, because this study only focussed on vegetation growth and productivity. Climate change may however also result in a change of species composition. A different type of vegetation and species may be better adapted to warmer and drier conditions or can possibly cause completely different growth patterns and productivity.

The changes in vegetation growth may have large consequences for the landscape development; rainfall interception is lowered which may lead to increased runoff and associated hazard

of flooding and soil erosion. The lower growth potential also causes the vegetation to be less resilient against grazing, logging or other forms of human pressure.

8. Synthesis

The Mediterranean region is one of the richest areas of the world with respect to history, geography and biodiversity. The unique landscape and climate draw many people to the region to settle, work, and for recreation. The pressure of economic activity on Mediterranean environmental resources is high and generally increasing (Grenon and Batisse, 1989; UNEP, 2009) while at the same time climate change may decrease water availability and plant growth.

The Mediterranean climate is characterized by long dry periods in summer, mild winters and concentrated rainfall events in spring and autumn. Persistent drought during the warm summer season is the most important constraint on growth, enhanced by the often marginal, degraded and shallow soils. Climate change scenarios predict that the extreme character of the Mediterranean climate will further increase: higher temperatures especially during the summer, and decreasing summer precipitation. These changing environmental conditions may have a deteriorating impact on the Mediterranean ecosystems with decreasing vegetation cover and lower productivity or they may cause shifts in vegetation type and species composition.

Timely mitigation of, or adaptation to the effects of climate change requires a thorough understanding of the landscape and ecosystem, and the possibility to accurately and early detect changes in vegetation development. Projections of future vegetation development based on possible climate-change scenarios are of great interest to policy makers and the general public. Improved knowledge and understanding of ecosystem functioning may indicate vulnerabilities of the Mediterranean landscape and in addition it may yield notions for possible measures to reduce adverse effects.

This thesis presents a collection of studies on the Mediterranean evergreen vegetation of the Peyne area in southern France. The evergreen forests and shrub lands in the Peyne area stand model for many areas in the European Mediterranean basin and other Mediterranean areas across the globe. In this thesis I focus on the physical characteristics of the vegetation like leaf area, biomass and productivity. A probable climate scenario for 2070 predicts a temperature increase of 2°C in winter and 5°C in summer plus a decrease of summer precipitation by 40% (Gao and Giorgi, 2008). Based on this climate, the Forest-BGC vegetation productivity model predicts a decrease of leaf area by 25%, and potentially over 50% less production of woody biomass in the area. Such changes in vegetation growth may have large consequences on the landscape and land use possibilities in the region. This thesis combines remote sensing, plot-based field data on biophysical vegetation parameters, geophysical exploration, tree-ring analysis, and dynamical production modelling. It contributes to the advance of our capabilities to monitor the growth and development of evergreen Mediterranean vegetation and to improve the projections of vegetation change in the next decennia as an effect of anticipated climate change.

Optimizing spatial support

Detection of biophysical vegetation parameters like leaf area and aboveground biomass is important for this study investigating the state of the ecosystem and its dynamics. Remote sensing offers a suitable tool to obtain spatially continuous data on vegetation characteristics. The spatial resolution of imaging systems is ever increasing and has developed to a point that it is possible to derive quantitative data on natural vegetation in fragmented and hence heterogeneous landscapes typical to the Mediterranean. The availability of such high-resolution earth observation imagery increases the importance of accounting for scale effects. Careful consideration of the spatial scale of mapping is important because, as stated in the Modifiable Area Unit Problem (Openshaw, 1984), the choice for the spatial unit affects the outcome of the analysis, implicating the existence of an optimal unit for quantitative analysis.

In the natural vegetation of the Peyne area, the optimal support for detection of stand-level vegetation parameters was determined by combining high resolution (5 by 5m pixels) hyperspectral images and an extensive field-plot-based dataset of leaf area and aboveground biomass. Use of the optimal support size of 55m (leaf area) to 95m (aboveground biomass) resulted in an increase in mapping accuracy by 7 and 17 percent for leaf area and aboveground biomass, respectively (Chapter 3). Although these results are specific to the study area, landscape, and vegetation type, general recommendations can be made based on the analysis of spatial image derivatives like variograms, and average local variance functions. To improve detection accuracy of stand level biophysical parameters the image support should be chosen such that: 1) Spectrally different scene sub-elements are averaged within the measurement unit to create a homogeneous spectrum at the studied scene scale. 2) The spatial variability of the mapped parameter is preserved through observation and mapping. 3) Neighbouring or intersecting scene elements are well separable. In any remote-sensing mapping project, the scale of analysis needs to be carefully considered as optimizing the measurement support can seriously improve mapping accuracy.

Multi-temporal imaging of vegetation development

When monitoring vegetation development with remote sensing images, it is important to consider the inherent temporal integration of each analyzed parameter. Biomass accumulates tree growth over several decades. Leaf area changes at seasonal or yearly timescales, while transpiration and light use show daily or even hourly variation depending on weather conditions and time of day. A second issue is the spatial properties of the image data and the error introduced by misalignment of the temporal image series. The spatial errors are specifically important in strongly fragmented landscapes like Peyne, where misalignment errors will have a relatively large effect compared to more homogeneous areas. Multi-temporal image analysis by an object-based approach may decrease alignment errors in a time series of images and may reduce edge effects between landscape units.

To detect changes in vegetation vigour and to assess the sensitivity of vegetation to seasonal drought, 12 ASTER images acquired between 2002 and 2008 were analysed (Chapter 4). The applied object-based analysis allowed detection of small differences in vegetation dynamics. The relation between the geological substrates and seasonal patterns in NDVI and thermal brightness indicates a close relation between the substrates, water availability and vegetation

vigour. Monitoring vegetation characteristics using remote-sensing images and analysing spatial temporal patterns at multiple scales, does reveal pertinent information on ecosystem development and the effect of variability in climate and stand characteristics on plant growth. Detailed monitoring of natural vegetation development using satellite images may contribute to early detection of ecosystem degradation and also may provide useful information on plant growth in the spatial landscape setting.

Soil water use and rooting depth

Vegetation growth in Mediterranean ecosystems is greatly dependent on moisture availability from the soil, as little precipitation is available during the growing season. Information on soil characteristics, water availability, and rooting depth, is therefore crucial to understand the relation between the climate and tree growth in a landscape context. However, a gap exists between hydrological measurements that are based on electrical soil probes with a very small support size, and measurements from earth observation images available at regional or continental scales. Accurate moisture measurements in many forested Mediterranean areas are difficult because of high spatial variability and coarse, shallow soils. Trees on these shallow soils are known to have extensive root systems growing deeply into the fissured bedrock to reach water during periods of drought.

The gap in soil-moisture measurement scale corresponds to the scale of individual trees to forest stands. To bridge this measurement gap, and to obtain data from inaccessible depths and substrates, the application of Electrical Resistivity Tomography (ERT) was evaluated (Chapter 5). ERT is a method to measure soil characteristics using electrodes placed in the top soil, and provides information on the spatial patterns within the soil reaching depths otherwise inaccessible. In heterogeneous soils, lithological and moisture effects in the measurements were separated using multi-temporal data collected over the dry summer season. Absolute calibration to moisture content was possible for some cases, but strongly dependent on lithological substrate. The ERT measurements confirmed that although the soils in the study area are shallow and rocky, plant roots penetrate deeply into the fractured and weathered bedrock, and vegetation subtracts water from depths down to 6 m and below. Substrates with deeper root growth and water abstraction support more vegetation and sustain the tree growth potential longer during the dry season. This information is important for understanding soil–vegetation interactions, and may be used to improve vegetation-development and productivity models. ERT measurements, although laborious, provide a new source of data for evaluation of soil-moisture content, soil-moisture redistribution processes, and water availability to plant growth. In the shallow and rocky soils typical to Mediterranean areas this data was unavailable using any other currently available measurement method.

Sensitivity of tree ring growth to climate variability

Predicting possible effects of climate change on Mediterranean forest ecosystems relies on understanding the relationship between plant growth and the most influential climate variables. Study of the relation between climate and plant growth can be done either by detailed analysis of physiological processes at the tree or leaf scale, or by evaluating long-term datasets of tree growth and climatic conditions. Stem-growth increments as recorded in annual tree rings are an accurate record of past stem growth and more generally of past forest productivity. In high altitude or

latitude areas tree rings are commonly used for measuring forest growth and as proxies for temperature reconstruction for periods past the measured data range. Mediterranean evergreen trees have a weaker seasonality in their growth, making accurate dating and measurements of annual rings difficult. Variability in their growth is influence by both temperature and drought, complicating the interpretation of Mediterranean tree rings. However, if sufficient care is taken in sampling, dating and analysing stem increments, tree rings of Mediterranean areas are very useful to derive time series of past tree growth.

Combining ring-width chronologies with meteorological records provides useful information on vegetation functioning and climate sensitivity. The analysis of 34 tree disk samples from the Peyne area, showed consistent ring-width patterns, and a strong response of tree growth to climate variability were found (Chapter 6). The analyses show a significant statistical relation between annual stem increments and monthly meteorological variables. Tree growth in the Peyne has a strong positive response to May and June precipitation, as well as a significant positive influence of early-spring temperatures and a negative growth response to summer heat. Comparing these ring-width data with detailed productivity measurements from a flux tower in two contrasting years confirms these observations and shows a strong productivity limiting effect of low early-summer precipitation. The tree-ring analysis provides a source of reference data towards the evaluation of simulation models, both at a longer (decadal) temporal scale as on the shorter (monthly or seasonal) scale. This type of data can be useful especially in areas where no direct measurements of productivity are available as stem increments are archived and readily available in almost all forest areas.

Modelling future vegetation growth

Dynamic modelling of vegetation productivity are a way of formalizing our understanding of ecosystem functioning into a mathematic system. If properly parameterized and validated, productivity models can be used to evaluate the possible effects of climate-change scenarios on tree growth. Modelling forests in a Mediterranean climate sets specific demands on the model principles, because the vegetation is mostly limited in its growth by the typical climate with long dry and very warm periods during the summer. Anticipated climate change may further increase these limitations because of higher temperatures and increasing aridity during summer. It is therefore crucial to use a model with an accurate process description with respect to water shortage and with the ability to capture the seasonal variability in rainfall and the resulting water stress.

To improve future projections of vegetation development the dynamical vegetation model Forest-BGC is used (Chapter 7). The model is first parameterized and validated against past tree-growth records from annual tree rings and current field measurements of leaf area and aboveground biomass. Most of the model parameters were already determined for the nearby Puechabon forest (Hoff et al., 2002), but some changes were made to account for the differences in soil conditions, biomass and leaf area between the Peyne and Puechabon. Runs of forest productivity over the past 60 years agree well with the field data and also show the same monthly sensitivity patterns the climate variability as the tree ring records. Simulations of forest growth based on the most probable climate scenario predict a decrease of leaf area by 25%, and potentially over 50% less production of woody biomass in the area. The seasonal character of

the expected climate change where the temperature increase is highest in summer, combined with a decrease in summer precipitations has a strong deteriorating effect on the vegetation. The current climate is already highly limiting on the productivity and the least productive areas are expected to be the most vulnerable to the anticipated changes. Model results indicate that for the Puechabon area woody biomass will halve, but in the Peyne area where the current biomass is a lot lower, hardly any allocation to woody biomass will occur. These changes in productivity are large, the results therefore indicate that serious changes are to be expected and a shift in species composition may be very likely.

Recommendations for further research

This thesis aimed at improving the understanding and prediction of Mediterranean vegetation growth within the framework of anticipated climate change and increasing human pressure on the region. The focus is on the role of landscape conditions on the vegetation. Climate change is expected to influence not only the amount of precipitation, but also the temporal distribution as rainfall may occur in fewer but more intense events. Concentration of precipitation in time may result in increased surface runoff causing less water to be available to the vegetation. In the modelling and field studies presented in this thesis, this type of change is not evaluated, but more detailed study of the relation between rainfall distribution and water availability is necessary. Monitoring of infiltration and soil-water use at daily or even smaller intervals should give more information on the influence of the temporal distribution of precipitation on water availability to plant growth. ERT measurements are non-invasive and non-destructive to the soil profile and provide a better spatial coverage than other available techniques. Installation of a permanent measurement array would facilitate local calibration to absolute moisture contents and high-resolution detection of infiltration, water redistribution and plant-water use. The high sensitivity of the Mediterranean forest to water availability, especially in combination with the expected changes in precipitation may require more detailed modelling of the water balance for productivity models. The detailed approach would at least include the infiltration of water into the soil and a distinction between the shallow (loose) and deeper (fissured rock) layers in the substrate.

This study used airborne and spaceborne earth observation imagery acquired by ASTER and HyMap to monitor the changes of ecosystem variables like leaf area and aboveground biomass over time. Long-term time series of earth observation imagery are a vital condition to evaluate changes of ecosystems over larger areas. For the Peyne area I present optimal sampling scales for leaf area and aboveground biomass. Further research is however required to evaluate whether this optimal mapping scale also holds for other Mediterranean areas with the same level of accuracy. Planned spaceborne remote sensing systems like the spectrometers EnMap (DLR) and HyspIRI (NASA) are well suited instruments for such studies.

The studies presented in this thesis centre on the vegetation growth and dynamics in the Peyne area in southern France. Although this study area is relatively small, the variability in vegetation cover and substrates provides a sufficiently wide range of conditions to study plant growth in a spatial perspective. The Earth observation methods and modelling are specifically suited to expand vegetation studies to a regional or even larger scale. However, availability of field data on such scales is low and sufficient validation of the results may therefore be difficult. To improve

our understanding of landscape and vegetation processes, local studies remain vitally important because of their strength in combining field observations, remote methods and modelling. The connection between different disciplines that exists based on a shared study area may yield profound new insights. Scientific progress is thereby aided by a strong common focus and good local produce.

References

Aber, J.D. and Federer, C.A., 1992. A generalized, lumped-parameter model of photosynthesis, evapotranspiration and net primary production in temperate and boreal forest ecosystems. Oecologia 92: 463–474.

Addink, E.A., S.M. De Jong, S.M., and Pebesma, E.J., 2007. The importance of scale in object-based mapping of vegetation parameters with hyperspectral imagery. Photogrammetric Engineering and Remote Sensing 73: 905–912.

Aerts, R., 1995. The advantages of being evergreen. Trends in Ecology & Evolution 10: 402–407.

Alabouvette, B., 1982. Carte Géologique de la France 1:50 000. Feuille Lodève; BRGM, Orléans

Allard, V., Ourcival, J.M., Rambal, S., Joffre, R., and Rocheteau, A., 2008. Seasonal and annual variation of carbon exchange in an evergreen Mediterranean forest in Southern France, Glob. Change Biol. 14: 714–725.

Archie, G.E., 1942. The Electrical Resistivity Log as an aid determining some characteristics. Transactions of American Institute of Mining. Metallurgical and Petroleum Engineers 145: 54–62.

ASTER, 2005. Advanced Spaceborne Thermal Emission and Reflection Radiometer (ASTER). http://asterweb.jpl.nasa.gov.

Atkinson, P.M., and Aplin, P., 2004. Spatial variation in land cover and choice of spatial resolution for remote sensing. International Journal of Remote Sensing 25: 3687–3702.

Atkinson, P.M., and Curran, P.J., 1997. Choosing an appropriate spatial resolution for remote sensing investigations . Photogrammetric Engineering & Remote Sensing 63: 1345–1351.

Atkinson, P.M., and Tate, N.J., 2000. Spatial scale problems and geostatistical solutions: a review. Professional Geographer 52: 607–623.

Atzberger, C., 2004. Object-based retrieval of biophysical canopy variables using artificial neural nets and radiative transfer models, Remote Sensing of Environment 93: 53–67.

Baldocchi, D.D., Xu, L., 2007. What limits evaporation from Mediterranean oak woodlands-The supply of moisture in the soil, physiological control by plants or the demand by the atmosphere? Advances in Water Resources 30: 2113–2122.

Barnsley, M.J., and Barr, S.L., 1996. Inferring urban land use from satellite sensor images using kernel-based spatial reclassification. Photogrammetric Engineering & Remote Sensing 62: 949–958.

Blamey, M. and Grey-Wilson, C., 2004 Wild Flowers of the Mediterranean: A Complete Guide to the Islands and Coastal Regions, 2nd edn., A&C Black Publishers Ltd., London.

Bøcher, P.K., and McCloy, K.R., 2006a. The fundamentals of Average Local Variance - part I: detecting regular patterns. IEEE Transactions on Image Processing 15: 300–310.

Bøcher, P.K., and McCloy, K.R., 2006b. The fundamentals of Average Local Variance - part II: sampling simple regular patterns with optical imagery. IEEE Transactions on Image Processing 15: 311–318.

Bonfils, P., 1993. Carte Pédologique de la France 1:100 000; Feuille Lodève. INRA, Olivet

Briffa, K. R., 2000. Annual climate variability in the Holocene: interpreting the message of ancient trees, Quaternary Sci. Rev., 19: 87–105.

Briffa, K. R., Osborn, T. J., and Schweingruber, F. H., 2004. Large-scale temperature inferences from tree rings: a review, Global Planet. Change, 40: 11–26.

Brolsma, R.J., and Bierkens, M.F.P., 2007. Groundwater –soil water– vegetation dynamics in a temperate forest ecosystem along a slope. Water Resources Research 43: W01414.

Bunn, A. G., 2008. A dendrochronology program library in R (dplR), Dendrochronologia 26: 115–124.

Büntgen, U., Esper, J., Frank, D. C., Nicolussi, K., and Schmidhalter, M., 2005. A 1052-year tree-ring proxy for Alpine summer temperatures, Clim. Dynam. 25: 141–153.

Büntgen, U., Frank, D., Trouet, V., and Esper, J., 2010. Diverse climate sensitivity of Mediterranean tree-ring width and density, Trees-Struct. Funct. 24: 261–273.

Campelo, F., Gutiérrez, E., Ribas, M., Nabais, C., and Freitas, H., 2007. Relationships between climate and double rings in Quercus ilex from Northeast Spain, Can. J. Forest Res. 37: 1915–1923.

Campelo, F., Nabais, C., Garcia-Gonzalez, I., Cherubini, P., Gutiérrez, E., and Freitas, H., 2009. Dendrochronology of Quercus ilex L. and its potential use for climate reconstruction in the Mediterranean region, Can. J. Forest Res. 3: 2486–2493.

Campelo, F., Nabais, C., Gutiérrez, E., Freitas, H., and García-González, I., 2010. Vessel features of Quercus ilex L. growing under Mediterranean climate have a better climatic signal than tree-ring width, Trees-Struct. Funct. 24: 463–470.

Canadell, J., Jackson, R.B., Ehleringer, J.R., Mooney, H.A., Sala, O.E. and Schulze, E.-D., 1996. Maximum rooting depth of vegetation types at the global scale. Oecologia 108: 583–595.

Case, R. A. and MacDonald, G. M., 1995. A dendroclimatic reconstruction of annual precipitation on the Western Canadian Prairies since AD 1505 from Pinus flexilis James, Quaternary Res. 44: 267–275.

Chason, J.W., Baldocchi, D.D., and Huston, M.A., 1991. A comparison of direct and indirect methods for estimating forest canopy leaf area. Agricultural and Forest Meteorology 57: 107–128

Cherubini, P., Gartner, B.L., Tognetti, R., Braeker, U.O., Schoch, W., and Innes, J.L., 2003. Identification, measurement and interpretation of tree rings in woody species from Mediterranean climates, Biol. Rev. 78: 119–148.

Chiesi, M., F. Maselli, M. Bindi, L. Fibbi, L. Bonora, A. Raschi, R. Tognetti, J. Cermak, and N. Nadezhdina. 2002. Calibration and application of FOREST-BGC in a Mediterranean area by the use of conventional and remote sensing data. Ecological Modelling 154: 251–262.

Chiesi, M., Maselli, F., Bindi, M., Fibbi, L., Cherubini, P., Arlotta, E., Tirone, G., Matteucci, G., and Seufert, G., 2005. Modelling carbon budget of Mediterranean forests using ground and remote sensing measurements, Agr. Forest Meteorol. 135: 22–34.

Chiesi, M., Maselli, F., Moriondo, M., Fibbi, L., Bindi, M., Running, S.W., 2007. Application of BIOME-BGC to simulate Mediterranean forest processes. Ecological modelling 206: 179–190.

Cohen, W.B., and S.N. Goward. 2004. Landsat's role in ecological applications of remote sensing. BioScience 54: 535–545.

Cohen, W.B., Spies, T.A., and Bradshaw, G.B., 1990. Semivariograms of digital imagery for analysis of conifer canopy structure Remote Sensing of Environment 34: 167–178.

Combal, B., Baret, F., Weiss, M., Trubuil, A., Mace, D., Pragnere, A., Myneni, R., Knyazikhin, Y., and Wang, L., 2003. Retrieval of canopy biophysical variables from bidirectional reflectance—using prior information to solve the ill-posed inverse problem, Remote Sensing of Environment 84: 1–15.

Curran, P.J., 1988. The semivariogram in remote sensing: An introduction. Remote Sensing of Environment 24: 493–507.

Damesin, C. and Rambal, S., 1995. Field study of leaf photosynthetic performance by a Mediterranean deciduous oak tree (Quercus pubescens) during a severe summer drought. New Phytologist 131: 159–167.

De Jong, S.M., and Jetten, V.G., 2007. Estimating spatial patterns of rainfall interception from remotely sensed vegetation indices and spectral mixture analysis. International Journal of Geographical Information Science 21: 529–545.

De Jong, S.M., Pebesma, E.J., and Lacaze, B., 2003. Above-ground biomass assessment of Mediterranean forests using airborne imaging spectrometry: de DAIS Peyne experiment. International Journal of Remote Sensing 24: 1505–1520.

Debussche, M., Escarré, J., Lepart, J., Houssard, C., and Lavorel, S., 1996. Changes in Mediterranean plant succession: old-fields revisited. Journal of Vegetation Science 7: 519–526.

Definiens, 2009. e-Cognition. http://www.ecognition.com

Di Castri, F. and Mooney, H.A., 1973. Mediterranean type ecosystems: origin and structure, Ecological studies 7, Springer, Berlin.

Di Castri, F., Goodall, D.W., Specht, R.L., 1983. Mediterranean-type shrublands. Plant Ecology 53: 96–96.

Driessen, P., Deckers, J., Spaargaren, O., Nachtergaele, F., 2001. Lecture notes on the major soils of the world. World Soil Resources Reports 64, FAO, Rome, pp 334.

Fensholt, R., I. Sandholt, and M.S. Rasmussen., 2004. Evaluation of MODIS LAI, fAPAR and the relation between fAPAR and NDVI in a semi-arid environment using in situ measurements. Remote Sensing of Environment 91: 490–507.

Field, C.B., Randerson, J.T., and Malmström, C.M., 1997. Global net primary production: Combining ecology and remote sensing. Remote Sensing of Environment 51: 74–88.

Fisher, P., 1997. The pixel: A snare and a delusion. International Journal of Remote Sensing 18: 679–685.

Floret, C., Galan, M. J., Floch, E., and Romane, F., 1992. Dynamics of holm oak (Quercus ilex L.) coppices after clearcutting in southern France, Plant Ecology 99-100: 97–105.

Friedman, S.P., 2005. Soil properties influencing apparent electrical conductivity: a review. Computers and Electronics in Agriculture 46: 45–70.

Fritts, H. C., 1976. Tree Rings and Climate, Academic Press, London.

Fritts, H. C., 1991. Reconstructing Large-Scale Climatic Patterns from Tree-Ring Data, Tree-Ring Bulletin 51: 39–41, 1991.

Gamon, J.A., Field, B.C., Roberts, D.A., Ustin, S.L., and Valentini, R., 1993. Functional patterns in an annual grassland during an AVIRIS overflight, Remote Sensing of Environment 44: 239–253.

Gao, X. and Giorgi, F., 2008. Increased aridity in the Mediterranean region under greenhouse gas forcing estimated from high resolution simulations with a regional climate model. Global and Planetary Change 62: 195–209.

Gea-Izquierdo, G., Martín-Benito, D., Cherubini, P., and Isabel, C., 2009. Climate-growth variability in Quercus ilex L. West Iberian open woodlands of different stand density, Ann. Forest Sci.,66: 802, doi:10.1051/forest/2009080.

Gibelin, A. L. and Déqué, M., 2003. Anthropogenic climate change over the Mediterranean region simulated by a global variable resolution model, Clim. Dynam., 20: 327–339.

Giorgi, F., Lionello, P., 2008. Climate change projections for the Mediterranean region. Global and Planetary Change 63, 90–104.

Glassy, J.M., Running, S.W., 1994. Validating diurnal climatology logic of the MT-CLIM model across a climatic gradient in Oregon. Ecological Applications 4: 248–257.

Gomez-Campo, C. ed., 1985. Plant conservation in the Mediterranean area. Geobotany 7. Dordrecht, the Netherlands, 269 pp.

Gracia, C., Tello, E., Sabate, S., and Bellot, J., 1999. GOTILWA: an integrated model of water dynamics and forest growth. Ecological Studies 137: 163–179.

Gratani, L., and L. Varone., 2004. Adaptive photosynthetic strategies of the Mediterranean maquis species according to their origin. Photosynthetica 42: 551–558.

Grenon, M., Batisse, M., 1989. Le plan bleu: avenirs du bassin méditerranéen. Economica, Paris, pp 279.

Grissino-Mayer, H. D., 2002. Research report evaluating crossdating accuracy: a manual and tutorial for the computer program COFECHA, Tree-Ring Res. 57: 205–221.

Grudd, H., Briffa, K. R., Karlen, W., Bartholin, T. S., Jones, P. D., and Kromer, B., 2002. A 7400-year tree-ring chronology in Northern Swedish Lapland: natural climatic variability expressed on annual to millennial timescales, Holocene 12: 657–665.

Guiot, J., 1991: The bootstrapped response function, Tree-Ring 51: 39–41.

Hanson, P. J., Amthor, J. S., Wullschleger, S. D., Wilson, K. B., Grant, R. F., Hartley, A., Hui, D., Hunt, E. R., Johnson, D. W., Komball, J. S., King, A. W., Luo, Y., McNulty, S. G., Sun, G., Thornton, P. E., Wang, S., Williams, M., Baldocchi, D. D., and Cushman, R. M., 2004. Oak forest carbon and water simulations: model intercomparisons and evaluations against independent data, Ecol. Monogr. 74: 443–489.

Hastie, T., Tibshirani, R., and Friedman, J., 2001. The elements of statistical learning: data mining, inference, and prediction. Springer-Verlag, New York.

He, Y., Guo, X., Wilmshurst, J., and Si, B.C., 2006. Studying mixed grassland ecosystems II: optimum pixel size. Canadian Journal of Remote Sensing 32: 108–115.

Hertig, E., Jacobeit, J., 2008. Downscaling future climate change: Temperature scenarios for the Mediterranean area. Global and Planetary Change 63: 127–131.

Hoff, C. and Rambal, S., 2003. An examination of the interaction between climate, soil and leaf area index in a Quercus ilex ecosystem. Annals of Forest Science 60: 153–161.

Hoff, C., Rambal, S., and Joffre, R., 2002. Simulating carbon and water flows and growth in a Mediterranean evergreen Quercus ilex coppice using the FOREST-BGC model. Forest Ecology and Management 164: 121–136.

Holmes, R. L., 1983. Computer-assisted quality control in tree-ring dating and measurement, TreeRing Bull. 43: 69–78.

Holstein, E., 1980. Mitteleuropäische Eichenchronologie. Philip von Zabern, Mainz.

HyVista, 2003. HyVista Corporation website. http://www.hyvista.com

Ibàñez, J.J., Lledó, M.J., Sánchez, J.R., and Rodà, F. (1999). Stand structure, aboveground biomass and production. In: Rodà, F., Retana, J., Gracia, C.A., and Llebot, J. (Eds.), Ecology of Mediterranean Evergreen Oak Forests (pp. 31–45). Springer, Berlin.

IPCC, 2007. Climate change 2007: The physical science basis. Contribution of Working Group I to the fourth assessment report of the Intergovernmental Panel on Climate Change. New York: Cambridge University Press, pp 996.

Isaaks, E.H., and Srivastava, R.M., 1989. An introduction to applied geostatistics. Oxford University Press, New York.

Jansma, E., 1995. RemembeRINGs. The development and application of local and regional tree-ring chronologies of Oak for the purposes of archaeological and historical research in the Netherlands. Dissertation Amsterdam University. Nederlandse Archeologische Rapporten 19.

Jayawickreme, D.H., Van Dam, R.L., Hyndman, D.W., 2008. Subsurface imaging of vegetation, climate, and root-zone moisture interactions. Geophysical Research Letters 35: L18404.

Joffre, R., Rambal, S., 2001. Mediterranean Ecosystems, in: John Wiley & SonsLtd (Eds.), Encyclopedia of Life Sciences. John Wiley & Sons, Ltd, Chichester, UK. doi:10.1038/npg.els.0003196

Jonckheere I., S. Fleck, K. Nackaerts, B. Muysa, P. Coppin, M. Weiss, and F. Baret., 2004. Review of methods for in situ leaf area index determination Part I. Theories, sensors and hemispherical photography. Agricultural and Forest Meteorology 121: 19–35.

Jones, P. D., Briffa, K. R., Barnett, T. P., and Tett, S. F. B., 1998. High-resolution palaeoclimatic records for the last millennium: Interpretation, integration and comparison with general circulation model control-run temperatures, Holocene, 8: 455–471.

Ju, J., Gopal, S., and Kolaczyk, E.D., 2005. On the choice of spatial and categorical scale in remote sensing land cover classification. Remote Sensing of Environment 96: 62–77.

Khatouri, M., 1992. Growth and yield of young Quercus ilex coppice stands in the Tafferte forest (Morocco), Plant Ecology 99-100: 77–82.

Kimball, J.S., Running, S.W., Nemani, R., 1997. An improved method for estimating surface humidity from daily minimum temperature. Agricultural and Forest Meteorology 85: 87–98.

Klein Tank, A.M.G., Wijngaard, J.B., Können, G.P., Böhm, R., Demarée, G., Gocheva, A., Mileta, M., Pashiardis, S., Hejkrlik, L., Kern-Hansen, C., 2002. Daily dataset of 20th-century surface air temperature and precipitation series for the European Climate Assessment. International Journal of Climatology 22: 1441–1453.

Knibbe, B., 2010. PAST4. SCIEM scientific engineering and manufacturing, available at: http://www.sciem.com, last acces: 9 February 2010.

Kummerow, J., 1981. Structure of roots and root systems. In: Castri, F, di, Goodall, D, W, , Specht, R, L (eds). Ecosystems of the World: 11. Mediterranean-type shrublands. Elsevier, Amsterdam. 269–288

Landsberg, J.J. and Waring, R.H., 1997. A generalized model of forest productivity using simplified concepts of radiation-use efficiency, carbon balance and partitioning. Forest Ecology and Management 95: 209–228.

Larsson, L., 2010. CooRecoreder User Manual, Cybis Elektronik and Data AB, available at: www.cybis.se/forfun/dendro/, last acces: 10 February 2010.

Lavorel, S., Canadell, J., Rambal, S., Terradas, J., 1998. Mediterranean terrestrial ecosystems: research priorities on global change effects. Global Ecology and Biogeography Letters 7: 157–166.

Lillesand, T.M., and Kiefer, R.W., 2004. Remote Sensing and Image Interpretation. John Wiley & Sons, New York.

Limousin, J.M., Rambal, S., Ourcival, J.M., Rocheteau, A., Joffre, R., Rodriguez-Cortina, R., 2009. Long-term transpiration change with rainfall decline in a Mediterranean Quercus ilex forest. Global Change Biology 15: 2163–2175.

Llorens, L., J. Peñuelas, and I. Filella., 2003. Diurnal and seasonal variations in the photosynthetic performance and water relations of two co-occurring Mediterranean shrubs, Erica multiflora and Globularia alypum. Physiologia Plantarum 118: 84–95.

Lowrie, W., 2007. Fundamentals of Geophysics. Cambridge University Press, Cambridge, pp 392.

Lu, D., 2006. The potential and challenge of remote sensing-based biomass estimation. International Journal of Remote Sensing 27: 1297–1328.

Marceau, D.J., and Hay, G.J. 1999. Remote sensing contributions to the scale issue. Canadian Journal of Remote Sensing 25: 357–366.

Marceau, D.J., Gratton, D.J., Fournier, R.A., and Fortin, J.P., 1994. Remote sensing and the measurement of geographical entities in a forested environment. 2. The optimal spatial resolution. Remote Sensing of Environment 49: 105–117.

Martín-Benito, D., Cherubini, P., del Río, M., and Cañellas, I., 2008. Growth response to climate and drought in Pinus nigra Arn. trees of different crown classes, Trees-Struct. Funct. 22: 363–373.

Martinelli, N., 2004. Climate from dendrochronology: latest developments and results, Global Planet. Change 40: 129–139.

Maselli, F., A. Rodolfi, L. Bottai, S. Romanelli, and C. Conese., 2000. Classification of Mediterranean vegetation by TM and ancillary data for the evaluation of fire risk. International Journal of Remote Sensing 21: 3303–3313.

Mather, A.S., Fairbairn, J., and Needle, C.L., 1999. The course and drivers of the forest transition: The case of France. Journal of Rural Studies 15: 65–90.

McCloy, K.R., and Bøcher, P.K., 2007. Optimizing image resolution to maximize the accuracy of hard classification. Photogrammetric Engineering & Remote Sensing 73: 893–903.

Médail, F. and Quezél, P. 1999. Biodiversity Hotspots in the Mediterranean Basin: Setting Global Conservation Priorities, Conservation Biology 13: 1510–1513.

Meteo-France, 2008. Meteo France – Climatologie. http://www.meteofrance.com.

Michot, D., Benderitter, Y., Dorigny, A., Nicoullaud, B., King, D., and Tabbagh, A., 2003. Spatial and temporal monitoring of soil water content with an irrigated corn crop cover using surface electrical resistivity tomography, Water Resources Research 39: 1138.

Miller, J. and Gaskin, G., 2008. ThetaProbe ML2x Principles of Operation and Applications. Macaulay Land Use Research Institute, Aberdeen.

Miller, P.C. and Hajek, E., 1981. Resource availability and environmental characteristics of Mediterranean-type ecosystems. In: Miller, P.C. (ed). Resource use by chaparral and matorral. Springer-Verlag, New York: 17–41.

Monteith, J.L., 1965. Evaporation and environment, in: Symp. Soc. Exp. Biol.: 205–234.

Mooney, H.A., Dunn, E.L., 1970. Convergent evolution of Mediterranean-climate evergreen sclerophyll shrubs. Evolution 292–303.

Mouillot, F., Rambal, S., and Joffre, R., 2002. Simulating climate change impacts on fire frequency and vegetation dynamics in a Mediterranean-type ecosystem. Global Change Biology 8: 423–437.

Mouillot, F., Ratte, J.P., Joffre, R., Mouillot, D., Rambal, S., 2005. Long-term forest dynamic after land abandonment in a fire prone Mediterranean landscape (central Corsica, France). Landscape Ecology 20: 101–112.

Muñoz-Carpena, R., Shukla, S., and Morgan, K., 2004. Field Devices for Monitoring Soil Water Content. University of Florida Cooperative Extension Service, Institute of Food and Agricultural Sciences, EDIS.

Nabais, C., Freitas, H., and Hagemeyer, J., 1998. Tree-rings to climate relationships of Quercus ilex L. in the NE-Portugal, Dendrochronologia, 16: 37–44.

Naveh, Z. and Kutiel, P., 1990. Changes in vegetation of the Mediterranean Basin in response to human habitation, in: The earth in transition, patterns and processes of biotic impoverishment, edited by: Woodwell, G. M., Cambridge University Press, Cambridge, 259–300.

Nemani, R. R., Keeling, C. D., Hashimoto, H., Jolly, W. M., Piper, S. C., Tucker, C. J., Myneni, R. B., and Running, S.W., 2003. Climate-Driven Increases in Global Terrestrial Net Primary Production from 1982 to 1999, Science 300: 1560–1563.

Nicault, A., Alleaume, S., Brewer, S., Carrer, M., Nola, P., and Guiot, J., 2008. Mediterranean drought fluctuation during the last 500 years based on tree-ring data, Clim. Dynam. 31: 227–245.

Nijland, W., E.A. Addink, S.M. De Jong, and F.D. Van der Meer. 2009. Optimizing spatial image support for quantitative mapping of natural vegetation. Remote Sensing of Environment 113: 771–780.

Nijland, W., Jansma, E., Addink, E.A., Domínguez Delmás, M., De Jong, S.M., 2011. Relating ring width of Mediterranean evergreen species to seasonal and annual variations of precipitation and temperature. Biogeosciences 8, 1141–1152.

Nijland, W., van der Meijde, M., Addink, E.A., de Jong, S.M., 2010. Detection of soil moisture and vegetation water abstraction in a Mediterranean natural area using electrical resistivity tomography. CATENA 81: 209–216.

Ogaya, R., J. Peñuelas, J. Martínez-Vilalta, and M. Mangirón. 2003. Effect of drought on diameter increment of Quercus ilex, Phillyrea latifolia, and Arbutus unedo in a holm oak forest of NE Spain. Forest Ecology and Management 180: 175–184.

Openshaw, S., 1984. The Modifiable Areal Unit Problem. Concepts and Techniques in Modern Geography (CATMOG) 38.

Pastor, J., and W.M. Post., 1986. Influence of climate, soil moisture, and succession on forest carbon and nitrogen cycles. Biogeochemistry 2: 3–27.

Patón, D., García-Herrera, R., Cuenca, J., Galavis, M., and Roig, F. A., 2009. Influence of climate on radial growth of holm oaks (Quercus ilex subsp. Ballota desf) from SW Spain, Geochronometria 34: 49–56.

Pereira, J. S., Mateus, J. A., Aires, L. M., Pita, G., Pio, C., David, J. S., Andrade, V., Banza, J., David, T. S., Pac¸ o, T. A., and Rodrigues, A., 2007. Net ecosystem carbon exchange in three contrasting Mediterranean ecosystems – the effect of drought, Biogeosciences 4: 791–802.

Pereira, J.M.C., T.M. Oliveira, and J.P.C. Paul., 1994. Fuel mapping in a Mediterranean shrubland using Landsat TM imagery; In: Kennedy, P.J. and Karteris, M. (Eds.) Proc. International Workshop on Satellite technology and GIS for Mediterranean forest mapping fire management (pp 97–106). Office for Official Publications of the European Communities, Luxembourg.

Poole, D.K., Roberts, S.W., and Miller, P.C., 1981. Water utilization. Resource use by chaparral and matorral. Springer-Verlag, New York: 123–149.

Rahman, A.F., Gamon, J.A., Sims, D.A., and Schmidts, M., 2003. Optimum pixel size for hyperspectral studies of ecosystem function in southern California chaparral and grassland. Remote Sensing of Environment 84: 192–207.

Rambal, S., 2001. Hierarchy and productivity of Mediterranean-type ecosystems, in: Terrestrial Global Productivity, Saugier, B. and Mooney, H. A. Academic Press, London, 315–344.

Rambal, S., Ourcival, J.M., Mission, L., 2008. Level 4 dataset CEIP_EC_L4_FRPue in CarboeuropeIP Ecosystem Component Database. http://gaia.agraria.unitus.it/database.

Raven, P.H., Di Castri, F., Mooney, H.A., 1973. Mediterranean type ecosystems: origin and structure. Ecological studies 7. Springer-Verlag.

Reichstein, M., Ciais, P., Papale, D., Valentini, R., Running, S., Viovy, N., Cramer, W., Cranier, A., Ogee, J., Allard, V., Aubinet, Marc, Bernhofer, C., Buchmann, N., Carrara, Grunwald, T., Heimann, M., Heinesch, Bernard, Knohl, A., Kutsch, W., Loustau, D., Manca, G., Matteucci, G., Miglietta, F., Ourcival, Jm., Pilegaard, K., Pumpanen, J., Rambal, S., Schaphoff, S., Seufert, G., Soussana, Jf., Sanz, Mj., Vesala, T., Zhao, M., 2007: Reduction of ecosystem productivity and respiration during the European summer 2003 climate anomaly: a joint flux tower, remote sensing and modelling analysis. Global Change Biology 13: 634–651.

Reichstein, M., Tenhunen, J., Roupsard, O., Ourcival, J.M., Rambal, S., Miglietta, F., Peressotti, A., Pecchiari, M., Tirone, G., Valentini, R., 2003. Inverse modeling of seasonal drought effects on canopy CO2/H2O exchange in three Mediterranean ecosystems. J. Geophys. Res 108, 4726, doi:10.1029/2003JD003430.

Richard, Y., and I. Poccard., 1998. A statistical study of NDVI sensitivity to seasonal and interannual rainfall variations in Southern Africa. International Journal of Remote Sensing 19: 2907–2920.

Richter, R., and Schläpfer, D., 2002. Geo-atmospheric processing of airborne imaging spectrometry data. Part 2: atmospheric/topographic correction. International Journal of Remote Sensing 23: 2631–2649

Robinson, D.A., Campbell, C.S., Hopmans, J.W., Hornbuckle, B.K., Jones, S.B., Knight, R., Ogden, F., Selker, J., and Wendroth, O., 2008. Soil moisture measurement for ecological and hydrological watershed-scale observatories: a review. Vadose Zone Journal 7: 358–389.

Robinson, D.A., Jones, S.B., Wraith, J.M., Or, D., and Friedman, S.P., 2003. A review of advances in dielectric and electrical conductivity measurement in soils using time domain reflectometry. Vadose Zone Journal 2: 444–475.

Rodá, F., Gracia, C., Retana. J., Bellot, J., 1999 The ecology of Mediterranean evergreen oak forests. Ecological studies 137, Springer, Berlin. Pp 381

R-Team., 2006. R: A language and environment for statistical computing. R Foundation for Statistical Computing, Vienna. http://www.r-project.org

Running, S. W. and Gower, S. T., 1991. FOREST-BGC, a general model of forest ecosystem processes for regional applications. II. Dynamic carbon allocation and nitrogen budgets. Tree Physiology 9: 147–160.

Running, S.W. and Coughlan, J.C., 1988. A general model of forest ecosystem processes for regional applications. I. Hydrologic balance, canopy gas exchange and primary production processes. Ecological Modeling 42: 125–154.

Running, S.W., Coughlan, J.C., 1988. A general model of forest ecosystem processes for regional applications. I. Hydrologic balance, canopy gas exchange and primary production processes. Ecological Modelling 42: 125–154.

Sabaté, S., Gracia, C.A., Sánchez, A., 2002. Likely effects of climate change on growth of Quercus ilex, Pinus halepensis, Pinus pinaster, Pinus sylvestris and Fagus sylvatica forests in the Mediterranean region. Forest Ecology and Management 162: 23–37.

Sala, A. and Tenhunen, J. D., 1996. Simulations of canopy net photosynthesis and transpiration in Quercus ilex L. under the influence of seasonal drought. Agricultural and Forest Meteorology 78: 203–222.

Scarascia-Mugnozza, G., Oswald, H., Piussi, P., Radoglou, K., 2000. Forests of the Mediterranean region: gaps in knowledge and research needs. Forest Ecology and Management 132: 97–109.

Schläpfer, D., and Richter, R., 2002. Geo-atmospheric processing of airborne imaging spectrometry data. Part 1: parametric orthorectification. International Journal of Remote Sensing 23: 2609–2630.

Schlerf, M., Atzberger, C., and Hill, J., 2005. Remote sensing of forest biophysical variables using HyMap imaging spectrometer data. Remote Sensing of Environment 95: 177–194.

Schmugge, T., A. French, J.C. Ritchie, A. Rango, and H. Pelgrum., 2002. Temperature and emissivity separation from multispectral thermal infrared observations. Remote Sensing of Environment 79: 189–198.

Schweingruber, F. H., 1993. Trees and Wood in Dendrochronology: Morphological, Anatomical, and Tree-Ring Analytical Characteristics of Trees Frequently used in Dendrochronology, Springer-Verlag, Berlin.

Schweingruber, F. H., Eckstein, D., Serre-Bachet, F., and Bräker, O.U., 1990. Identification, presentation and interpretation of event years and pointer years in dendrochronology, Dendrochronologia 8: 9–38.

Sluiter, R., 2005. Mediterranean land cover change: modelling and monitoring natural vegetation using GIS and remote sensing. Nederlandse Geografische Studies.

Sluiter, R., and De Jong, S.M., 2007. Spatial patterns of Mediterranean land abandonment and related land cover transitions. Landscape Ecology 22: 559–576.

Sluiter, R., De Jong, S.M., Van der Kwast, J., and Walstra, J., 2004. A Contextual Approach to Classify Mediterranean Heterogeneous Vegetation using the Spatial Reclassification Kernel and DAIS7915 Imagery. In: De Jong, S.M., and Van der Meer, F.D. (Eds.) Remote Sensing Image Analysis: Including the Spatial Domain (pp. 291–310). Kluwer Academics, Dordrecht.

Solomon, S., Qin, D., Manning, M., Marquis, M., Averyt, K., Tignor, M.M.B., Miller, H.L., Chen, Z., 2007. Climate Change 2007: the physical science basis: contribution of Working Group I to the Fourth Assessment Report of the Intergovernmental Panel on Climate Change. Cambridge Univ Pr, Cambridge, pp 996.

Srayeddin, I., and Doussan, D., 2009. Estimation of the spatial variability of root water uptake of maize and sorghum at the field scale by electrical resistivity tomography. Plant Soil 319: 185–207.

Strahler, A.H., C.E. Woodcock, and J.A. Smith. 1986. On the nature of models in remote sensing. Remote Sensing of Environment 20: 121–139.

Telford, W.M., Geldart, L.P., and Sheriff, R.E., 1990. Applied Geophysics. Cambridge University Press, Cambridge, pp792.

Tessier, L., Nola, P., and Serre-Bachet, F., 1994. Deciduous Quercus in the Mediterranean region: tree-ring/climate relationships, New Phytol., 126: 355–367.

Thornton, P.E., Running, S.W., 1999. An improved algorithm for estimating incident daily solar radiation from measurements of temperature, humidity, and precipitation. Agricultural and Forest Meteorology 93: 211–228.

Tichonov, A.N., and Arsennin, V.J., 1977. Solutions of ill-posed problems. Wiley, New York.

Tomaselli, R., 1981. Relations with other ecosystems: temperate evergreen forests, Mediterranean coniferous forests, savannahs, steppes and desert shrublands. In: Di Castri, F., Goodall, D.W., and Specht, R.L. Ecosystems of the world 11. Mediterranean-type shrublands (pp 123–130). Elsevier, Amsterdam.

Touchan, R., Xoplaki, E., Funkhouser, G., Luterbacher, J., Hughes, M., Erkan, N., Akkemik,Ü., and Stephan, J., 2005. Reconstructions of spring/summer precipitation for the Eastern Mediterranean from tree-ring widths and its connection to large-scale atmospheric circulation, Clim. Dynam., 25: 75–98.

Tucker, C.J. 1979. Red and photographic infrared linear combinations for monitoring vegetation. Remote Sensing of Environment 8: 127–150.

UNEP, 2009. MAP-Plan Bleu, State of the environment and development in the Mediterranean, UNEP/MAP-Plan Bleu. Athens, pp 200.

Van Der Tol, C., Dolman, A.J., Waterloo, M.J., Raspor, K., 2006. Topography induced spatial variations in diurnal cycles of assimilation and latent heat of Mediterranean forest. Biogeosciences Discussions 3: 1631–1677.

Van Keulen, H. and Wolf, J., 1986. Modelling of Agricultural Production: Weather, Soils and Crops, Pudoc, Wageningen.

Van Reeuwijk (Ed.), 2002. Procedures for Soil Analysis. International Soil Reference and Information Centre (ISRIC), Wageningen.

Vennetier, M., Ripert, C., 2009. Forest flora turnover with climate change in the Mediterranean region: A case study in Southeastern France. Forest Ecology and Management 258: 56–63.

Vogiatzakis, I.N., Mannion, A.M., Griffiths, G.H., 2006. Mediterranean ecosystems: problems and tools for conservation. Progress in Physical Geography 30, 175–200.

Walther, G.R., E. Post, P. Convey, A. Menzel, C. Parmesan, T.J.C. Beebee, J.M. Fromentin, O. Hoegh-Guldberg, and F. Bairlein., 2002. Ecological responses to recent climate change. Nature 416: 389–395.

Watson, D. J., 1947. Comparative physiological studies in the growth of field crops. I. Variation in net assimilation rate and leaf area between spedies and varieties, and within and between years. Ann. Bot. 11: 41–76.

Webster, R., and Oliver, M.A., 2001. Geostatistics for environmental scientists. John Wiley & Sons Ltd., Chichester, pp286.

Weiss, M., Baret, F., Smith, G.J., Jonckheere, I., Coppin, P., 2004. Review of methods for in situ leaf area index (LAI) determination Part II. Estimation of LAI, errors and sampling. Agricultural and Forest Meteorology 121, 37–53.

Wonnacott, T. H., and Wonnacott, R. J., 1990. Introductory statistics. John Wiley and Sons Ltd, New-York.

Woodcock, C.E., and Strahler, A.H., 1987. The factor scale in remote sensing. Remote Sensing of Environment 21: 311–332.

Woodcock, C.E., Strahler, A.H., and Jupp, D.L.J., 1988a. The use of variograms in remote sensing: I Scene models and simulated images. Remote Sensing of Environment 25: 323–348.

Woodcock, C.E., Strahler, A.H., and Jupp, D.L.J., 1988b. The use of variograms in remote sensing: II Real digital images. Remote Sensing of Environment 25: 349–379.

Xiao, X., Q. Zhang, B. Braswell, S. Urbanski, S. Boles, S. Wofsy, B. Moore, and D. Ojima. 2004. Modeling gross primary production of temperate deciduous broadleaf forest using satellite images and climate data. Remote Sensing of Environment 91: 256–270.

Yamaguchi, Y., A.B. Kahle, H. Tsu, T. Kawakami, and M. Pniel. 1998. Overview of advanced spaceborne thermal emission and reflection radiometer (ASTER). IEEE Transactions on Geoscience and Remote Sensing 36: 1062–1071.

Zhang, S. H. and Romane, F., 1991. Variations de la croissance radiale de Quercus ilex L. en fonction du climat, Ann. Sci. Forest. 48: 225–234.

Summary

Vegetation development in Mediterranean landscapes is often a slow process. The typical Mediterranean climate -with long dry periods in summer, mild winters and concentrated rainfall events in spring and autumn- is an important constraint on growth, enhanced by the often marginal and degraded soil conditions. Climate change scenarios predict that the extreme character of the Mediterranean climate will increase: higher temperatures especially in the summer, and decreasing summer precipitation. These changing environmental conditions may have a deteriorating impact on the Mediterranean ecosystems. The Mediterranean climate does not only limit vegetation productivity, it also attracts human activity. Pressure on environmental resources is therefore increasing by population growth, economic development and recreation.

Natural vegetation in Mediterranean areas is characterized by the dominance of broadleaved evergreen species that are adapted to summer drought. The evergreen leather-like leaves limit evaporation and allow these species to grow in a landscape where summer drought and poor soil conditions strongly limit plant productivity. The low growth potential and slow succession make the Mediterranean landscape vulnerable to disturbances and modern climate change. It is thus important to create reliable predictions of future vegetation development and to have accurate methods to monitor the natural areas. Analysis of the current spatial patterns and temporal variability in key vegetation characteristics such as biomass, leaf area, water use, and growth provides information on the ecosystem that can be used to create more accurate projections for future development of the landscape and vegetation. The objective of this thesis is therefore: To increase our understanding of, and abilities to monitor the growth and development of evergreen Mediterranean vegetation and to improve the projections of vegetation change as an effect of modern climate change.

Optimal spatial support for monitoring

High-spatial-resolution images allow detailed detection of vegetation parameters like leaf area and aboveground biomass. With high resolution images it is important to consider the spatial scale of the analysis, because the resolution may have a large influence on mapping accuracy. In order to optimize quantitative image analysis, airborne hyperspectral imagery was combined field data to find the optimal spatial resolution for the mapping of natural vegetation in a Mediterranean environment. The optimal pixel size for the forests and shrub lands in the Peyne area was 50 to 100m and resulted in an improvement of mapping accuracy of 7 to 17%. This shows that in any remote sensing project, the scale of analysis has to be carefully considered as optimizing the measurement support can seriously improve mapping accuracy.

Detection of ecosystem functioning with optical and thermal imagery

Accurate detection of tree growth and ecosystem functioning in naturally vegetated areas is of interest to many applications, but changes are often small when compared to normal spatial and seasonal variability, or occur gradually over time. Use of object-based image analysis for time-series analysis of vegetation functioning improves the ability to detect small differences because the objects coincide better with ecological units in the field than pixels. A single segmentation

of multi-temporal data aligns all available data to a single object framework, reducing the effects of spatial misalignment between multi-temporal data. The images are recorded before, during, and after the dry summer season, and thus show the effect of summer drought on the vegetation in our study area. The relation between the geological substrates and seasonal patterns in NDVI and thermal brightness indicates a close relation between the substrates, water availability and vegetation vigour.

Soil water use and rooting depth

Accurate moisture measurements in naturally vegetated areas are difficult because of high spatial variability and coarse, shallow soils. Electrical Resistivity Tomography (ERT) is a method to measure soil characteristics using electrodes placed at the surface, and provides information on the spatial patterns within the soil reaching depths otherwise inaccessible. In heterogeneous soils, lithological and moisture effects are differentiated in the measurements using multi-temporal data. Absolute calibration to moisture content was sometimes possible, but strongly location dependent. Based on the ERT measurements, plant roots were found to penetrate deeply into the fractured and weathered bedrock, subtracting water from the soil at depths down to 6m and below. The evaluation of rooting depth and soil water abstraction on different substrates shows that lithology is an important factor controlling water availability, water storage capacity, and maximum root penetration depth. Soils with deeper root growth and water abstraction are able to support more vegetation and sustained growth potential during the dry season.

Sensitivity of tree ring growth to climate variability

To improve the understanding of forest sensitivity to annual and seasonal climatic variability, tree-ring measurements of two Mediterranean evergreen tree species: *Quercus ilex* and *Arbutus unedo* are used. 34 stems were sampled on three different types of substrates. The resulting chronologies were analysed in combination with 38 years of monthly precipitation and temperature data to reconstruct the response of stem growth to climatic variability. Results indicate a strong positive response to May and June precipitation, as well as a significant positive influence of early-spring temperatures and a negative growth response to summer heat. Comparison of the data with more detailed productivity measurements in two contrasting years confirms these observations and shows a strong productivity limiting effect of low early-summer precipitation. The tree-ring analysis provides an important source of reference data towards the evaluation of simulation models, both at a longer (decadal) temporal scale as on the shorter (monthly or seasonal) scale

Modelling future vegetation growth.

Anticipated climate change for the upcoming century will intensify the warm and dry character of the climate which may lead to decreased water availability and changes in vegetation growth. To improve the future projections of vegetation development the dynamical vegetation model forest-BGC is used. The model is first parameterized and validated against past tree-growth records from annual tree rings and current field measurements of leaf area and aboveground biomass. The past runs agree well with the field data and also show the same monthly sensitivity patterns the climate variability as the tree ring records. Secondly, the model is run with possible climate scenarios for 2070 with yearly and seasonal changes in temperature and precipitation. A probable climate scenario predicts a temperature increase of 2˚C in winter and 5˚C in

summer plus a decrease of summer precipitation by 40%. Based on this climate, the Forest-BGC vegetation productivity model predicts a decrease of leaf area by 25%, and potentially over 50% less production of woody biomass in the area. These results indicate that a change in species composition may be likely because a forest cannot sustain itself if there is so little wood production. Both a large change in productivity and vegetation cover and a shift in species composition will have significant consequences for the landscape and land use possibilities in the region.

My study contributes to improving the understanding and prediction of Mediterranean vegetation growth within the framework of anticipated climate change and increasing human pressure on the region. Spatial and temporal patterns in vegetation growth and water availability were detected using earth observation, geophysical measurements, field plots, and tree-ring samples. By combining novel detection and monitoring methods and dynamical productivity modelling, this study contributes to the advance of vegetation monitoring and the ability to project future vegetation growth based on climate-change scenarios.

Samenvatting

Vegetatie ontwikkeling in Mediterrane landschappen is meestal een langzaam proces. Het typisch mediterrane klimaat –met lange droge periodes in de zomer, milde winters en geconcentreerde neerslag in de lente en de herfst– is een belangrijke beperking voor groei, versterkt door de vaak marginale en gedegradeerde bodems. Klimaatscenario's voorspellen dat het extreme karakter van het Mediterrane klimaat zal toenemen: hogere temperaturen en nog minder neerslag tijdens de zomer. Deze veranderende milieu-omstandigheden kunnen een negatieve invloed hebben op Mediterrane ecosystemen. Het Mediterrane klimaat beperkt niet alleen de productiviteit van de vegetatie, het trekt ook menselijke activiteit aan. De druk op natuurlijke bronnen neemt dan ook toe door bevolkingsgroei, economische ontwikkeling, en recreatie.

De natuurlijke vegetatie in de mediterrane gebieden wordt gekenmerkt door de dominantie van groenblijvende boom- en struiksoorten die zijn aangepast aan de droge zomers. De altijdgroene leerachtige bladeren remmen de verdamping zodat deze soorten kunnen groeien in een landschap waar de droogte en karige bodems de productiviteit beperken. Door het lage groeipotentieel en de trage successie is het mediterrane landschap kwetsbaar voor verstoringen en klimaatverandering. Het is daarom belangrijk om toekomstige vegetatieontwikkeling betrouwbaar te voorspellen en om nauwkeurige methoden te ontwikkelen voor het monitoren van de natuurlijke gebieden. Analyse van de huidige ruimtelijke patronen en temporele variabiliteit in belangrijke vegetatie kenmerken zoals biomassa, bladoppervlakte, watergebruik, en groei geeft informatie over het ecosysteem die kan worden gebruikt voor het maken van accurater prognoses van de toekomstige ontwikkelingen in het landschap. Het doel van dit proefschrift is dan ook: Het vergroten van ons begrip, en de mogelijkheden voor het monitoren, van de groei en ontwikkeling van groenblijvende Mediterrane ecosystemen om de projecties voor toekomstige verandering als gevolg van klimaatverandering te verbeteren.

Optimale ruimtelijke eenheden voor de monitoring

Beelden met een hoge ruimtelijke resolutie maken het mogelijk om vegetatie parameters zoals bladoppervlakte en bovengrondse biomassa in groot detail te detecteren. Het is met deze hoog resolutie beelden belangrijk om de ruimtelijke schaal van analyse te overwegen, omdat de resolutie een grote invloed kan op de nauwkeurigheid van het eindproduct. Om kwantitatieve beeldanalyse te optimaliseren, heb ik hyperspectrale vliegtuigbeelden gecombineerd met veld gegevens om de optimale ruimtelijke resolutie te vinden voor het in kaart brengen van Mediterrane natuurlijke vegetatie. De optimale pixelgrootte voor de bossen en struiken in het Peyne gebied was van 50 tot 100m het gebruik van deze optimale grootte en resulteerde in een verbetering van de nauwkeurigheid van 7 tot 17%. Dit onderzoek toont aan dat in elk aardobservatie project, de schaal van analyse moet zorgvuldig worden bekeken, omdat het optimaliseren van de resolutie een significante verbetering kan opleveren voor de detectie nauwkeurigheid.

Detectie van vegetatieontwikkeling met optische en thermische beelden

Nauwkeurige detectie van de groei en functioneren van natuurlijke gebieden is van belang voor vele toepassingen, maar veranderingen in het systeem zijn vaak klein in vergelijking met normale ruimtelijke- en seizoenschommelingen, of lopen geleidelijk in de tijd. Door object-gebaseerde beeldanalyse voor tijdreeksen van natuurlijke mediterrane vegetatie is het mogelijk om kleinere verschillen te detecteren, omdat de objecten beter samenvallen met ecologische eenheden in het veld dan pixels. Door één segmentatie te gebruiken voor de multitemporele gegevens worden alle beschikbare gegevens uitgelijnd op het zelfde object frame, waardoor het effect van fouten in de uitlijning van de verschillende beelden word verminderd.. De gebruikte beelden zijn opgenomen voor, tijdens en na het droge zomer seizoen, en laten dus het effect zien van de zomer droogte op de vegetatie in ons studiegebied. Het verband tussen de substraten in het gebied en seizoenspatronen in NDVI en thermische helderheid geeft een nauwe relatie weer tussen het substraat, waterbeschikbaarheid, en groei en stress van de vegetatie.

Beschikbaarheid van bodemvocht en worteldiepte

Nauwkeurige metingen van bodemvocht in begroeide Mediterrane gebieden zijn moeilijk vanwege de hoge ruimtelijke variabiliteit en de grove en dunne bodem. Electrical Resistivity Tomography (ERT) is een methode om bodemeigenschappen te bepalen met aan het oppervlakte geplaatste elektroden en geeft informatie over de ruimtelijke patronen in de bodem op diepten die anders ontoegankelijk zijn. In heterogene gronden, zijn de effecten van de lithologie en vocht te onderscheiden door het gebruik van multitemporele metingen. Absolute kalibratie van het vochtgehalte was soms mogelijk, maar sterk afhankelijk van de lokatie. Op basis van de ERT metingen zijn de effecten van boomwortels gevonden die diep in het gebarsten gesteente doordringen om water te onttrekken tot 6m of dieper. De analyse van de worteldiepte en bodemwater onttrekking op verschillende substraten laat zien dat lithologie een bepalende factor is in de waterbeschikbaarheid, wateropslagcapaciteit de maximale diepte van doorworteling. Bodems met diepere wortelgroei en wateronttrekking hebben meer vegetatie en een groter groeipotentieel tijdens het droge seizoen

Gevoeligheid van jaarring groei voor klimaatvariabiliteit

Voor het beter begrijpen van de gevoeligheid van bossen voor seizoenale en jaarlijkse variabiliteit van het klimaat, zijn jaarring metingen van gebruikt van twee soorten Mediterrane groenblijvende soorten gebruikt: *Quercus ilex* en *Arbutus unedo* gebruikt. 34 stammen werden bemonsterd op drie verschillende soorten substraten. De resulterende chronologieën zijn geanalyseerd in combinatie met 38 jaar maandelijkse neerslag en temperatuur data, om de reactie van stamgroei op klimaatvariaties te reconstrueren. De resultaten geven een sterke positieve relatie met neerslag in mei en juni, evenals een significante positieve relatie met de temperaturen vroeg in de lente en een negatieve relatie met zomerse hitte. Vergelijking van de gegevens gedetailleerde metingen van productiviteit in twee tegengestelde jaren bevestigt de gevonden relaties en laat een sterk beperkend effect zien op de stamgroei van weinig neerslag in de vroege zomer. De jaarringanalyse is een belangrijke bron van referentiedata voor de evaluatie van de simulatiemodellen, zowel op een langer (decade) temporele schaal als op de kortere (maandelijks of seizoenale) schaal

Modelleren van de toekomstige vegetatiegroei.

De verwachte klimaatverandering voor de komende eeuw geeft een intensivering van het warme en droge karaktervan het Mediterrane klimaat wat kan leiden tot een verminderde waterbeschikbaarheid en veranderingen in vegetatiegroei. Voor verbeteren van toekomst projecties van vegetatieontwikkeling wordt het dynamische vegetatie model Fores-BGC gebruikt. Het model wordt eerst geparameteriseerd en gevalideerd tegen het jaarring gegevens van de afgelopen 38 jaar en recente velddata van bladoppervlak en bovengrondse biomassa. De veldgegevens komen goed overeen met modelsimulaties voor de laatste halve eeuw en laten ook dezelfde maandelijkse patronen zien in klimaatgevoeligheid als de jaarring data. Als tweede is het model gedraaid met klimaatscenario's voor 2070 met een jaarlijkse of seizoenale verandering in temperatuur en neerslag. Het meest waarschijnlijke klimaatscenario voorspelt een temperatuurstijging van 2°C in de winter en 5°C in de zomer, plus een daling van de zomerse neerslag met 40%. Op basis van dit klimaat voorspeld Forest-BGC een vermindering van bladoppervlak met 25%, en mogelijk een reductie van 50% in de productie van houtige biomassa. Deze resultaten geven aan een verandering van de soortsamenstelling waarschijnlijk is omdat een bos zich niet kan handhaven bij zulke lage houtproductie. Zowel grote veranderingen in de productiviteit als een verschuiving in de soortensamenstelling zal grote gevolgen hebben voor het landschap en landgebruiksmogelijkheden in de regio

Mijn studie draagt bij aan een verbeterd begrip en mogelijkheden voor het voorspellen van Mediterrane vegetatiegroei binnen het kader van de verwachte klimaatverandering en de toenemende menselijke druk op de regio. Ruimtelijke en temporele patronen in de vegetatie en de beschikbaarheid van water werden in kaart gebracht met behulp van aardobservatie, geofysische metingen, proefvelden, en jaarring monsters. Door het combineren van nieuwe detectie en monitoring methoden en het dynamisch modelleren van productiviteit draagt deze studiebij aan de vooruitgang in vegetatie monitoring en de mogelijkheden voor het voorspellen van toekomstige groei op basis van klimaatscenario's

About the author

Wiebe Nijland was born on 12 February 1983 in Taarlo, The Netherlands. He went to primary school at the 'Meester Croneschool' in Oudemolen, travelling to school by bike along the beautiful Drentsche Aa stream valley every day. Through the 'PCB Beemte' and 'KSG Apeldoorn' he graduated high school at the 'RSG Pantarijn' in Wageningen. During his high school and study time he spent most of his spare time strolling through nature with the ´Nederlandse Jeugdbond voor Natuurstudie´ (NJN), looking for all kinds of insects and anything living in water, especially along the sea shore.

At Utrecht University Wiebe studied Physical Geography starting in 2001. He specialized in remote sensing and land degradation writing his MSc. Thesis on the 'Spatial variance of Mediterranean vegetation in relation to remote sensing image analysis'. Before starting on a PhD project in the same Mediterranean study area in southern France, Wiebe went for an internship to the northern interior of British Columbia, Canada. With the forest service in Prince George, he studied the relations between landslide hazards and pine-beetle killed forests using satellite imagery to detect dead forest areas. In October 2006 Wiebe started his PhD research on the evergreen forests in the Peyne catchment, France. Next to his research he was chair of the PhD platform for two years, and involved in teaching remote sensing, supervising MSc students for their work in Peyne, and supervising the first year field course in the French Alps.

After the PhD project Wiebe got a one year part-time appointment as junior assistant professor with the earthsciences faculty at Utrecht University in which he participated in teaching classes in natural hazards, remote sensing, GIS, and several other courses, excursions and fieldwork. In most of his time at Utrecht University, Wiebe was also a member of the emergency response team as a fist aid provider. Starting in November 2011 Wiebe will move to Vancouver, Canada to work as a postdoc with the Integrated Remote Sensing Studio of the Forest Sciences Centre at The University of British Columbia (UBC). In this new environment he will further explore the use of remote sensing in forest ecosystems, but in a very different climate and landscape.

List of publications:

Journal Papers

Nijland, Wiebe, Elisabeth A. Addink, Steven M. de Jong, & Freek D. van der Meer, (2009). Optimizing spatial image support for quantitative mapping of natural vegetation. Remote Sensing of Environment 113 (4), 771-780.

Nijland, Wiebe, Mark van der Meijde, Elisabeth A. Addink, & Steven M. de Jong, (2010). Detection of soil moisture and vegetation water abstraction in a Mediterranean natural area using electrical resistivity tomography. CATENA 81 (3), 209-216.

Nijland, Wiebe, Esther Jansma, Elisabeth A. Addink, Marta Domínguez-Delmás, & Steven M. de Jong, (2011). Relating ring width of Mediterranean evergreen species to seasonal and annual variations of precipitation and temperature. Biogeosciences 8, 1141-1152.

Other Publications

Nijland, Wiebe, Esther Jansma, & Elisabeth A. Addink, (2011) Using tree ring data in modelling seasonal and annual dynamics of Mediterranean evergreen forests. 2011 US-IALE Symposiuim, Sustainability in Dynamic Landscapes. April 3-7 2011, Portland, Oregon.

De Jong, Steven M., Elisabeth A. Addink, Priscilla E. Hoogenboom, & Wiebe Nijland, (2011). A laboratory experiment to investigate the spectral response of Buxus sempervirens to differences types of stress. Proceedings of the EARSeL 7th SIG Imaging Spectroscopy workshop. Edinburgh, 11-13 April. 10pp.

Nijland, Wiebe, Elisabeth A. Addink, Steven M. de Jong, & Freek D. van der Meer, (2010). Detection of ecosystem functioning using object-based time-series analysis. In: Addink, E.A. and F.M.B. Van Coillie (Eds). GEOBIA 2010-Geographic Object-Based Image Analysis. Ghent University, Ghent, Belgium, 29 June – 2 July. ISPRS Vol.No. XXXVIII-4/C7.

Nijland, Wiebe, Mark van der Meijde, Elisabeth A. Addink, Steven M. de Jong, & Freek D. van der Meer, (2009). Electrical resistivity tomography detection of vegetation water use. Geophysical Research Abstracts Vol.11, EGU General Assembly 2009, Vienna.

Addink, Elisabeth A., Steven M. de Jong, Edzer J. Pebesma, & Wiebe Nijland, (2007). Estimating Biomass and LAI in Mediterranean Forests From Hymap Data Using Object-Oriented Image Analysis. How to Define Optimal Objects? Proceedings ForestSAT2007 conference. 5-7 November 2007 at Montpellier. CDRom Publication 5pp.